INSIGHTS INTO THE ROLE OF GRIM-19 IN MITOCHONDRIAL FUNCTION AND INTERFERON - RETINOIC ACID INDUCED CELL DEATH PATHWAY

BHAVANI K
(B. Tech)

A THESIS SUBMITTED

FOR THE DEGREE OF MASTER OF SCIENCE

DEPARTMENT OF BIOLOGICAL SCIENCES

NATIONAL UNIVERSITY OF SINGAPORE

2014

DECLARATION

I hereby declare that this thesis is my original work and it has been written by me in its entirety. I have duly acknowledged all the sources of information which have been used in the thesis.

This thesis has also not been submitted for any degree in any university previously.

_____

Bhavani K

23 December 2014

ACKNOWLEDGEMENT

This thesis has definitely come out the way it has, only with the help and support of some very special and important people who have contributed to all my learning, understanding and implementation of ideas. I am so grateful to all of them.

First and foremost I would like to thank my supervisor Dr. Liou Yih-Cherng who has been more than just a guide for my research. Apart from sharing his expertise in the subject, he has always been very supportive, encouraging and motivating which has definitely helped me a lot during testing times professionally and personally.

At this juncture, I would like to extend my gratitude to Dr. Low Boon Chuan and Dr. Cynthia He for being very kind and supportive throughout my program. I am also thankful for their critical suggestions with respect to my project.

Life in the lab would definitely not have been the same without my kind labmates. They were always there for me, very caring and helpful. Xiao Bin and Xiao Lin helped me learn all my mitochondrial techniques. Jian Yuan, Chenyu, Yajun, Lora and Qiaoyun were always ready to extend their help and spend time in any difficulty that I faced inside and outside of lab. Lastly Hongxu and Zhang Rui, my sweet juniors who help make the lab livelier.

Finally, I would like to dedicate this work to my parents who have been immensely supportive of my interests in life and always stood by me and loved me unconditionally. Without them, I would not be the person I am today. My lovely sister, Haripriya and the most wonderful friend one can ask for, Tg, without your constant support and help in every which way, I don't think this would have been possible.

To have been blessed with the best things in life, I am eternally grateful to my Guru and the Almighty.

TABLE OF CONTENTS

SUMMARY

Interferons (IFN) are cytokines that regulate anti tumour, immune and anti viral responses in vertebrates. Retinoic acid (RA) is a metabolite of vitamin A that has profound effects on metabolism, cell growth and differentiation. The combinatorial therapeutic effect of IFN/RA has been shown to be more potent in fighting cancer cells than that of either drug alone. GRIM-19 is a protein that was identified to be one of the downstream players of the IFN/RA induced cell death pathway. Subsequent studies showed that it is a subunit of mitochondrial complex I. However, little is known about the role of GRIM-19 in maintaining mitochondrial homeostasis and IFN/RA mediated cell death. As mitochondria are highly dynamic organelles, in this study, we tried to explore the role of GRIM-19 in maintaining the morphology and other vital functions of the mitochondria.

The localization of GRIM-19 was controversial with studies reporting that it is present in the cytoplasm and the nucleus apart from the mitochondria. Here, I show that GRIM-19 clearly localizes only to the mitochondria. The results also show that GRIM-19 over expression or knock down (KD) does not affect the morphology or dynamics of mitochondria. While studying the role of GRIM-19 in mitochondrial functions, I observed that ROS increases upon GRIM-19 KD. Apart from this, I also investigated the characteristics of three GRIM-19 mutants

which had lost the capacity to inhibit STAT3-induced cellular transformation identified from human patient tumour samples. These mutants are not able to rescue the increase in ROS production caused by the knock down of GRIM-19. Down-regulation of GRIM-19 has been reported in several cancers. Research has also shown that cancer cells exhibit a higher level of ROS than do normal cells. With these results and further studies on the physiological significance of the interaction of STAT3 and GRIM-19 with respect to the mitochondria, it would be possible to elucidate the mechanism by which absence or mutations of GRIM-19 promote tumour growth.

LIST OF TABLES

LIST OF FIGURES

LIST OF ABBREVIATIONS

ATP	Adenosine triphosphate
DHE	Dihydroethidium
DMEM	Dulbecco's modified eagle medium
DMSO	Dimethyl sulfoxide
dNTP	Deoxynucleoside triphosphate
Drp1	Dynamin related protein 1
ETC	Electron transport chain
FACS	Fluorescence-activated cell sorting
Fis1	Mitochondrial fission 1
FRAP	Fluorescence Recovery after photobleaching
GFP	Green fluorescence protein
GRIM	Genes associated with Retinoid Interferon induced mortality
HEPES	4-(2-hydroxyethyl)-1-piperazineethanesulfonic acid
HRP	Horseradish peroxidase
IMM	Inner mitochondrial membrane
IMS	Intermembrane space
Mfn1/2	Mitofusin ½
MOMP	Mitochondrial outer membrane permeabilization
mtDNA	Mitochondrial DNA
NADPH	Reduced nicotinamide adenine dinucleotide phosphate
OMM	Outer mitochondrial membrane
OPA1	Optic atrophy 1
OPA1	Optic atrophy 1
PBS	Phosphate-buffered saline
PCR	Polymerase chain reaction
PVDF	Polyvinylidene difluoride
ROS	Reactive oxygen species
ROS	Reactive oxygen species
RT-PCR	Reverse transcription polymerase chain reaction
S.D	Standard deviation
S.E.M	Standard error of mean
SDS	Sodium dodecylsulphate
SDS-PAGE	Sodium deodecyl sulfate polyacrylamide gel electrophoresis
shRNA	Short hairpin RNA
siRNA	Short interfering RNA
TEMED	Tetramethylethylenediamine
WT	Wild type

Chapter 1 INTRODUCTION

1.1 MITOCHONDRIA

1.1.1 Origin

Multicellular organisms are composed of variety of tissues which are in turn made up of individual functional units called cells. Each cell is made up of a myriad of sub cellular organelles. Amongst them, one of the most important is the mitochondrion. According to the endosymbiotic theory, mitochondria are descendants of ancient bacteria that entered into a symbiotic relationship with primitive host cells (Gray et al., 1999). They retain several features of their putative bacterial ancestors like the double membrane, a proteome similar to that of α-proteobacteria and the ability to synthesize ATP through a proton gradient generated across their inner membrane. Mitochondrial morphologies vary widely among different cell types. Fibroblast mitochondria, for instance, are usually long filaments (1 to 10 μm in length with a reasonably constant diameter of ~700 nm), whereas hepatocyte mitochondria are more uniformly spheres or ovoids (Youle and van der Bliek, 2012). The number of mitochondria in a cell can also vary widely depending on the organism, tissue, and cell type. For example, red blood cells have no mitochondria, whereas liver cells can have more than 2000. Since their main role is production of energy, they are referred to as the "powerhouse of the cell" and are

abundant in cells that have a high energy requirement like neurons and cardiomyocytes.

1.1.2 Structure

Mitochondria are semi-autonomous organelles that contain their own genome and protein synthesis machinery. These are enclosed in a double membrane that is made up of phospholipids and proteins. There are four main parts to the structure of a mitochondrion, namely the outer mitochondrial membrane (OMM), the inter-membrane space (IMS), the inner membrane (IMM) and the matrix (Friedman and Nunnari, 2014).

OMM contains large numbers of integral proteins called *porins*. These porins form channels that allow molecules 5000 Daltons or less in molecular weight to freely diffuse from one side of the membrane to the other. Proteins larger can enter the mitochondrion if their N-terminus hosts a signalling sequence that binds to a large multi-subunit protein called translocase of the outer membrane, which then actively moves them across the membrane (Hay et al., 1984).

IMS also called the peri-mitochondrial space is the space between the outer and the inner membranes. Of late, many studies have revealed the protein composition of the IMS. One important protein that is localized to this compartment is cytochrome c which plays a significant role in the apoptotic signalling cascade (Chipuk et al., 2006). It is an essential component of the respiratory electron transport chain, and has been identified as a potent activator of apoptosis when released into the

cytosol. Other potential killers residing within the IMS are proapoptotic members of the caspase family : caspase-9, caspase-2 and caspase-3 and a flavoprotein known as an apoptosis-inducing factor (AIF) (Alnemri, 1999).

IMM has a high protein to phospholipid ratio and is made up of proteins with highly specific functions for the synthesis of ATP. These are discussed in detail in the following sub-headings. Unlike the OMM, the IMM does not contain porins and is highly impermeable. Most of the ions and molecules require special membrane transporters to enter or exit the matrix. Proteins are ferried into the matrix via the translocase of the inner membrane (TIM) complex or via Oxa1 (Herrmann and Neupert, 2000). In addition, there is a membrane potential across the inner membrane, generated by the action of the enzymes of the electron transport chain (Tupper and Tedeschi, 1969). The IMM is compartmentalized into numerous cristae, which help to expand the surface area, enhancing its ability to produce ATP. The ratio of the area of the OMM and the IMM is variable and mitochondria in cells that have a greater demand for ATP, such as muscle cells, contain much more cristae than normal cells. These folds are embedded with small round bodies known as F_1 particles or oxysomes. These invaginations of the IMM can affect overall chemiosmotic function (Mannella, 2006). A recent study using mathematical modelling has suggested that the optical properties of the cristae in filamentous mitochondria may affect the generation and propagation of light within the tissue (Thar and Kuhl, 2004).

Matrix is the space enclosed by the IMM. It houses about two-thirds of the total protein in a mitochondrion. The matrix aids in the production of ATP with the help of the ATP synthase contained in the inner membrane. It contains a highly concentrated mixture of hundreds of enzymes, mitochondrial ribosomes, tRNA, apart from several copies of the mitochondrial DNA. The major functions of the enzymes include oxidation of pyruvate and fatty acids, and the citric acid cycle. As mentioned earlier, mitochondria are semi-autonomous organelles meaning that they have the ability to self replicate with the help of their exclusive mitochondrial DNA (mt DNA) (Gray, 1989). In addition, they also possess the necessary machinery to manufacture their own RNAs and proteins. Research on human mitochondrial DNA sequence revealed that it is 16,569 base pairs long, encoding 37 total genes: 22 tRNA, 2 rRNA, and 13 polypeptide genes (Anderson et al., 1981). The 13 mitochondrial polypeptides in humans are integrated into the inner mitochondrial membrane complexes about which the later sections describe in more detail.

1.1.3 Function

On the one hand, mitochondria produce metabolic energy in the form of ATP; on the other hand, they are involved in the process of apoptosis or programmed cell death, and harbour proteins that are potentially lethal to vertebrate cells. The following sections aim to give a comprehensive overview of these functions of the mitochondria.

1.1.4 Respiratory chain (or ETC), OXPHOS and the production of ROS

Most eukaryotic mitochondria produce ATP from products of the citric acid cycle, fatty acid oxidation, and amino acid oxidation. On the mitochondrial inner membrane, electrons from NADH and succinate go through the electron transport chain to oxygen, which is eventually reduced to water. The electron transport chain is made up of an enzymatic series of electron donors and acceptors. Each electron donor shuttles electrons to a more electronegative acceptor, which in turn donates these electrons to another acceptor, a process that continues down the series until electrons are passed to oxygen, the most electronegative and terminal electron acceptor in the chain (Tzagoloff, 1974). Shuttle of electrons between donor and acceptor releases energy, which is used to create a proton gradient across the mitochondrial membrane by actively "pumping" protons into the IMS, producing a thermodynamic state (Gibb's free energy) that has the potential to do work. The entire phenomenon is called oxidative phosphorylation, since ADP is phosphorylated to ATP using the energy of hydrogen oxidation in many steps.

A note worth mention is that a small percentage of electrons do not complete the whole sequence and instead directly leak to oxygen, resulting in the formation of the free-radical superoxide, a member of the highly reactive oxygen molecules (ROS) that contributes to oxidative stress and has been implicated in a number of diseases. Four membrane-bound complexes have been known in mitochondria (Tzagoloff, 1974).

Each is an extremely complex trans-membrane structure made up of several sub-units and embedded in the inner membrane. Three of them are proton pumps. The structures are electrically linked by lipid-soluble electron carriers and water-soluble electron carriers. In summary, the flow of electrons is as described here. Complex I (NADH coenzyme Q reductase) accepts electrons from the Krebs cycle electron carrier NADH, and passes them to coenzyme Q (ubiquinone), which also receives electrons from complex II (succinate dehydrogenase). UQ transports electrons to complex III (cytochrome bc_1 complex), which passes them to cytochrome *c* (cyt *c*). Cyt *c* then transfers electrons to Complex IV (cytochrome *c* oxidase; labeled IV), which utilizes the electrons and hydrogen ions to reduce molecular oxygen to water.

The efflux of protons from the mitochondrial matrix creates an electrochemical gradient (a.k.a proton gradient). This gradient is used by the F_0F_1 ATP synthase complex (sometimes referred to as Complex V of the ETC) to make ATP via oxidative phosphorylation.

1.1.5 Membrane potential and its significance

The oversimplified view that mitochondria are purely metabolic organelles was discarded with the finding that the disruption of the mitochondrial trans-membrane potential ($\Delta\psi m$) forms an early and irreversible step in the cascade of events that lead to apoptotic cell death (Zamzami et al., 1995).

The mitochondrial potential ($\Delta\psi_m$) provides the charge gradient required for mitochondrial Ca^{2+} sequestration, and regulates reactive oxygen species (ROS) production, and thus is also a central regulator of cell health (Ly et al., 2003). Under cellular stress, $\Delta\psi_m$ may be altered by dysregulated intracellular ionic charges [e.g., Ca^{2+} or K^+], subsequently changing the total force driving protons into the mitochondria and thus ATP production. When ionic fluxes exceed the ability of mitochondria to buffer these changes, ultimately $\Delta\psi_m$ along with its components may collapse, leading to a failure of ATP production and bioenergetic stress. The approximate physiological value of mitochondrial potential is $\Delta\psi_m$ = 150 mV (Perry et al., 2011).

1.1.6 In apoptosis/programmed cell death

The apoptotic pathway that involves the mitochondria is activated by many triggers, such as growth factor deprivation, glucocorticoids, cytotoxic agents and mitogenic oncogenes. These stimuli in some way lead to an increase in the permeability of the OMM and promote the release of cytochrome *c* into the cytosol (Alnemri, 1999).

One of the first cues that mitochondria participate in the regulation of apoptosis stemmed from the observation that in *Caenorhabditis elegans,* CED-9 (the worm orthologue of human B cell lymphoma 2 (BCL-2)), a constituent of the core apoptotic machinery, is tethered to the mitochondrial outer membrane. Although mitochondria were initially thought to operate as mere signalling scaffolds in this

framework, it soon became clear that they actively regulate programmed cell death in an extensive group of organisms, ranging from lower eukaryotes like yeast to humans. In fact, mitochondrial outer membrane permeabilization (MOMP) represents a near-universal event that marks an irreversible point followed by multiple signal transduction cascades, leading to cell death be it through apoptosis or regulated necrosis (Chipuk et al., 2006). Thus, it is unambiguous that mitochondria occupy a central position in the regulation and execution of cell death. Hence, understandably, defects that alter the ability of mitochondria to execute MOMP are associated with a variety of human pathologies, including infectious diseases, ischaemic conditions, neurodegenerative disorders and cancer (Galluzzi et al., 2012; Kroemer et al., 2007; Tait and Green, 2010). Moreover, it has recently been proved that mitochondria also release mitochondrial DNA (mtDNA), metabolic by-products such as reactive oxygen species (ROS) and specific nucleus-encoded proteins as danger signals to alert the cell of perturbations in mitochondrial homeostasis (Krysko et al., 2011). Apart from the aforesaid functions, they also contribute to the biosynthesis of pyrimidines, amino acids, phospholipids, nucleotides, folate coenzymes, heme, urea, and many other metabolites.

1.1.7 Dynamics

Mitochondria viewed in live cells reveal that their morphologies are far from static. Their shapes change constantly through the combined actions of fission, fusion, and motility. Recurrent cycles of fusion and fission result

in the intermixing of the mitochondrial population in the cell (Chan, 2012). Increased fusion or reduced fission causes the formation of elongated mitochondrial networks, while increased fission or reduced fusion leads to mitochondrial fragmentation. The key molecules in both fusion and fission are large GTP-hydrolysing enzymes of the dynamin superfamily. Mitochondrial fusion involves two sequential steps: first, the outer membranes (OMMs) of two mitochondria fuse followed by the fusing of their inner membranes (IMMs). OMM fusion is carried out by mitofusin 1 (MFN1) and mitofusion 2 (MFN2), which are dynamin-related GTPases located at the OMM. IMM fusion is mediated by the dynamin-related protein optic atrophy 1 (OPA1) (Refer Figure 1.1). While cells that lack both MFNs have no mitochondrial OMM fusion, cells lacking OPA1 exhibit OMM fusion events, but the fusion intermediates cannot progress to IMM fusion. The opposite process of mitochondrial fission involves the recruitment of dynamin-related protein 1 (DRP1) from the cytosol to the OMM. Assembly of DRP1 on the mitochondrial surface causes the formation of a ring structure at the point of constriction of the mitochondria leading to the eventual division of the organelle into two separate units (Chan, 2006; Mishra and Chan, 2014)

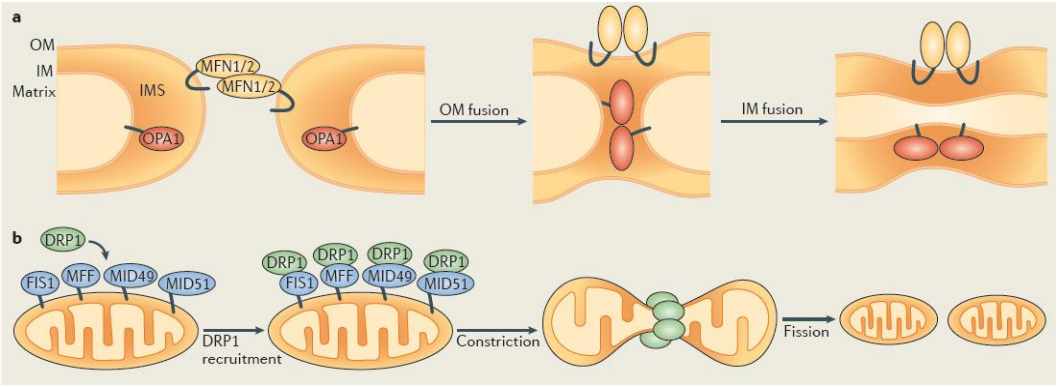

Figure 1-1: Fusion and Fission of mitochondrial membranes
a) Fusion of OMM is mediated by MFN1/2 whereas IMM fusion is mediated by OPA1.
b) Once recruited on to the OMM, Drp1 aids in the fission of mitochondria through the formation of a ring structure (Adapted from Mishra et al., 2014)

1.2 INTERFERON-RETINOIC ACID INDUCED CELL DEATH PATHWAY

1.2.1 Interferon signalling

Cytokines are small proteins that play an important role in cell signalling. They include chemokines, interferons, interleukins, lymphokines, tumour necrosis factors with the exception of hormones and growth factors. They are secreted by a broad range of cells, including immune cells like macrophages, B lymphocytes, T lymphocytes and mast cells, as well as endothelial cells, fibroblasts, and various stromal cells. Cytokines protect the host from infectious pathogens (Evan and Vousden, 2001).

The interferon (IFN) family of cytokines regulates antiviral, antitumor, and immunoregulatory activities (Sen, 2000). IFNs used two classes of transcription factors, Janus tyrosine kinases (JAK)-Signal Transducing Activator of Transcription (STAT) pathway (Levy and Darnell, 2002) and Interferon gene-Regulatory Factors (IRFs) (Fujita et

al., 1989) to stimulate the expression of a number of cellular genes, which bring about their diverse actions. IRFs primarily regulate the expression of IFN genes and some Interferon stimulated genes (ISGs) while the STATs mostly regulate ISGs. However, it was observed that these factors cross-regulate each other and form complexes with other factors to deliver specific biological responses, based on the elements present in the ISG promoter (Ozato et al., 2007). For example, the Interferon-Stimulated Response Element (ISRE) binds to a heteromeric transcription factor, ISGF3, consisting of IRF9, STAT1 and STAT2, for inducing transcription of certain ISGs (Stark et al., 1998). Similarly, the binding of activated STAT1 dimer to Gamma-Activated Sites (GAS) of some ISGs stimulates gene expression in response to IFN-γ (Shuai et al., 1992). Cytokine-induced responses driven by STATs are controlled by feedback mechanisms, which regulate gene expression.

Transcription factors as they are, STAT1 and IRFs, their inhibitory effects on growth are eventually dependent on the downstream gene products induced by them. Among these products, two antiviral enzymes, protein kinase R (PKR) and Ribonuclease L (RNaseL) have been found to be important in stress-induced and spontaneous apoptosis (Balachandran et al., 1998; Zhou et al., 1997). Nevertheless, growth suppressive actions of IFNs independent of PKR and RNaseL have also been described (Kalvakolanu, 2000; Levy-Strumpf and Kimchi, 1998). The other proteins that are regulated by IFNs are pRB, which is a growth suppressor and is activated (Resnitzky et al., 1992); c-myc, E2F and cyclin D3 which are pro-

proliferation genes down regulated in certain lymphoblastoid tumor cell lines (Tiefenbrun et al., 1996).

1.2.2 Interferons and cell cycle regulation

As mentioned above, IFNs inhibit cell growth by inducing either growth arrest or apoptosis. Although growth arrest in some cases leads to the activation of apoptosis, these events are clearly regulated by different gene products. Of note is the fact that cell death can occur independently of growth arrest. IFNs target specific proteins involved in growth arrest and cell death responses. Whether one or both of these processes are activated in cells is dependent on the cell type (Hertzog and Williams, 2013). IFNs either alter the activities of proteins that control the cell cycle or IFN-induced proteins interact with the cell cycle machinery for inducing growth arrest. For instance, IFN-γ activates the expression of p21/WAF/Cip-1, a cyclin dependent kinase inhibitor, to cause growth arrest in some cell types (Chin et al., 1996). It is important to note that induction of p21/WAF/Cip-1 by IFN-γ does not involve p53 (el-Deiry, 1998), a typical inducer of this inhibitor. STAT1 directly induces the p21/WAF/Cip-1 gene. IFNs also inhibit cell growth by downregulating c-*myc* expression (Raveh et al., 1996), inactivating the transcription factor E2F (Melamed et al., 1993) and inducing/dephosphorylating the retinoblastoma tumor suppressor (pRb) in lymphoid tumor cells (Resnitzky et al., 1992). In the context of apoptosis, some studies suggest that caspases are activated by IFNs. Not surprisingly, IFN-γ induced apoptosis requires JAK1 and STAT1, and an induced expression of

caspase-1 (Chin et al., 1996). It was found that STAT binding sites are present in the promoter of caspase 1. However, the role of caspase-1 in apoptosis is less known, since mice lacking this gene exhibit normal apoptotic response (Kuida et al., 1995). Interestingly, TNF-α induced apoptosis is also found to be defective in STAT1 null cells.

1.2.3 IFN and cancer

An important role for IFNs in controlling carcinogenic cell growth was highlighted by observations such as an increased occurrence of carcinogen-induced tumors in the IFN-γ receptor-/- and STAT1-/- mice, and an inability of the immune system to reject the STAT1-null tumors (Kaplan et al., 1998). Some IFN-regulated factors such as IRF-1 and IFN-consensus sequence binding protein (ICSBP) behave as tumor growth suppressors. Mutations in these genes have been reported in the development of myeloid leukemias with the deletion of IRF8 gene causing a CML-like disease in mice (Holtschke et al., 1996; Willman et al., 1993). Also, loss of IRF8/ICSBP expression of occurs in CML patients (Schmidt et al., 1998); whereas re-expression of IRF8 suppressed BCR-ABL oncogene-induced CML-like disease in mouse models (Hao and Ren, 2000).

Though the effectiveness of IFNs has been proven in the therapy of certain leukaemias, they yield poor results in the case of solid tumors (Gutterman, 1994). In an effort to overcome this drawback, a number of combination therapies have been studied for their enhancement of effectiveness. Among these, the combination of IFNs with retinoids was found to be most potent against several tumors (Moore et al., 1994).

1.2.4 Retinoids signalling

Retinoids are produced from dietary vitamin A, in particular from eggs, milk, butter and fish-liver oils, and the pro-vitamin β-carotene of plant source. Once taken up by the intestinal mucosa cells, retinol is esterified to retinyl esters subsequently passing into the lymphatic system and transported by the blood in chylomycrons, from where they are taken up by the liver and stored. After it is mobilized, retinol is oxidized to retinal and retinoic acid (RA) by cleavage of retinyl esters (Altucci and Gronemeyer, 2001). Gene-ablation experiments (Niederreither et al., 1999) show that the production of retinoic acid by the retinaldehyde dehydrogenase-2 enzyme is required for mouse embryo survival and early morphogenesis. A very small proportion of plasma and tissue retinol (0.2–5%) is converted to all *trans* RA (ATRA), the main activator of RA receptors that can drive all functions of vitamin A except vision (Love and Gudas, 1994). RA is a crucial regulator of embryogenesis, and its production needs to be carefully controlled for proper organogenesis. Very little vitamin A leads to severe malformation whereas high concentrations of retinoids are teratogenic, strengthening the idea that RA may play the role of a morphogen during early embryogenesis (Altucci and Gronemeyer, 2001).

Retinoids employ two structurally similar, but genetically distinct, classes of nuclear transcription factors, viz., Retinoic Acid Receptors (RARs) and Retinoid X Receptors (RXRs) to drive the expression of genes that contain the Retinoic Acid Response Elements (RARE) (Mangelsdorf

and Evans, 1995; Nagpal et al., 1992). Targeted gene disruption experiments have shown that nearly all the congenital malformations that are caused by vitamin A deficiency are due to the absence of RAR or RXR functions (Kastner et al., 1995). The RAR: RXR heterodimers bind to RARE constitutively, whose transcriptional activity is held in check by several co-repressor molecules. Binding of RA to the RAR induces a conformational change that allows the recruitment of nuclear receptor co-activators, which promote transcription. A number of isotypes and subtypes of RARs and RXRs (α, β and γ) participate in retinoid-induced transcription in a gene- and cell specific manner. Most RAR and RXR genes are constitutively expressed except for the RARβ gene whose expression is up-regulated by RA treatment (Chambon, 1996)

1.2.5 RA and cancer

Deprivation of dietary vitamin A results in an increase in incidence of cancers in experimental animals such as leukemias and an abnormal rise in myelopoiesis owing to a loss of spontaneous apoptosis which was reversed by RA treatment (Bjelke, 1975; Kuwata et al., 2000). Mutations in the RAR and RXR genes occur rarely. A perplexing number of RAR and RXR isoforms present in mammalian cells mediate the processes of growth inhibition of retinoids. The expression of RARβ gene is inhibited in some cancers and its re-expression restores growth arrest in response to RA (Liu et al., 1996). Transgenic mice expressing anti-sense RARβ gene develop lung cancers, although the exact mechanisms is unclear (Berard et al., 1996). One of the well-defined mutations that involve RARs is a

reciprocal translocation that occurs between the RARα (human chromosome 17) and the promyelocytic leukemia (human chromosome 15) in some forms of acute promyelocytic leukemia (APL) (de The et al., 1991). Despite this translocation the resultant fusion protein, PML-RARα, responds to RA treatment and leukemic cell growth are successfully controlled in APL patients (Chomienne et al., 1990).

Based on this observation, an oncogenic role for the chimeric PML–RARα product has been suggested. The PML protein forms a nuclear body consisting of several IFN-inducible genes, ubiquitin ligases and other proteins with indeterminate functions. It is known to collaborate with p53 tumor suppressor and is also implicated in DNA repair, regulation of apoptosis, antigen presentation and viral replication. The PML gene is induced by IFNs via a STAT1 dependent pathway and implicated in the antiviral actions of IFNs (Kalvakolanu, 2004).

1.2.6 Growth suppressive effects of retinoids

Retinoids inhibit pro growth transcription factor E2F to suppress growth in some cell types (Lee et al., 1998). The other known effects of retinoids include their inhibition of the transcription factor AP1 (Fanjul et al., 1994). It is likely that retinoids inhibit tumor growth by blunting the expression of AP1dependent pro-growth genes. The growth suppressive effects of synthetic retinoids are mediated by a RAR-RXR dependent and independent manner (Liu et al., 1996). One of the retinoids, 4-HPR, showed an excellent *in-vitro* activity against tumor cell lines and in animal models with one of its actions involving mitochondria related cell death

pathways, activately translocating the orphan nuclear receptor TR3 from nucleus to mitochondria, and the consequent release of cytochrome c to induce apoptosis (Li et al., 2000). In one of the scenarios, interestingly, induction of caspase-dependent cleavage of the ubiquitous transcription factor Sp1 by certain synthetic retinoids occurs independent of transcription to activate apoptosis (Piedrafita and Pfahl, 1997). On a similar note, a number of reports of synthetic retinoids inducing cell death by a p53-dependent or caspase-dependent manner has been recorded (Sun et al., 1999).

Although primarily developed for cancer therapy, the receptor selective retinoids may also be valuable in the treatment of other human diseases such as type II diabetes, psoriasis and acne (Thacher et al., 2000). Clinically, retinoids are useful in the treatment of APL, and primary cancers of the skin, and head and neck. Although less efficacious against advanced cancers, retinoids can reverse pre-malignant lesions and the development of second primary tumors in head and neck cancers and *Xeroderma pigmentosum* (Hansen et al., 2000).

1.2.7 Cross talk between IFNs and RA

Although IFN and RA use different signalling pathways, a cross talk between their growth suppressive pathways exists. PML-RARα, a mutant chimeric retinoic acid receptor found in certain acute promyelocytic leukemias responds to RA (Wang et al., 1998). Interestingly, this mutant receptor is induced by IFNs and has been reported to participate in the anti-cellular action of IFN-α (Chelbi-Alix et al., 1998; Nason-Burchenal et

al., 1996). As mentioned earlier, PML forms a nuclear body consisting of several IFN-inducible gene products (Gaboli et al., 1998; Gongora et al., 1997). PML is induced by IFNs and its promoter contains STAT1 binding sites (Pelicano et al., 1997). In certain IFN-resistant cells, RA induces STAT1 levels resulting in an enhancement of IFN-responses and a mutant STAT1 inhibits RA-induced differentiation in embryonic stem cells (Gianni et al., 1997; Kolla et al., 1997; Matikainen et al., 1997). RA has also been shown to induce some ISGs directly (Pelicano et al., 1997). RA is known to induce the expression of the RIG-G gene (Yu et al., 1997), a member of the ISG54 family. However, it is not yet known whether RIG-G, like p56, also regulates mRNA translation. A more compelling connection between IFN and retinoid-like receptors comes from a recent study that reports that in the liver and macrophages, liver X receptor (LXR), a structural homologue of retinoid receptors (RXR), regulates expression of the genes involved in cholesterol metabolism. LXRs also appear to be markers for atherogenesis. In response to microbial pathogens, the cellular toll-like receptors (TLR), which bind to bacterial and viral products, such as LPS, flagellae, and dsRNA, stimulate expression of the IFN-β gene (Toshchakov et al., 2002). Though these receptors are known to activate multiple pathways and their corresponding transcription factors, IRF3 is the most significant transcriptional regulator for IFN-β gene induction. Among the ten known TLRs, TLR3 and TLR4 stall cholesterol metabolism in a ligand dependent manner. In particular, IRF3 inhibits transcriptional activity of LXRs by combining the promoter complexes in vivo, in the presence of inducers of TLR.

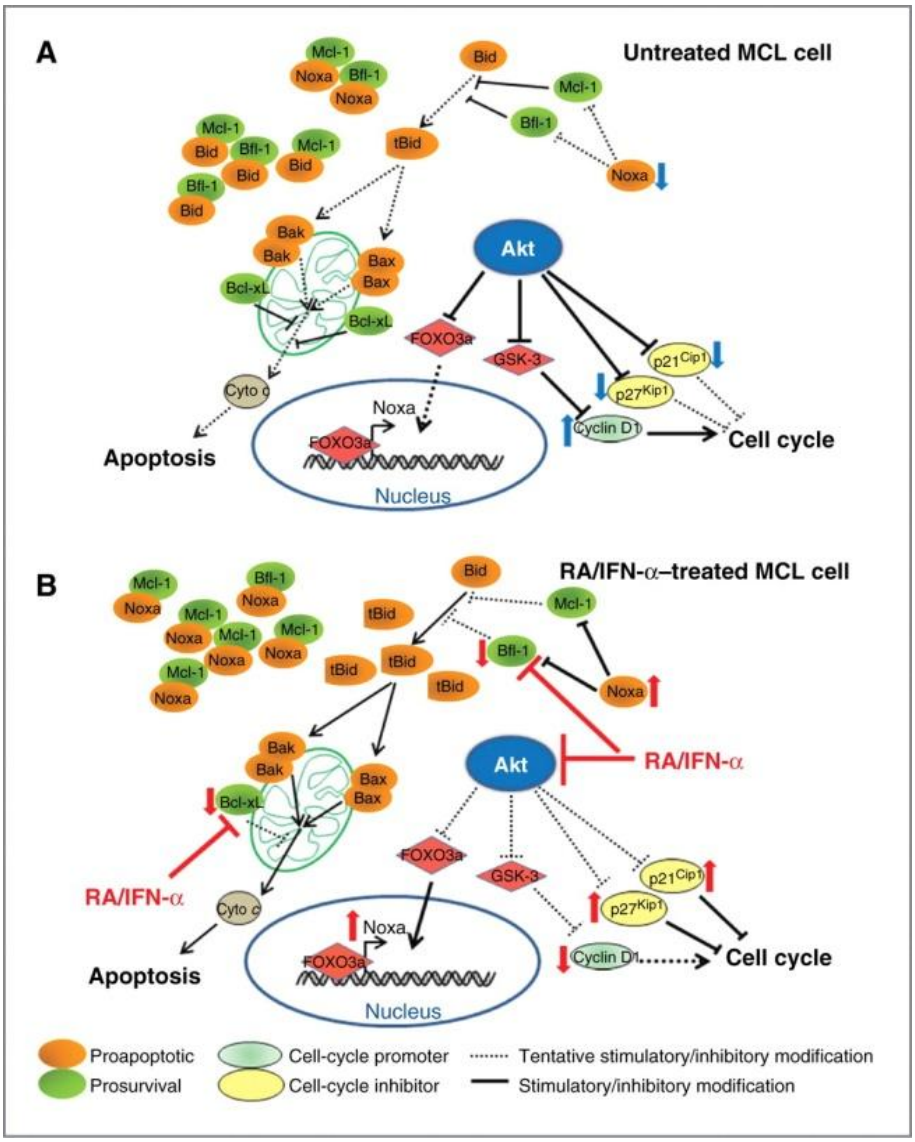

Figure 1-2: Antiproliferative and proapoptotic effects induced by IFN/RA

A) In untreated cells, the Akt pathway is functional and results in cell proliferation.

B) When the cells are treated with the combination of IFN/RA, it blocks Akt, Bcl-xL and Bfl-1 resulting in the release of cytochrome c from mitohcondria as well as upregulation of p21 and p27 eventually resulting in cell cycle prevention and cell death (Adapted from (Dal Col et al., 2012)).

There have been reports of a possible overlapping mechanism, shifting gears back to the clinical studies of the IFN/RA combination for cancer treatment, as mentioned briefly earlier. Experimental studies have shown that the IFN/RA combination is a more potent inhibitor of cell growth than either drug alone (Lindner et al., 1997; Moore et al., 1994). In locally advanced squamous cell carcinomas of the skin and cervix and small cell lung carcinomas the combination of 13-*cis* RA and IFN-α2a showed significantly higher overall clinical response, compared to single agents (Ruotsalainen et al., 2000). IFN/RA has only modest effects on metastatic cancers (Stadler et al., 1998). However, these cancers are also resistant to other modes of therapy. Lack of response in these studies could be owing to the doses used, the stage of the disease, and a low pharmacologic availability of IFN/RA in the tumor microenvironment. In summation, although persuasive anti-tumor effects of IFN/RA *in vitro* and *in vivo* are known, the molecular bases for such synergistic action are not clearly understood. Since the IFN and RA induced toxicities are non-overlapping, it makes them a good combination for clinical use. Figure 1.2 gives a more comprehensive view of the possible eventual downstream mechanism and effect of IFN/RA combination in cell death.

1.3 GRIM-19

1.3.1 Identification

The above mentioned characteristics and molecular signalling pathways employed by IFNs and RA led Angell et al., resort to devising a strategy to isolate genes that may be exclusive in the apoptotic pathway executed by the combination of IFN and RA treatment. (Angell et al., 2000). In this study, they employed an anti-sense technical knock-out screen which allows the isolation of cell death-associated genes based on their selective inactivation by over-expression of antisense cDNAs. Because the antisense mRNA silences gene expression of death-specific genes, transfected cells would survive in the presence death inducers, *i.e*. the combination of IFN and RA. Several Genes associated with Retinoid-IFN induced Mortality (GRIM) was identified using this approach. One such protein is GRIM-19. Its 552-base pair cDNA encodes a 16- kDa protein. Antisense expression of GRIM-19 conferred a strong resistance against IFN/RA-induced death by the reduction of the intracellular levels of GRIM-19 protein. However, in this study, they reported that GRIM-19 is primarily a nuclear protein. Whereas, our experiments indicate very clearly that GRIM-19 is present only in the mitochondrial inner membrane (see results section; Figure 3.1 and 3.2). Similar studies' outcomes and our results are discussed in the following sections.

1.3.2 Chromosomal location

Using Fluorescence In-Situ Hybridization, the chromosomal localization of GRIM-19 was mapped to be at p13.1–p13.2 (Chidambaram et al., 2000). Apparently, this locus has been shown to host a number of tumour suppressive genes such as *ICAM-1, Notch 3*, and *Stau* that can suppress prostate tumour cell growth (Gao et al., 1999). It is good to recollect from the earlier headings that IFNs regulate some tumour suppressors. In addition, the IFN regulatory factor-1 (IRF-1) and IFN consensus sequence binding protein (ICSBP) have tumour suppressor functions (Holtschke et al., 1996). The finding that GRIM-19 is an IFN/RA regulated protein and its chromosomal localization led the authors to propose that GRIM-19 might be a novel tumour suppressor.

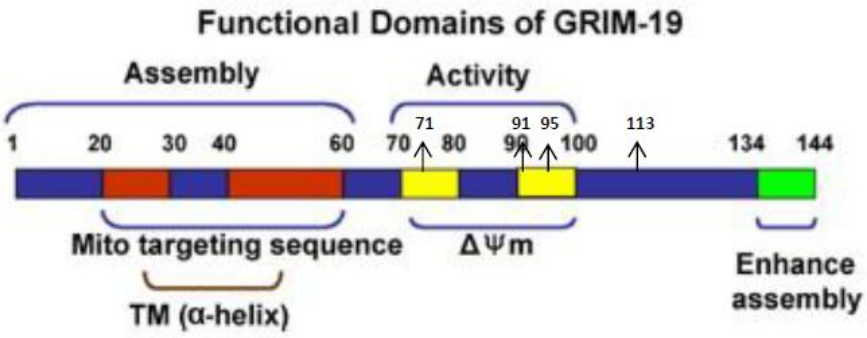

Figure 1-3: Domain architecture of GRIM-19

Predicted functional domains of GRIM-19. Arrow marks represent positions of GRIM-19 mutations chosen for this study (Adapted from Lu et al., 2008).

1.3.3 Domain architecture of GRIM-19

According to a study conducted by Lu and others using truncation mutants of GRIM-19, (Lu and Cao, 2008) they predict as shown in Figure 1.3, the plausible domain organization of the protein. As do most

mitochondrial proteins, GRIM-19 also hosts a mitochondria-targeting sequence on its N-terminal which helps to recruit the protein to the mitochondria. Based on the results of this study, the authors classify the region encompassed between amino acids (a.a) 20-30 and 40-60 as regions playing a vital role in the formation of the trans-membrane alpha helix of the protein; 70-80 and a.a 90-100 as important for the maintenance of mitochondrial potential; and regions spanning a.a 134-144 could be essential for the assembly of Complex I of the mitochondria. Also represented in the figure is the residues that are mutated in the three GRIM-19 mutants characterized in this study. These mutants were identified from human tumour samples by Nallar et al., which conferred the inhibitory nature to GRIM-19 to oppose STAT3-induced cellular transformation (Nallar et al., 2013). These mutations are L71P, L91P, A95T. The last mutation, T113A is a modification of a potential phosphorylation site identified through a proteomic screening study ((Palmisano et al., 2007).

1.3.4 Studies on Interaction with other proteins

After the identification of GRIM-19, there have been a number of studies which report the interaction of GRIM-19 with other proteins. Here, we will look into each of them to provide a comprehensive overview of the nature of our protein of interest.

1.3.4.1 HtrA2

A yeast two hybrid (Y2H) screen showed that GRIM-19 interacts with the serine protease HtrA2 (Ma et al., 2007). The group further went on to characterize this interaction in mammalian cells and the effect of IFN/RA on this interaction. HtrA2 belongs to a family of mammalian serine proteases which localize to the mitochondria (Suzuki et al., 2001). In mammalian cells, inhibitors of apoptosis proteins (IAPs) block caspase activation. One such protein, the XIAP, inhibits caspase-9. HtrA2 degrades XIAP to alleviate the inhibition of caspases (Hegde et al., 2002; Martins et al., 2002; van Loo et al., 2002). In this study, they show that the interaction is weaker at steady state and that IFN/RA enhances the interaction of HtrA2 and GRIM-19 for augmenting cell death.

The physiologic relevance of GRIM-19 and HtrA2 to IFN/RA-induced cell death has been shown using multiple approaches. Down regulation of either protein is sufficient for preventing cell death and a signal-induced degradation of XIAP. Similarly, a catalytically inactive HtrA2 mutant fails to augment cell death and the inactivation of XIAP. In addition, the results prove that recombinant GRIM-19 can promote the protease activity of HtrA2 *in vitro*. Thus it is shown that GRIM-19 and HtrA2 are mutually dependent on each other for executing cell death. The PDZ domain of HtrA2 is critical for regulating its activity. The isolation of the c-terminal 133 a.a of HtrA2 as a binding partner for GRIM-19 suggests that GRIM-19 associates with the PDZ to promote HtrA2 activity. Interestingly, they also show the relevance of these interactions to an

oncogenic process using the vIRF1 protein of HHV8. Earlier, studies have shown that vIRF1 transforms oncogenically NIH3T3 cells and represses IFN gene expression. Studies have shown that vIRF1 binds to GRIM-19 and inhibits apoptosis (Seo et al., 2002). Ma et al., have shown that vIRF1 disrupts the HtrA2 and GRIM-19 interactions, thereby ablating the IFN/RA induced anti-XIAP activity. vIRF1 is not a resident of mitochondria. However, it seems to leak into cytoplasm during IFN/RA treatment, for preventing XIAP degradation. Thus, the vIRF1 protein appears to have evolved for ablating specific cellular innate defence mechanisms that prevent virus replication and cellular transformation. Finally, they also report that vIRF1 disrupts these interactions to override GRIM-19-induced apoptosis.

1.3.4.2 P16ink4a

Previously, a proteomic analysis revealed that GRIM-19 also interacts with the cell cycle inhibitor CDKN2A (p16Ink4a) (Sun et al., 2010). P16 is a tumor suppressor, and mutations in its gene sequence or epigenetic repression of its expression have been described in a number of tumors. The activity of CDK can be blocked by CDK inhibitors, which fall within the two protein families Kip/Cip and Inhibitor of CDK kinase (INK). The INK4 family is made up of four proteins p15, p16, p18 and p19, which have been shown to interact with CDK4/6 in order to suppress cyclin-dependent phosphorylation of the retinoblastoma (RB) protein (Ruas and Peters, 1998). RB is a very well studied tumor suppressor and is known to inhibit the expression of proliferation-associated genes by

binding to the transcription factor E2F1 (Dyson, 1998). Sun et al., using MCF-7 cells, which lack endogenous p16, show that exogenous p16 expression led to significant repression of genes required in S-phase. This seems to occur because p16 prevents cyclin D1 association with CDK4 and subsequent expression of E2F1-responsive genes. Indeed, in the presence of GRIM-19, the association of p16 with CDK4 was high and caused a decrease in cyclin D1-bound CDK4. This effect was reversed by GRIM-19 depletion. Importantly, GRIM-19 and p16 co-expression synergistically suppressed E2F1-dependent gene expression resulting in cell cycle arrest. The physiological relevance of this interaction is further supported by in vivo experiments in which p16 and GRIM-19 co-expression caused a dramatic reduction in tumor size. However, since expression of GRIM-19 alone suppressed E2F1-driven transcription, it is possible that GRIM-19 is a novel E2F1 inhibitor. Even so, the mechanism underlying this inhibition has not been defined. In this study, the authors showed that deletion of the fourth ankyrin-like repeat or introduction of clinically observed mutations, abolished p16 interaction with GRIM-19 along with its ability to synergistically repress E2F1-driven transcription and tumour growth. This was the first report to identify a function for GRIM-19 in cell cycle control and to propose a functional interaction between two unrelated tumour suppressors.

1.3.4.3 GW112

A protein previously found to be over expressed in tumors of the digestive system, GW112 – has been shown to interact with GRIM-19

reducing its ability to mediate apoptotic cell death (Zhang et al., 2004). It was shown that GW112/OLFM4 is expressed at relatively low levels in normal tissues, including prostate, colon, breast and pancreas. However, its expression was dramatically higher in pancreatic, stomach and colon cancer tissues. Gene reporter experiments revealed that GW112/OLFM4 localized mainly in the cytoplasm but some foci could be observed in the nucleus as well. Interestingly, most of the cytoplasmic GW112 co-localized with a mitochondrial marker. Since GW112 was found to interact with GRIM19 in yeast two-hybrid assay, the authors then explored its role in inducing apoptotic cell death. Indeed, overexpression of GW112 was sufficient to reduce hydrogen peroxide and IFN-β/RA-induced apoptosis and apoptotic gene expression. The authors also demonstrated that overexpression of GW112 was capable of promoting tumor growth *in vivo*, as assessed by injecting mice with slow growing TRAMP-C1 prostate cancer cells expressing GW112. These results were further substantiated by another study that compared GW112 mRNA expression levels in colon, breast and lung cancer tissues with those of matched non-cancerous tissue (Koshida et al., 2007). A sample comparison revealed that the mRNA levels of GW112 were increased in 90%, 68.8% and 84.6% of the cases analyzed for colon, breast and lung cancer tissues, respectively. For colon and breast cancer tissues, high GW112 mRNA expression levels were present even in the early stages of disease. In the case of lung cancer, it was shown that GW112 levels were significantly higher in squamous cell carcinomas than in adenocarcinomas. In vitro experiments by the group show that in SBC-1

lung cancer cells, GW112 knock-down by siRNA dramatically decreased their growth capacity. A recent study explored more carefully the link between GRIM-19 and GW112/OLFM4, and their influence on tumor cell invasion and metastasis (Huang et al., 2010). In human gastric cancer SGC-7901 cells, upregulation of GRIM-19 suppressed the expression of GW112/OLFM4 resulting in decreasing the binding activity of nuclear factor-κB (NF-κB). NF-κB was previously shown to bind to the GW112/OLFM4 promoter and to regulate its expression. In the study by Huang et al., *in vitro* assays revealed that when GRIM-19 was upregulated, the ability of cells to adhere to Matrigel was significantly decreased. Metastatic assays in nude mice demonstrate that SGC-7901 cells over expressing GRIM-19 gave rise to fewer visible liver metastases. As cell invasion and metastasis are dependent on the cells' capacity to degrade extracellular matrix, the authors investigated the effect of GRIM-19 in the expression of matrix metalloproteinase (MMP)-2, MMP-9, urokinase-type plasminogen activator (u-PA) and vascular endothelial growth factor (VEGF), which are known to mediate this process. The authors observed that when GRIM-19 was upregulated, the cells secreted less MMP-2, MMP-9, u-PA and VEGF, leading them to propose that the inhibitory effect of GRIM-19 in gastric cancer metastasis is, at least in part, achieved through down regulation of these proteins.

1.3.4.4 Disruption of E6/E6AP complex

Previous studies had shown a down-regulation of GRIM-19 in primary human cervical cancers with restoration of GRIM-19 inducing

tumor regression (Zhou et al., 2009). The induction of tumor suppressor protein p53 ubiquitination and degradation by E6 oncoportein of high risk-human pappiloma virus (HPV) through forming a stable complex with E6AP is considered as a critical mechanism for cervical tumor development. Another recent study by the same group (Zhou et al., 2011) investigated the potential role of GRIM-19 in rescuing p53 protein and inducing cervical cancer cell apoptosis. The protein levels of GRIM-19 and p53 in normal cervical tissues and cervical cancer tissues from patients with non-metastatic squamous epithelial carcinomas were analyzed. Co-immunoprecipitation and GST pull-down assays were performed to examine the interaction of GRIM-19 with 18E6 and E6AP *in vivo* and *in vitro* respectively. To examine the disruption of E6/E6AP complex by GRIM-19, the competition of 18E6 with E6AP in binding GRIM-19 was observed by performing competition pull-down assays. As a result, the levels of GRIM-19 and p53 were concurrently down regulated in cervical cancers. The restoration of GRIM-19 was able to induce ubiquitination and degradation of E6AP, and disrupt the E6/E6AP complex through the interaction of N terminus of GRIM-19 with both E6 and E6AP, which protected p53 from degradation and promoted cell apoptosis. Tumor xenograft studies also revealed the suppression of p53 degradation in presence of GRIM-19. Through these data, authors suggested that GRIM-19 can block E6/E6AP complex, and synergistically suppressed cervical tumor growth with p53.

1.3.4.5 NOD2

Nucleotide oligomerization domain 2 (NOD2) functions as a mammalian cytosolic pathogen recognition molecule, and variants have been associated with risk for Crohn disease. NOD2 functions as an anti-bacterial factor limiting survival of intracellular invasive bacteria, to gain further insight into the mechanism of NOD2 activation and signal transduction. Barnich et al. performed yeast two-hybrid screening and demonstrated that GRIM-19 interacts with endogenous NOD2 in HT29 cells. GRIM-19 is required for NFκB activation following NOD2-mediated recognition of bacterial muramyl dipeptide. GRIM-19 is also shown to control pathogen invasion of intestinal epithelial cells. GRIM-19 expression was decreased in inflamed mucosa of patients with inflammatory bowel diseases. The authors propose that GRIM-19 may be a key component in NOD2-mediated innate mucosal responses and serve to regulate intestinal epithelial cell responses to microbes (Barnich et al., 2005).

1.3.4.6 STAT3

One of the most promising and highly reported interactions of GRIM-19 has been with STAT3. GRIM-19 directly interacts with STAT3, inhibiting its gene stimulatory function (Lufei et al., 2003; Zhang et al., 2003). STAT3 is constitutively active in a number of human cancers either by autocrine growth factors or activated oncogenes (Buettner et al.,

2002). Activated STAT3 induces the expression of a number of cellular proto-oncogenes, including c-myc, c-fos and c-met (Yang et al., 2005) cell cycle-regulating proteins, such as cyclin D1, cyclin B1 and CDK1/cdc2 (Bromberg et al., 1999) and anti-apoptotic proteins, suchas B-cell lymphoma protein 2 (Bcl-2),myeloid cell leukemia sequence 1 (mcl-1) and Bcl-XL (Buettner et al., 2002). All of these are known to promote tumor growth. Zhang and others in their study showed that STAT3 bound to GRIM-19 in unstimulated cells and that the amount of STAT3 coimmunoprecipitated with GRIM-19 increased after IFN-β/RA treatment. Remarkably, this interaction is restricted to STAT3, as experiments performed failed to detect any interaction between GRIM-19 and STAT1, STAT2 or STAT5, despite their abundant expression in the cells used. The authors further demonstrated that GRIM-19 inhibited STAT3-induced gene expression, but not its activation or ability to bind to DNA. By mutation analysis, the authors were able to map the transactivation domain (TAD) as the region on STAT3 targeted by GRIM-19, and that the phosphorylation of a serine residue at position 727 (S727), within the TAD, was essential for binding. Considering the known role of activated STAT3 in tumor growth, it is tempting to predict that GRIM19 inhibition of STAT3 is anti-oncogenic. Another study, by Lufei et al., also found that GRIM-19 bound to STAT3 inhibiting it. However, the authors proposed that such an inhibition of STAT3 occured by impeding its translocation to the nucleus. It remains to be clarified exactly how GRIM-19 inhibits STAT3 function.

Later, two studies explored in more detail the tumor suppressive role of GRIM-19 through interaction with STAT3 (Kalakonda et al., 2007a; Kalakonda et al., 2007b). In one of these studies, the authors examined GRIM-19 function in the presence of constitutively active STAT3. Chronic tyrosyl phosphorylation of STAT3, rendering the protein constitutively active, was sufficient to induce oncogenic transformation and has been described in a number of human tumors and tumor cell lines (Bromberg et al., 1999; Buettner et al., 2002). The authors showed that GRIM-19 counteracted constitutive STAT3-induced cellular transformation and suppressed the expression of genes involved in cell proliferation. In another study, it was shown that GRIM-19 was able to suppress src-induced cellular transformation. The src family of tyrosine kinases is known to control several cellular activities, including motility and invasion (Martin, 2001). The current study unveiled that in the presence of GRIM-19, the number of src-transformed soft-agar colonies significantly decreased and these were much smaller as well GRIM-19 was also able to inhibit src-induced cell motility and growth in vitro, and tumor formation *in vivo*. The authors demonstrated that GRIM-19 inhibition of src-induced cellular transformation was mediated by downregulation of a number of STAT3-dependent genes. However, not all of the GRIM-19 effects observed were dependent on STAT3, as GRIM-19 inhibition of src-induced phosphorylation of cellular proteins still occurred even when STAT3 was knocked-down. Actually, the study demonstrated that GRIM-19 dramatically suppressed src-induced tyrosyl phosphorylation of cortactin, an F-actin-bundling protein that localizes to

podosomes and lamellipodia, which may explain the suppressive role of GRIM-19 on src-induced cell motility (Sun et al., 2009). These studies highlight that GRIM-19 functions as a tumor suppressor seems to occur at multiple levels and that the mechanisms underlying these are still far from clear.

Interestingly, it was also reported that STAT3 regulates a metabolic function in the mitochondria as a modulator of mitochondrial respiration (Wegrzyn et al., 2009). It was observed that STAT3 was present in the mitochondria of cultured cells and primary tissues, although in a smaller amount than in the cytosol. Importantly, mitochondrial STAT3 was shown to regulate complexes I and II, as the activities of these were significantly decreased in STAT3 knock-out cells. These roles were dependent on STAT3 targeting to mitochondria and phosphorylation of S727, but had no relationship with its classical function in the nucleus (Wegrzyn et al., 2009). Another study showed that this mitochondrial STAT3 is also essential for Ras-induced cellular transformation (Gough et al., 2009). Expression of oncogenic Ras (H-RasV12) conferred to cells the ability to grow into colonies in soft agar, which was impaired without STAT3. Noticeably, STAT3 function was dependent on S727 but not on phosphorylation of a tyrosine residue at position 705 (T705) or DNA-binding domains. These results were also verified for the other members of the Ras family, N and K-Ras. Mitochondrial STAT3 was also essential for tumor growth *in vivo* and seemed to be involved in the metabolic shift characteristic of cancer cells.

Having known of the results of these studies on GRIM-19 and that of STAT3's role in mitochondria, it is indeed tempting to characterize the dependency of mito-STAT3's function on GRIM-19. The forthcoming paragraphs also throw some light on GRIM-19 recruiting STAT3 to the mitochondria. Bearing these in mind, plausible mechanisms and knowledge gaps are covered in the discussion section.

Recently, another study brought new insights into how GRIM-19 restrains cell growth via STAT3 inhibition (Nallar et al., 2010). It was found that a motif in the N terminus of GRIM-19 protein was essential for its function as a tumor suppressor. This motif is formed by the four amino acids glutamic acid, aspartate, methionine and proline (QDMP) and exhibits structural similarities with some viral RNA proteins. Point mutations in the DMP residues strongly impaired the ability of GRIM-19 to suppress colony formation in soft-agar in comparison to the wildtype protein. Mutation in the Q residue also caused loss of the ability to suppress anchorage-independent growth, but the results were not as dramatic as those obtained with the other mutants. In addition, it was previously reported that GRIM-19 inhibits cell motility (Kalakonda et al., 2007a), a very prominent feature of cancer cells that is required for metastasis. On a similar line, in the current study, authors reported that mutants lost the ability to suppress cell motility as assessed by wound-healing assays. It was also demonstrated that, unlike the wild-type protein, these mutants were incapable of restraining cell growth. These results clearly reveal that the tumor suppressive function of GRIM-19

occurs in different cellular processes. However, the authors claimed that the results obtained with the mutants cannot be explained by altered localization of these within the cells, since immunofluorescence and cell fractionation experiments revealed that they were present in the nucleus, mitochondria and cytoplasm just like the wild-type protein. This last finding is highly disputable since a) the mutations were most likely done in the N-terminal region that hosts the mitochondrial targeting sequence and b) they report that the wild-type protein was found in the nucleus and cytoplasm apart from the mitochondria which may not reflect the right localization in itself. Our own results and others stand evidence for this.

Similarly, a tumor-derived mutation in the N terminus, which was previously described by a different group (Maximo et al., 2005) that results in a lysine to asparagine substitution at residue 5 (K5N), also led to the failure of GRIM-19 to inhibit colony formation in soft-agar and limit cell growth (Nallar et al., 2010). The *in vitro* data was further supported by *in vivo* experiments in which it was shown that mutant-expressing tumors grew significantly faster than those expressing the empty vector or wild-type GRIM-19. To explore in more detail the mechanisms on the basis of the observations for the mutant proteins, the authors analyzed their ability to suppress STAT3-dependent gene expression. As expected, while the wild-type protein clearly inhibited the expression of STAT3-responsive genes, this anti-STAT3 activity was dramatically reduced in some of the mutants. This anti-STAT3 activity was determined not only

through real-time PCR and reporter gene assays but also by expressing a constitutively active STAT3 in cells and then evaluating the effect of the mutants in STAT3-induced gene expression. The authors performed an additional experiment where the effect of the selected mutants was assessed on cellular transformation induced by src, which is a known STAT3 activator. As anticipated, the mutant lacking the N terminus completely lost the anti-transforming activity observed with wild-type GRIM-19. Immunoprecipitation experiments demonstrated that this loss was due to their inability to interact with STAT3.

1.4 GRIM-19 AND CANCER

1.4.1 Physiological significance of the interaction between STAT3 and GRIM-19: Clinical aspects

Apart from these studies discussed above, there are numerous other studies which report the significance of the interaction of GRIM-19 and STAT3 in several carcinomas. For instance, Zhou et.al, observed through immunohistochemical (in 108 breast samples) and western blotting analysis (in 20 breast cancer tissues) that GRIM-19 expression was severely impaired in breast carcinoma and that there was a corresponding increase in the expression of STAT3. The reduction in expression of GRIM-19 was associated with lymph node metastasis, advanced tumor node metastasis stage and triple negative phenotype (Zhou et al., 2013). Various other researchers have also shown that activated STAT3 plays a critical role in the pathogenesis of breast cancer,

including its metastatic progression and response to therapy. High concentrations of activated STAT3 inversely correlated with a complete pathologic response of breast cancers to neoadjuvant chemotherapy. Activation of STAT3 significantly modulated the biological and clinical behaviour of breast cancer (Diaz et al., 2006; Ranger et al., 2009).

A similar scenario was reported by Li et.al, wherein downregulation of GRIM-19 was associated with hyper activation of p-STAT3 in hepatocellular carcinoma (HCC). GRIM-19 and p-STAT3 expression levels were analyzed in HCC and adjacent non tumorous liver tissues (ANLT) by immunohistochemistry, Western blot analysis, and RT-PCR. the expression of GRIM-19 protein was predominantly located in the cytoplasm with weak staining in the nucleus in ANLT, but only located in the cytoplasm in HCC tissues. HCC samples exhibited low levels of GRIM-19 and moderate to high levels of p-STAT3 expression. In contrast, ANLT was characterized by high levels of GRIM-19 and low levels of p-STAT3 expression (Li et al., 2012).

Extending the relationship between GRIM-19 and STAT3 to cervical cancers, Zhou et al., show that reduction in GRIM-19 protein levels occur in a number of primary human cervical cancers. Consequently, these tumors tend to express a high basal level of STAT3 and its downstream target genes. More importantly, using a surrogate model, they show that restoration of GRIM-19 levels re-establishes the control over STAT3-dependent gene expression and tumor growth *in vivo*. GRIM-19 suppressed the expression of tumor invasion and angiogenesis-

associated factors to limit tumor growth. Tumor samples from mice when subjected to Western blot analysis and RT-PCr revealed that the expression of STAT3, Cyclin B1 and Bcl2-L1 were decreased in the presence of GRIM-19. In addition, expression of Survivin, an antiapoptotic protein regulated by STAT3, was also strongly diminished. Apart from this, proliferation-associated antigen Ki67's expression was extremely reduced in tumors expressing GRIM-19 compared to control tumors. Lastly, Western blot analysis revealed similar results to a study referred much earlier in the section that the expression of GRIM-19 significantly suppressed the expression of VEGF and matrix metalloproteases, MMP-2 and MMP-9, involved in tumor invasion (Zhou et al., 2009).

Another study by Zhang et al. inclined towards the translational aspect of cancer therapy reports that co-expressed Stat3-specific shRNA and GRIM-19 synergistically and more effectively suppresses prostate tumor growth and metastases when compared with treatment with either single agent alone. As mentioned earlier, persistent activation of STAT3 and its overexpression contribute to the progression and metastasis of several different tumor types. For this reason, STAT3 is a reasonable target for RNA interference mediated growth inhibition. Blockade of STAT3 using shRNA could significantly reduce prostate tumor growth in mice but was not able to fully ablate target gene expression in vivo, owing to the idiosyncrasies associated with shRNAs and their targets. To enhance the therapeutic efficacy of Stat3-specific shRNA, the group applied a combination treatment involving expression of GRIM-19 as an

inhibitor of STAT3 and Stat3-specific shRNAs that were used to create a dual expression plasmid vector in vitro and in mouse xenograft models in vivo. The study concludes that the simultaneous use of two specific, but mechanistically different, inhibitors of STAT3 activity exerts enhanced antitumor effects than either single agent alone (Zhang et al., 2008). A very similar study conducted on thyroid cancer cells *in vitro* and *in vivo* reports that simultaneous expression of pSi-Stat3-GRIM-19 in SW579 cancer cells was found to significantly suppress the proliferation, migration and invasion *in vitro* and tumor growth *in vivo*, when compared to the controls either Stat3-specific siRNA or GRIM-19 alone (Wang et al., 2014).

In line with these translation efforts, another group, Okamoto *et al*. tried another approach to suppress tumour growth. They used the nona-arginine (R9)-protein transduction domain (R9-PTD) as a protein carrier to induce high levels of GRIM-19 expression in vitro and in vivo. They generated an R9-PTD-containing GRIM-19 fusion protein (rR9-GRIM19) and successfully induced over expression in cancer cells. Analysis of the expression of downstream molecules of STAT3 confirmed that in vitro rR9-GRIM19 treatment of constitutively activated STAT3 (STAT3c) cancer cells significantly reduced STAT3-dependent transcription. Moreover, intra-tumoral injections of rR9-GRIM19 in STAT3c cancer-bearing mice significantly suppressed tumor growth. These results lead the authors to suggest that intra-tumoral injections of rR9-GRIM19 have potential as a novel anticancer therapy in STAT3c cancer due to their ability to inhibit

STAT3-mediated signal transduction without major systemic side effects (Okamoto et al., 2010).

Another study on parallel areas with clinical significance demonstrates that GRIM-19 expression was lower in patients with radiotherapy-resistant tumors compared to patients with radiotherapy-sensitive tumors. In order to further investigate the effects of GRIM-19 expression on the radiation response in gastric cancer cells, they established BGC-803 clones stably expressing exogenous GRIM-19. It was found that the percentage of apoptotic cells was higher in cells expressing GRIM-19 than untransfected cells post-radiation treatment. Furthermore, caspase-3, -8, and -9 activity was significantly increased in GRIM-19-expressing cells compared to untransfected cells after radiation. Finally, the study demonstrates that expression of GRIM-19 in BGC-803 cells suppresses accumulation of STAT3. Taken together, these data may indicate that GRIM-19 expression sensitizes BGC-803 cells to radiation, and this is likely due to suppression of STAT3 accumulation. Summing up, the results show that GRIM-19 expression might be a useful therapy to enhance apoptosis in gastric cancer cells in response to radiation treatment (Bu et al., 2013).

Apart from a number of studies reporting the linkage of GRIM-19 and STAT3 expression levels in various cancers, there are numerous independent studies which report the abnormality of GRIM-19 in several carcinomas. The passages below mention aim to cover majority of the findings reported. Alchanati et al. report a severe to complete loss of

GRIM-19 in a number of human renal cell carcinomas (RCC). More importantly, they show the relevance of these data to RCC growth, wherein down regulation of GRIM-19 provides growth advantage and over-expression enhances cell death via an augmentation of STAT3 dependent gene activation (Alchanati et al., 2006). In another study, the authors investigated GRIM-19 expression pattern which appeared to correlate with hepatocellular carcinoma (HCC) invasive properties. Downregulation of GRIM-19 in the hepatic and HCC cell lines enhanced adhesive and invasive potential of these cells. While dissecting the possible mechanisms by which GRIM-19 mediates tumor invasion, they suggest a suppressive effect of GRIM-19 on HCC invasion via modulating epithelial–mesenchymal transition (EMT) and cell contact inhibition. GRIM-19 has hence been proposed as a new potential target for adjuvant treatment of aggressive and invasive HCCs besides surgical resection (Hao et al., 2012).

That downregulation of GRIM-19 promotes growth and migration of human glioma cells has been demonstrated by observing GRIM-19 mRNA and protein expression being markedly lower in gliomas than in control brain tissues, which negatively correlated with the malignancy of gliomas (Zhang et al., 2011). They also show that downregulation of GRIM-19 in glioma cells significantly enhanced cell proliferation and migration, whereas overexpression of GRIM-19 showed the opposite effects (Zhang et al., 2011). Lower expressions of GRIM-19 in lung cancers were reported by two groups (Fan et al., 2012; Wang et al., 2011)

while others reported that upregulation of GRIM-19 provided resistance to metastasis and suppressed tumour invasion in gastric cancer cell lines and oral carcinomas (Huang et al., 2010; Li et al., 2014). Among the differentially expressed proteins in malignant and benign adrenocortical tumors, GRIM-19 levels werefound to be significantly lower in malignant tumors (Kjellin et al., 2014). Mechanistic insights into the downstream factors of GRIM-19 in glioblastoma cell lines have identified hypoxia-inducible factor 1α (HIF1α) as a potential candidate. The study (Liu et al., 2013) shows that downregulation of GRIM-19 promotes HIF1α synthesis in a STAT3-dependent manner, which acts as a potential competitive inhibitor for von Hippel-Lindau (pVHL)–HIF1α interaction, and thereby prevents HIF1α from pVHL-mediated ubiquitination and proteasomal degradation (Liu et al., 2013). Taken together, they conclude that GRIM-19 could be a potential tumor suppressor gene, performing its function in part *via* regulating glioblastoma metabolic reprogramming through STAT3-HIF1α signaling axis. Interestingly, one study reported that alternatively spliced forms of GRIM-19 were detected in kidney tumor tissues with intron 3 by reverse transcriptase PCR. This splicing variant was found in kidney tumor tissues but not in matched normal tissues. Furthermore, the research also found that in addition to GRIM-19, the protein levels of NDUFS3, which is another mitochondrial complex I subunit, were also diminished in kidney tumor tissues when compared with paired normal tissues. The authors suggested that the alternative splicing forms of GRIM-19 were tumor tissue specific (He and Cao, 2010).

Yet another study provided evidence for an observation that monoallelic loss of GRIM-19 sufficient to induce squamous cell carcinoma in mice. The authors generated a genetically modified mouse in which Grim-19 could be conditionally inactivated. Deletion of Grim-19 in the skin significantly increased the susceptibility of mice to chemical carcinogenesis, resulting in development of squamous cell carcinomas. These tumors had high Stat3 activity and an increased expression of Stat3-responsive genes. With regard to the mitochondrial function, loss of Grim-19 also caused mitochondrial electron transport dysfunction, resulting from failure to assemble electron transport chain complexes and altered the expression of several cellular genes involved in glycolysis (Kalakonda et al., 2013). These observations add further proof to the critical role of GRIM-19 as a tumor suppressor.

Consistent with its regulation by IFNs that are key in immune responses, an interesting study that investigates the pathogenesis of H5N1 viral infection which is associated with the ability of the virus to induce apoptotic cell death, reports that H5N1 virus is able to up-regulate the expression GRIM-19 in human monocyte-derived macrophages (hMDMs). The percentage of apoptotic cells was significantly decreased in H5N1-infected GRIM-19 depleted hMDMs, which was also associated with a decrease of BH3-interacting domain death agonist cleavage and apoptosis-inducing factor (AIF) release to the cytosol. Furthermore, neutralizing-IFN-β Ab is able to suppress GRIM-19 expression in H5N1-infected cells resulting in a decrease in apoptotic cell number, indicating

that IFN-β secreted by H5N1-infected hMDMs regulates GRIM-19 expression leading to apoptosis (Ekchariyawat et al., 2013). This is consistent with other studies referred to earlier, reporting that GRIM-19 expression could be induced by IFN-β and RA.

1.5 MITOCHONDRIAL FUNCTIONS OF GRIM-19

At the time of the discovery of GRIM-19 protein, 42 subunits of Complex I of the mitochondrial respiratory chain were defined with 35 nuclear encoded genes and 7 mitochondrially encoded proteins. Fearnly et al., using a mass spectrometric analysis revealed that GRIM-19 is a subunit of Complex I of the mitochondria which did not correspond to any known subunit of the complex assembly at the time. However, this study does not provide any evidence at the cellular level for the localization of GRIM-19 (Fearnley et al., 2001). A study referred to earlier, by Angell et al., the founders of the GRIM-19 protein, reveal a predominantly nuclear staining and possibly punctae in the cytoplasm corresponding to the mitochondria (Angell et al., 2000). Nevertheless, the images provided are far from convincing. As this has been dealt with in our study, a comparison and discussion of both the results are done in the discussion section.

During one of the early studies on the interaction between GRIM-19 and STAT3, the authors tried to investigate the cellular localization of GRIM-19 and report that it is majorly found as punctae in the cytoplasm and aggregates around the perinuclear region coinciding with COX

protein. They also state that the results show a minor distribution in the nucleus. Both the fractions witnessed an increase in the presence IFN/RA (Lufei et al., 2003). The group further claims that GRIM-19 suppresses STAT3 via functional interaction thus preventing STAT3 from entering the nucleus and up-regulating downstream genes in the cascade. However, there are a few glitches in the experimental design and the immunofluorescence results that are discussed in detail in the discussion section.

The same group further took to in vivo analysis of the function of GRIM-19 by generating a mouse knock out model. In this study, they report that homologous deletion of *GRIM-19* causes embryonic lethality at embryonic day 9.5. *GRIM-19*-/- blastocysts show retarded growth in vitro and, strikingly, display abnormal mitochondrial structure, morphology, and cellular distribution (The quality of the image does not allow any conclusion to be made with enough confidence. As this also contradicts with our results, more detailed discussion is made under the discussion section). Although, they claim to have re-examined the cellular localization of GRIM-19 in various cell types and found its primary localization in the mitochondria, the results for the same are not clear and the mitochondria looks highly fragmented not to mention the staining being non-specific (Huang et al., 2004). A subsequent study by the group involved knockdown of GRIM-19 in *Xenopus laevis* embryos. A severe deficiency in heart formation was observed, and the deficiency could be rescued by reintroducing human *GRIM-19* mRNA. The mechanism

involved was further investigated. It was found that the activity of NFAT, a transcription factor family that contributes to early organ development, was downregulated in GRIM-19 knockdown embryos. Furthermore, the expression of a constitutively active form of mouse *NFATc4* in these embryos rescued the heart developmental defects. Since NFAT activity is controlled by a calcium-dependent protein phosphatase, calcineurin, it suggests that calcium signaling could be disrupted by GRIM-19 knockdown. Indeed, both the calcium response and calcium-induced NFAT activity were found to be impaired in the GRIM-19 or NDUFS3 (another complex I subunit) knockdown cell lines. They also showed that NFAT can rescue expression of Nkx2.5, which is one of the key genes for early heart development (Chen et al., 2007). Of note is the result of the same group in a study that shows that GRIM-19 is necessary for maintenance of mitochondrial membrane potential with the use of truncation mutants (Lu and Cao, 2008). This also has contradictions with what we observe in our data and hence is taken up for discussion in the upcoming sections.

In the most recent study by Chen et al., from the same group, the authors observe that GRIM-19 +/- mice were more prone to urinary tract infection and that the macrophages from these mice have compromised mitochondrial complex I activity and increased ROS levels (Chen et al., 2012). In addition, production of pro-inflammatory cytokines, such as interleukin (IL)-1, IL-12, IL-6, and interferon (IFN)-γ induced by both bacterial infection and lipopolysaccharide (LPS) and

monodansylcadaverine treatment, is also decreased in the GRIM19+/- macrophages. Inhibition of mitochondrial RC activity by inhibitors showed a similar reduction on the cytokine production.

1.5.1 Does GRIM-19 recruit STAT3 to mitochondria?

Previous studies conducted in the background of necroptosis, indicated that GRIM-19 mediated translocation of STAT3 to the mitochondria plays an essential role in the execution of the process. Tumor necrosis factor (TNF) can induce necroptosis, wherein inhibition of caspase activity prevents apoptosis but initiates an alternative programmed necrosis. The activity of receptor-interacting serine/threonine-protein kinase 1 (RIPK-1) is required for necroptosis to proceed, with suppression of RIPK-1 expression or inhibition of RIPK-1 activity with necrostatin-1 preventing TNF-induced necroptosis. Downstream from the TNF receptor, the generation of reactive oxygen species at the mitochondria has been identified as necessary for the execution of necroptosis; with antioxidants and inhibitors of mitochondrial complex I preventing TNF-induced cytotoxicity. However, components of the signaling pathway that lie between activated RIPK-1 and the mitochondria are unknown. In this study they demonstrate that during TNF-induced necroptosis, STAT3 is phosphorylated on serine 727, which is dependent on RIPK-1 expression or activity. The phosphorylation of STAT3 induced interaction with GRIM-19, a subunit of mitochondrial complex I, with a resultant translocation of STAT3 to the mitochondria, where it induces an increase in ROS production and cell

death. As much as the idea could be thought of as a reasonable one, there is not much of raw data that is presented by the study except for western blots whose quality still stands highly arguable (Shulga and Pastorino, 2012).

A recent study by Tammineni et al., showed convincingly through a thorough *in vitro* analysis that the import of STAT3 into the mitochondria depends on GRIM-19. The authors showed that GRIM-19 acts as a chaperone to recruit STAT3 into inner mitochondrial membrane. In addition, GRIM-19 was shown to enhance the integration of STAT3 into complex I. A S727A mutation in STAT3 reduced its import and assembly even in the presence of GRIM-19 (Tammineni et al., 2013).

1.6 HYPOTHESIS

We hypothesized that GRIM-19 may play an important part in the dynamics of mitochondria, eventually acting as an inducer of cell death under stressful conditions. Since it was shown to be a part of Complex I, it could play an important role in the generation of ROS which may be, in part, the way in which it executes cell death through the IFN/RA cell death pathway. In the case of mutations found in GRIM-19 from tumour samples, these functions could be altered leading to abnormal proliferation and eventually cancer.

1.7 OBJECTIVES

With the pool of knowledge as mentioned above, when we embarked on our study, our aims were as follows:

- To unambiguously determine the sub cellular localization of GRIM-19 using protease protection assay and alkaline conditions on the mitochondrial fraction and immunofluorescence assays.
- To investigate if GRIM-19 has a role in mitochondrial dynamics by forming a part of the fission-fusion machinery of the mitochondria. This was studied using the FRAP assay under GRIM-19 over-expression and KD conditions (Fluorescence Recovery After Photobleaching)
- To study the mitochondrial functions of GRIM-19 such as its role in the production of ROS, maintenance of mitochondrial potential and production of ATP using dyes such as DHE and TMRM with Fluorescence Assorted Cell Sorting (FACS)
- To characterize certain tumour derived mutations of GRIM-19 with respect to its mitochondrial functions using Site-directed mutagenesis and subsequently the anomalies they cause in the normal functioning of the mitochondria.

Chapter 2 MATERIALS AND METHODS

2.1 GENE CLONING

2.1.1 RNA extraction

Total RNA was extracted from HEK 293T cells using Trizol (Invitrogen) according to the instructions provided by the manufacturer. Briefly, a total of 1 ml of Trizol was added to one well of a 6-well plate of HEK 293T cells. The cells were homogenized and incubated at room temperature for 5 min to allow nucleoproteins to dissociate before adding 200 µl chloroform. The mixture was shaken for 15 sec and incubated at room temperature for 2-3 min, followed by centrifugation at 12,000x g for 15 min at 4 °C in order to separate the aqueous and organic phases. An aliquot of 500 µl aqueous phase was transferred to a new tube and mixed with 500 µl isopropyl alcohol. The mixture was incubated at room temperature for 10 min and centrifuged for 15 min at 12,000xg at 4 °C. The supernatant was discarded and the pellet containing RNAs was washed with 70% ethanol and centrifuged at 7,500x g for 5 min at 4 °C. After the pellet was briefly air dried, it was dissolved into 20 µl Diethyl pyrocarbonate (DEPC) water. The isolated RNAs can now be used for downstream experiments immediately or be stored at -80 °C.

2.1.2 Reverse transcription polymerase chain reaction (RT-PCR)

SuperScript™ Reverse Transcriptase from Invitrogen was used to carry out RT-PCR. Firstly, a mixture of RNA template (11.5 µl), OligodT (1 µl) and dNTP (1 µl) was incubated at 65 °C for 5 min followed by chilling on ice. Subsequently, 5 X First strand buffer (4 µl), 0.1 M DTT (2 µl) and RNAas out™ (0.24 µl) were added and the mixture incubated for 2 min at 42 °C. Subsequently, SuperScript RTase™ (0.25) was added to the mixture and incubated for 50 min at 42 °C and 15 min at 70 °C. The synthesized cDNA was used for PCR immediately or be stored at -80 °C.

Components	Volume (µl)
RNA template(1 µg/µl)	2
dNTP (10 mM)	1
DTT (0.1 M)	2
Oligo-dT18 (100 µM)	1
Reverse transcriptase (200 U/µl)*	0.25
5 × first strand buffer	4
Sterile distilled water	10.75
Total	**20**

Table 2-1: Reverse transcription reaction

2.1.3 Polymerase Chain Reaction (PCR)

Amplification of the gene constructs from the cDNA was carried out using DyNAzyme™ EXT DNA polymerase (Finnzymes, Thermo Scientific). The reaction adopted, the PCR cycle parameters and the sequence of primers used are shown in Tables 2.2, 2.3 and 2.4 respectively.

Component	Volume (µl)
cDNA template (200ng/µl)	1-2
Forward primer (10 nM)	0.5
Reverse primer (10 nM)	0.5
dNTP (10 nM)	0.5
10 X 514 Buffer	2.5
DyNAzymeTM EXT	0.5
Double-distilled water	Top up to 25 µl
Total	**25**

Table 2-2: PCR reaction

Cycle	Step	Temperature (°C)	Time
1	Initialization	95	3 min
	Denaturation	95	30 s
25	Annealing	55	40 s
	Extension	72	1 min (1min/kb)
1	Final elongation	72	5 min
1	Final hold	4	∞

Table 2-3: PCR cycling parameters

Insert	Vector	Primer (5'-3')	Insertion site
GRIM-19	pXJ40	Forward-CGCGGATCCATGGCGGCGTCAAAGGTGAAG Reverse-CCGCTCGAGCTACGTGTACCACATGAAGCCG	BamH1 Xho1
GRIM-19	pEGFP-N1	Forward-CCCAAGCTTATGGCGGCGTCAAAGTGAAG Reverse-CGGGGTACCGTCGTGTACCACATGAAGCCGTG	Kpn1 HindIII
GRIM-19	c-Flag pcDNA3	Forward-CCCAAGCTTACCATGGCGGCGTCAAAGGTGAAG Reverse- CGGGGTACCCGTGTACCACATGAAGCCGTG	Kpn1 HindIII

Table 2-4: Sequences of primers for cloning

2.1.4 DNA ligation and transformation

All the genes amplified from the cDNA library or template were purified using QIAquick Gel Extraction Kit (Qiagen) after agarose gel electrophoresis and then subjected to double restriction enzymatic digestion. The restriction enzymes and buffers used in this study were

purchased from NEB. The reaction was incubated at 37 °C for 2-6 hours. The components of restriction digestion reaction were shown in Table 2.5

Component	Volume (µl)
Purified PCR product	16.5
Restriction enzyme 1	0.5
Restriction enzyme 2	0.5
10 X Buffer	2
BSA	0.5
Total volume	**20**

Table 2-5: Double digestion restriction system

The digested products were purified once again using QIAquick Gel Extraction Kit (Qiagen) and GRIM-19 was inserted into EGFP-N1 vector (Clonetech)to fuse GFP into the C terminus of GRIM-19, a pXJ40 vector with different tags namely, FLAG, GFP, c-myc or BFP (kindly dononated by Dr. Low Boon Chuan, Department of Biological Sciences, National University of Singapore) which fuses these tags to the N terminus of GRIM-19and C-Flag vector (Addgene) to fuse FLAG to the C terminus of GRIM-19. The restriction enzyme sites used for the cloning of these plasmids are mentioned in Table 2.4.

The ligation reaction was incubated at 4 °C overnight. The components added in the reaction are shown in Table 2.6. After ligation, the product was transformed into DH5α or TOP10 competent cells. The products of ligation were added into 100 µl DH5α or TOP10 competent cells and incubated on ice for 30 min. Subsequently, the mixture was heated at 42 °C for 90 sec and cooled on ice for 3 min. This was followed by addition of 1 ml of LB medium (Conda) and incubation at 37 °C shaker for 1 hour. After incubation, the mixture was centrifuged and supernatant

was removed. The pellet was resuspended to be spread and grown on LB agar plate supplemented with appropriate antibiotics for around 16 hours and the resulting colonies on the plate were picked for plasmid extraction.

Component	Volume (µl)
Double digested PCR product	7
Double digested vector	0.5
T4 ligase (Promega)	0.5
10 X T4 ligase Buffer (Promega)	1
Total volume	**10**

Table 2-6: Ligation reaction

Plasmid extraction was performed using miniprep plasmid extraction kit (Axygen) according to the protocol from the manufacturer. Double restriction enzymatic digestion was performed to the plasmids to verify the insertion and the plasmids with insertion were subject to DNA sequencing analysis to confirm the fidelity of the inserted segment.

2.1.5 DNA sequencing

DNA sequencing was carried out using ABI PRISM BIG DYE™ Terminator Cycle Sequencing Ready Reaction Kit (Applied Biosystems). The sequencing PCR mixture and cycling parameters are shown in Table 2.7 and Table 2.8, respectively.

Component	Volume (µl)
Terminator Ready Reaction Mix	2
1 mM sequencing primer	3
5 X sequencing reaction buffer	4
Template DNA (200-500 ng/µl)	1
Double-distilled water	10
Total volume	**20**

Table 2-7: DNA sequencing reaction

Cycle	Temperature (°C)	Time
1	95	1 min
	95	10 s
25	50	5 s
	60	1 min
1	4	∞

Table 2-8: Cycling parameters for DNA sequencing reaction

The PCR products were mixed with 20 µl of 3 M NaOAc (pH 4.6) and 50 µl of 95% ethanol and incubated at room temperature for 10 min. The samples were centrifuged at 13,200 rpm at 4 °C for 10 min. The supernatant was removed and the pellet was washed twice with 500 µl of 70% ethanol, centrifuging at 13,200 rpm for 5 min after each wash. The pellet of PCR product was air-dried at room temperature and dissolved in 15 µl HiDi and subject to automated sequencing on the ABI 377 sequencer system.

2.1.6 Site-directed mutagenesis

FLAG-GRIM19 and EGFPN1-GRIM-19 single point mutations were carried out by site-directed mutagenesis using QuickChange™ Site-Directed Mutagenesis Kit (Stratagene, CA). The experiments were performed following the manufacturer's instruction. The components

added into the PCR reaction are shown in Table 2.9. The PCR cycle parameters are shown in Table 2.9.

Component	Volume (µl)
Template plasmid (50 ng/µl)	1
Primer forward (10nM)	1
Primer reverse (10nM)	1
dNTP (10nM)	1
10 × buffer	5
Pfu Turbo DNA polymerase	1
Sterile distilled water	40
Total volume	**50**

Table 2-9: Site-directed mutagenesis PCR reaction system

Cycle	Step	Temperature (°C)	Time
1	Initialization	95	1 min
	Denaturation	95	1 min
18	Annealing	60	1 min
	Extension	72	6 min (1min/kb)
1	Final elongation	72	10 min
1	Final hold	4	∞

Table 2-10: Site-directed mutagenesis PCR cycle parameters

The PCR products were subsequently digested by Dpn I restriction enzyme (10 U/µl) for 2 hours at 37 °C and the digested products were transformed into DH5α or TOP10 competent cells for plasmid extraction. The mutations were verified by DNA sequencing.

2.2 WESTERN BLOT

Cells were washed by 1x PBS and placed on ice immediately. For 10-cm plates, 1 ml RIPA buffer (20 mM Tris-Cl at pH 8.0, 125 mM NaCl, 0.5% NP-40, 5% glycerol) with phosphatases inhibitors (20 mM NaF, 0.2 mM Na3VO4, 2 mM EDTA) and protease inhibitors (Sigma) was added to cover all the cells in the plate, which was then put on ice for 30 min with

occasional shaking. After the incubation, cells were transferred to a new tube and then centrifuged at maximum speed for 30 min at 4 °C. The supernatant was collected and the protein concentration was determined using Bradford Protein Assay reagent (Bio-Rad) according to manufacturer's instructions. An appropriate amount of 6 × SDS loading dye was added to each sample and boiled at 95 °C for 15 min before loading for SDS-PAGE. The proteins separated on SDS-PAGE in a SDS-running buffer (12.5 mM Tris-Cl [pH 7.4], 96 mM glycine, 1.7 mM SDS) were immediately transferred onto a PVDF (polyvinylidene difluoride) membrane. The membranes were then incubated in 5% BSA or 5% skimmed milk in TBST (20 mM Tris-Cl [pH 7.4], 137 mM NaCl, 0.1% Tween-20) for 1 hour, followed by washing with 1x TBST thrice, 10 min each time. After washing, the membranes were incubated in primary antibodies diluted in 1x TBST over night at 4 °C or at room temperature for 1 hour. After primary antibody incubation, the membranes were washed by 1x TBST again thrice and subsequently incubated in secondary antibodies for 1 hour at room temperature. Washing was carried out again at the end of secondary antibody incubation as described above. Proteins on membranes were detected by an enzyme-substrate reaction using an ECL kit (Pierce) and exposure to FUJI medical X-Ray film (FUJIFILM).

GRIM-19 antibody used for western blot was purchased from abcam (Anti-GRIM19 antibody [6E1BH7] ab110240). The product is a well validated one with clear bands at the predicted molecular weight of

GRIM-19 (around 16-17 kDa). Further to this, I have also carried out preliminary assays to verify the authenticity of the purchased antibody by western blots and immunoflourescence assays.

2.3 MITOCHONDRIAL EXTRACTION

HEK 293T, HeLa and MEF cells cultured in 10-cm dishes were washed with 1x PBS before being harvested with a pre-cold mitochondrial extraction buffer (220 mM mannitol, 70 mM sucrose, 20 mM Hepes-KOH, pH 7.5, 1 mM EDTA, 0.5 mM PMSF, and 2 mg/ml BSA) supplemented with protease inhibitors including 0.7 µg/ml pepstatin, 0.5 µg/ml leupeptin and 2.2 mg/ml Aprotinin. The cells were scrapped and transferred to a new 1.5 ml tube; subsequently, the cells were passed through a 25-G syringe (BD) for ten times on ice. The homogenized cells were centrifuged for 15 min at 4 °C, 1000xg. The supernatant was transferred to a new tube followed by another 20 min centrifugation at 4 °C, 10,000x g to pellet the mitochondria. The supernatant fraction contains the cytosolic protein.

2.4 MITOCHONDRIAL MEMBRANE ANALYSIS ASSAY AND PROTEINASE K DIGESTION

For mitochondrial membrane analysis and proteinase K digestion assay, mitochondria of HeLa cells were pelleted according to the method described previously. Mitochondrial samples were resuspended in freshly prepared 0.1 M Na2CO3, pH 11.5, and incubated on ice for 30 min with

vortexing every 10 min. After the incubation, membranes were centrifuged down to the pellet at 100,000 g for 30 min at 4 °C, and the supernatant was collected as inter-mitochondrial membrane space and matrix proteins.

For proteinase K digestion assay, isolated mitochondria were resuspended in mitochondrial isolation buffer and incubated with different proteinase K concentrations on ice for 30 min. PMSF was added to stop the digestion and the samples were precipitated by TCA. Pellets were resuspended in RIPA buffer (20 mM Tris-Cl [pH 8.0], 125 mM NaCl, 0.5% NP-40, 5% glycerol, 20 mM NaF, 0.2 mM Na3VO4, 2 mM EDTA, and protease inhibitors) for 30 min and subjected to SDS-PAGE and Western blotting.

2.5 IMMUNOFLUORESCENCE

HeLa cells were seeded on sterilized glass coverslips in 12-well plates 24 hours before transfection with indicated plasmids or siRNAs. After transfection, cells were cultured for the indicated time and fixed by freshly prepared 4% PFA (paraformaldehyde) for 10 min at room temperature. PFA was removed after fixation followed by 2 times wash with PBS and the coverslips were then incubated with 3% BSA + 0.1~0.5% Triton X-100 in PBS for 30 min at room temperature for blocking and permeabilization. After the incubation, coverslips were washed using PBS for 3 times and followed by incubation with primary antibodies diluted in 3% BSA for 1 hour at room temperature. After

primary antibody incubation, coverslips were washed again and incubated with fluorescence conjugated secondary antibodies for 45 min at room temperature. The secondary antibodies used were Alexa Fluor dye-conjugated IgG (488,568 and 642)(Molecular Probe, Invitrogen) After incubation, coverslips were washed with 1x PBS and DNA was stained by Hoechst 33342 (Invitrogen) for 15 minutes at room temperature. Cells stained by various dyes were mounted onto glass slides using FluorSaveTM reagent (Calbiochem) and preserved at 4 °C for further analysis. All fluorescent images were acquired on Ultraview Vox spinning disc confocal system (PerkinElmer) equipped with a 60× 1.2 N.A. objective (Olympus). The images were processed using Volocity Suite (PerkinElmer).

2.6 LIVE CELL IMAGING AND FLUORESCENCE RECOVERY AFTER PHOTOBLEACHING (FRAP)

For live cell imaging, HeLa cells seeded in a 35mm-glass-bottom dish with different treatments were incubated at 37 °C, 5% CO_2 chamber equipped on the microscope, and time lapse imaging was taken on Ultraview Vox spinning disc confocal system (PerkinElmer). Volocity™ (PerkinElmer) was used to control all the parameters used for image acquisition.

For FRAP analysis, HeLa cells stably expressing mito-Red were transfected with the indicated plasmids. The use of mito-Dsred for FRAP analysis is a validated method wherein the RFP is fused with a

mitochondrial protein to avoid usage of chemical stains that may interfere with the result of the experiment (Frohlich et al., 2013). Cells were placed on the live imaging system described above, and the laser line of 561 nm was used to bleach a 2 × 2 μm^2 area placed on the fiber of mitochondrial network. 20 sec of recovery time for each bleaching was used to make sure the recovery had reached their plateau. 60 FRAP curves with each treatment were analyzed by measuring the intensities of mito-Red fluorescence in the photobleached area.

2.7 ROS AND MITOCHONDRIAL POTENTIAL DETECTION

To test levels of ROS and mitochondrial potential, fluorescent indicator DHE (Invitrogen) and TMRM were used. Cells were harvested, washed in PBS and stained with 5 μM DHE or 50nM TMRM dye for 30 min or 20min respectively at 37 °C in the dark. Fluorescence was measured immediately with LSRFortessa (BD Biosciences), and the data was analyzed with the FACSDiva version 6.2 software (BD Biosciences). The fluorescence intensity of the red signal in DHE/TMRM stained cells indicates ROS level or the mitochondrial potential respectively. A total of 10,000 cells were counted in each population.

2.8 ATP PRODUCTION ASSAY

ATP was measured by using the ATP determination kit (Molecular Probes) according to manufacturer's instruction. In brief, HeLa cells transfected with control or GRIM-19 siRNAs were washed with 1 × PBS

and placed in ice-cold ATP buffer (20 mM Tris-HCl, PH7.5, 0.5% Nonidet P-40, 25 mM NaCl, and 2.5 mM EDTA) for 5 min. Lysates were then centrifuged at 13,000× g for 30 min at 4 °C and supernatants were collected and protein concentrations were measured using the Bradford Protein Assay reagent (Bio-Rad). ATP levels were determined by using 0.5 μg of proteins for each reaction and every sample was measured in triplicate.

2.9 CELL CULTURE AND TRANSFECTION

2.9.1 Cell lines

Human embryonic kidney epithelial cells (HEK 293T), human cervical cancer cells (HeLa) were used in the current studies. HEK 293T cells were mainly used for the biochemical assays for expression of vectors. While, HeLa cells were mainly used for biochemical assays of the mitochondrial fractionation and the imaging analyses of mitochondrial morphology.

2.9.2 Cell culture

HeLa and HEK 293T cells were maintained in Dulbecco's modified Eagle medium (DMEM) (Hyclone), supplemented with 10% (v/v) fetal bovine serum (FBS) (Hyclone) and 10U/ml Penicillin-streptomycin (Hyclone) unless otherwise noted. All cultures were maintained at 37 °C, 5% CO2.

2.9.3 Transfection

2.9.3.1 HEK 293T cell line transfection

Plasmid DNA was introduced into HEK 293T cells using calcium phosphate transfection. One day before transfection, cells were seeded in 10-cm plates. The transfection cocktail including 10 μg of the plasmid DNA, 500 μl of 2 × HBS and 50 μl of 2.5M $CaCl_2$ was topped up to 1ml with distilled water. After cells reach 50%-60% confluence, the transfection cocktail was added directly into the culture medium.

2.9.3.2 HeLa cell line transfection

For HeLa cells, EffecteneTM (Qiagen) was used to transfect plasmid DNA. At 70%-80% confluence, cells in 12- or 6-well dishes were transfected with 6 μl or 10 μl of Effectene reagent mixed with 0.3 μg or 0.4 μl of plasmid DNA and 2.4 μl or 3.2 μl of enhancer, respectively. PEI was also used to transfect HeLa cells. This protocol involved diluting the plasmid DNA in 1x PBS at 1μg plasmid DNA per well of a 12 well plate. Three times the amount of PEI was added to the diluted plasmid DNA and the mixture incubated for 20 minutes. It was later added directly added to cells on the corresponding plate.

2.9.3.3 siRNA transfection using lipofectamine

Transfection of siRNA into HeLa cells using OligofectamineTM (Invitrogen) was performed according to manufacturer's instructions. Briefly, cells at 60%-70% confluences in 12-well plates were changed to non-antibiotics medium before they were ready for transfection. A total of

3 µl of Lipofectamine 2000™ reagent mixed in 100µl of OPTI for 5 min was combined with 120 pmol siRNA mixed in 100 µl of OPTI. The transfection cocktail was incubated in room temperature for another 20 min, followed by adding into cells directly. 48 h after transfection, the knockdown efficiency of the target proteins were validated by Western blotting or immunofluorescence. All of the siRNA sequences listed in the table below were synthesized by Sigma.

GENE	shRNA	TARGET SEQUENCE
GRIM-19	Sense strand	UCUACGGGCACUGGAGCAUAAUGAA
	Anti sense strand	UUCAUUUAUGCUCCAGUGCCCGUAGA

Table 2-11: Sequences of siRNA

Chapter 3 RESULTS

3.1 CHARACTERIZATION OF GRIM-19 FUNCTION ON MITOCHONDRIAL MORPHOLOGY AND DYNAMICS

3.1.1 GRIM-19 localizes to the inner mitochondrial membrane

Ever since the identification of GRIM-19, its intracellular localization has been highly controversial. The founders of this protein suggested a nuclear localization, which was reported by a few other groups as well (Angell et al., 2000). However, subsequent research indicated mitochondrial localization (Huang et al., 2004). Nonetheless, these studies too fail to show convincing data for their claim. This led us to investigate and conclude unambiguously the intracellular localization of GRIM-19. To do the same, I performed immunostaining with HeLa cells using an anti-GRIM-19 antibody to locate endogenous GRIM-19. Figure 3.1 shows that GRIM-19 localizes to the mitochondria as indicated by Tom20, an outer mitochondrial membrane protein. Consistently, Western blot analysis revealed that GRIM-19 was present only in the mitochondrial fraction and not in the cytosolic fraction (Figure 3.2 A). The purity of the mitochondrial fraction is indicated by the non-leakage of cytochrome C to the cytosolic fraction and absence of tubulin contamination in the mitochondrial fraction. Further to this, I employed the Proteinase K protection assay to further ascertain the sub-

mitochondrial localization of GRIM-19. The Proteinase K digestion led to the disappearance of Tom20. The results, as seen from Figure 3.2 C, showed that GRIM-19 exhibited a similar pattern to the inner mitochondrial membrane protein Tim23, both being protected until Triton X-100 was added indicating that it is also present in the same compartment.

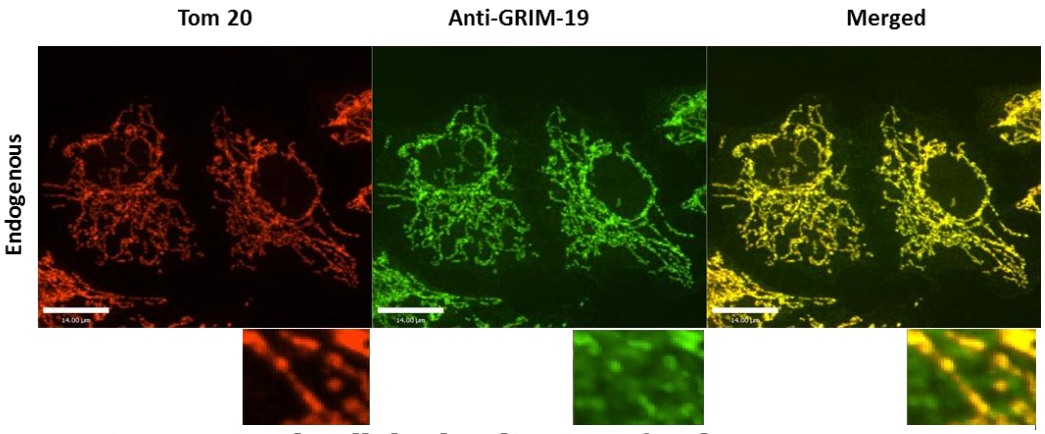

Figure 3-1: Sub cellular localization of endogenous GRIM-19

Sub cellular localization of endogenous GRIM-19. HeLa cells were fixed with 4% paraformaldehyde and permeablized by 0.5% Triton-X 100 in BSA for 30 min. Following this, the cells were stained with an anti-Tom20 antibody or anti-GRIM-19 antibody. Scale bar: 14μm

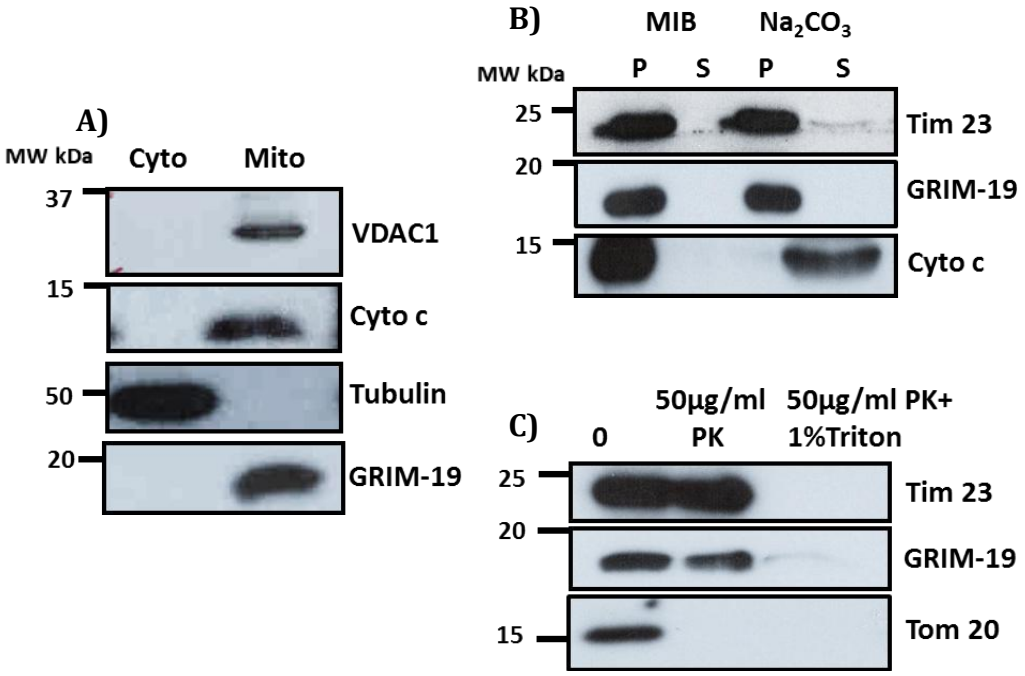

Figure 3-2: Sub cellular localization of endogenous GRIM-19

A) Mitochondrial extraction performed with HeLa cells. Cells were harvested using mitochondrial isolation buffer and separated into the mitochondrial (M) and cytosolic (C) fractions. VDAC1 and Tubulin were identified as mitochondrial and cytosolic markers respectively. Cytochrome C was used to indicate the purity of the mitochondrial fraction. This assay shows that Grim19 localizes to mitochondria. No detectable amount of protein was found in the cytosol.

B) Sub-mitochondrial localization of Grim19. Mitochondrial fractions were prepared as described in A. This was subjected to alkaline extraction using sodium carbonate (P and S represent the Pellet and Supernatant fractions obtained after alkaline extraction) or incubated with the indicated concentrations of Proteinase K (panel C) and immunoblotted for Tim 23, Tom 20 as inner and outer mitochondrial membrane markers respectively.

Following Proteinase K digestion, alkaline extraction using Na_2CO_3 was performed to study the membrane association of GRIM-19. As shown in Figure 3.2 B, GRIM-19 is detected in the mitochondrial pellet portions suggesting that GRIM-19 is integrated with membrane, consistent with Tim 23, an inner mitochondrial membrane bound protein. On the other hand, cytochrome C which is present in the inter-membrane space, purifies in the supernatant fraction of the mitochondria. Taken together, the Proteinase K protection assay and the alkaline extraction clearly show that GRIM-19 is part of the inner mitochondrial membrane.

3.1.2 Alteration to GRIM-19 does not affect the mitochondrial morphology

Once the endogenous localization of the protein was determined, I set out to characterize the over expression constructs of GRIM-19. I had designed GRIM-19 plasmids that fused tags on its N-terminal. As shown in Figure 3.3 A and Figure 3.3 B, the GFP and Flag tags present on the N-terminal of GRIM-19 appear to affect its proper localization to mitochondria. Instead, the tagged GRIM-19 protein forms abnormal punctae in the cytoplasm. This led us to clone constructs with the tags on the C-terminal of GRIM-19. When this tagged GRIM-19 were over-expressed in cells, the localization of the protein was primarily observed to be in the mitochondria, as shown in Figure 3.4 A and B.

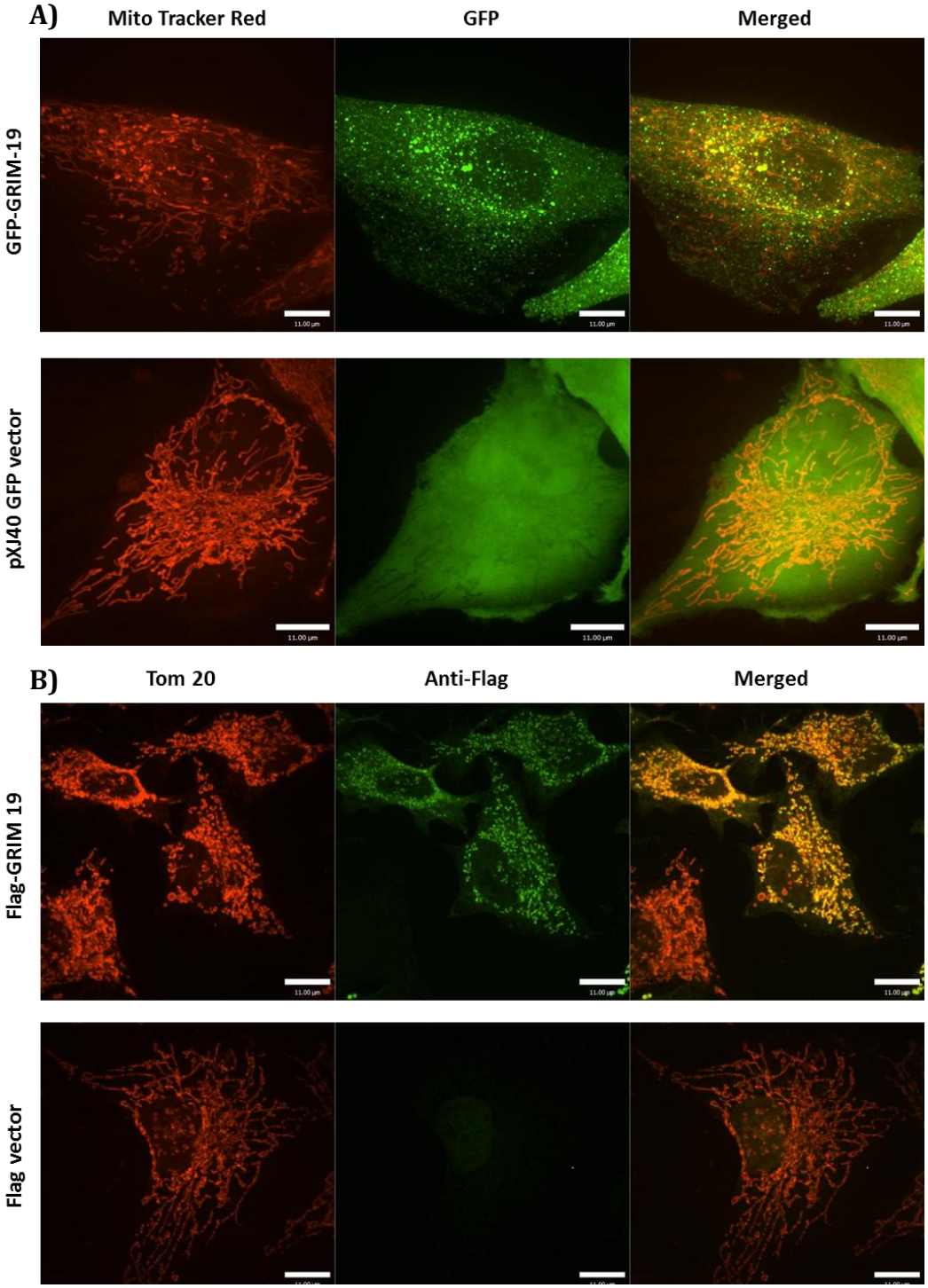

Figure 3-3: N-terminal tags affect the localization of GRIM-19

A) N terminal tags affect the localization of GRIM-19. HeLa cells were transfected with either pXJ40 GFP vector or GFP-GRIM-19. Cells were stained with Mito Tracker Red before performing live cell imaging. Results show that GFP-GRIM-19 forms aggregates/punctae in the cytoplasm devoid of a proper cellular localization pattern. However, this does not affect the morphology of mitochondria.

B) HeLa cells were transfected with Flag vector (pXJ40) or Flag-GRIM-19 and fixed with 4% paraformaldehyde and permeablized by 0.5% Triton-X 100 in BSA for 30 min. Following this, the cells were stained with Anti-Tom20 antibody and Anti-Flag antibody. Though GRIM-19 seems to localize to the mitochondria, the mitochondrial morphology is affected. Since, this method involves fixing the cells, any artefacts should be ruled out (GFP tags utilize live cell imaging and hence can be relied upon better). Scale bar: 11µm

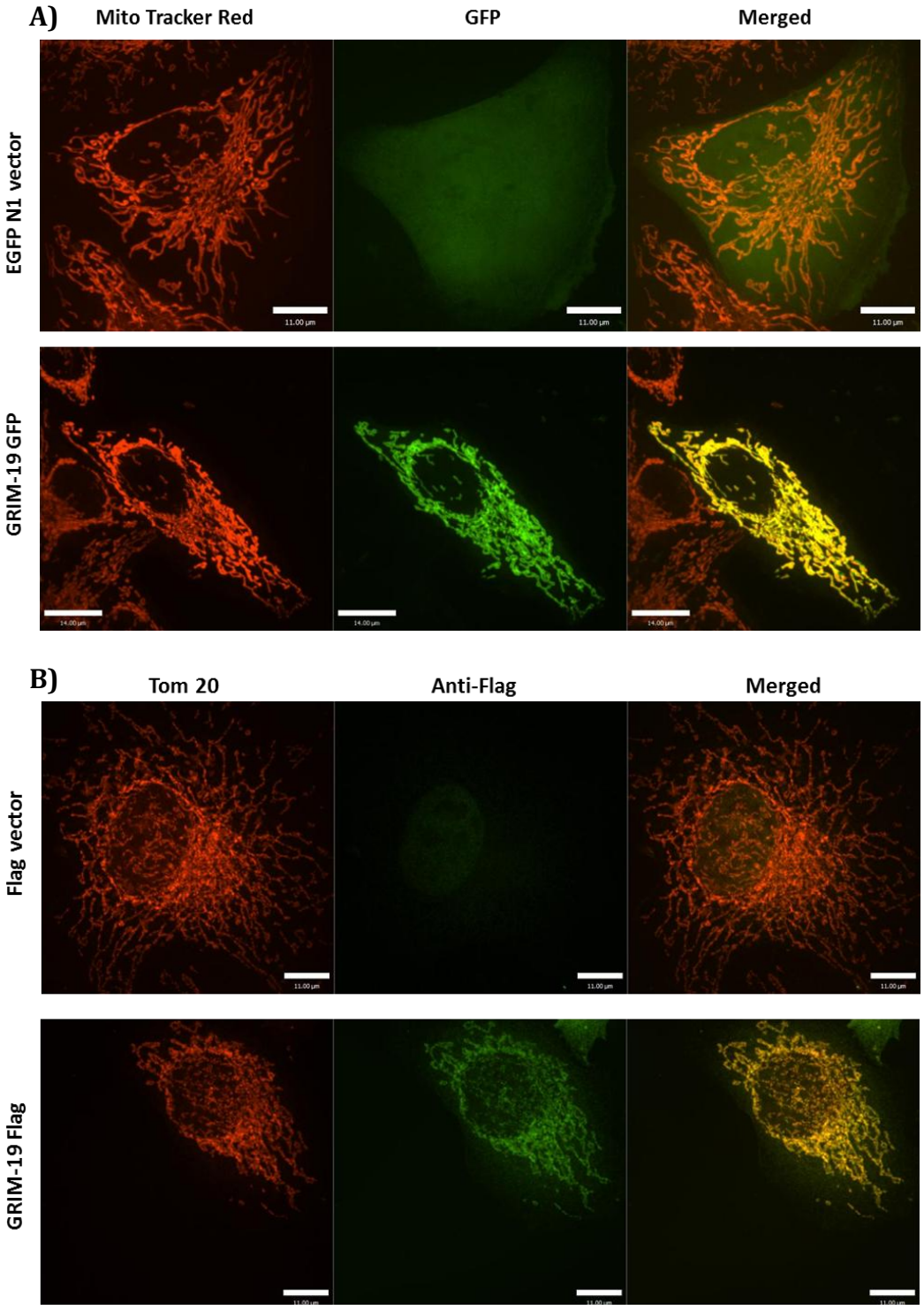

Figure 3-4: C-terminal tags facilitate proper localization of GRIM-19

A) HeLa cells were transfected with either an EGFP-N1 or GRIM-19-GFP plasmid. Cells were stained with Mito Tracker Red before performing live cell imaging. Results clearly indicate that GRIM-19 with a tag on the C-terminal can localize to the mitochondria without forming aggregates or affecting the morphology of the mitochondria.

B) HeLa cells were transfected with Flag vector (C-FLag) or GRIM-19-Flag and fixed with 4% paraformaldehyde and permeablized by 0.5% Triton-X 100 in BSA for 30 min. Following this, the cells were stained with Anti-Tom20 antibody and Anti-Flag antibody. These results complement the live cell imaging results proving that C-terminal tags facilitate proper localization of GRIM-19. Scale bar: 11µm

These results also indicated that the over expression of GRIM-19 using the right tags is critical and does not affect the morphology of the mitochondria.

Since other studies had shown that GRIM-19 knockout mice cannot survive beyond E 9.5 (Huang et al., 2004), I was interested in investigating the effects of knock down of GRIM-19 in mammalian cells, especially with regard to the mitochondria. A lentiviral system was used to generate a knock down stable line. Alternatively, I had also designed siRNAs to specifically knock down GRIM-19. From Figure 3.5 A and B, it is clear that both the methods mentioned above led to a significant depletion of GRIM-19 protein levels. These were verified by immunostaining as well. From the immunofluorescence, our results suggest that depletion of GRIM-19 does not change the mitochondrial morphology.

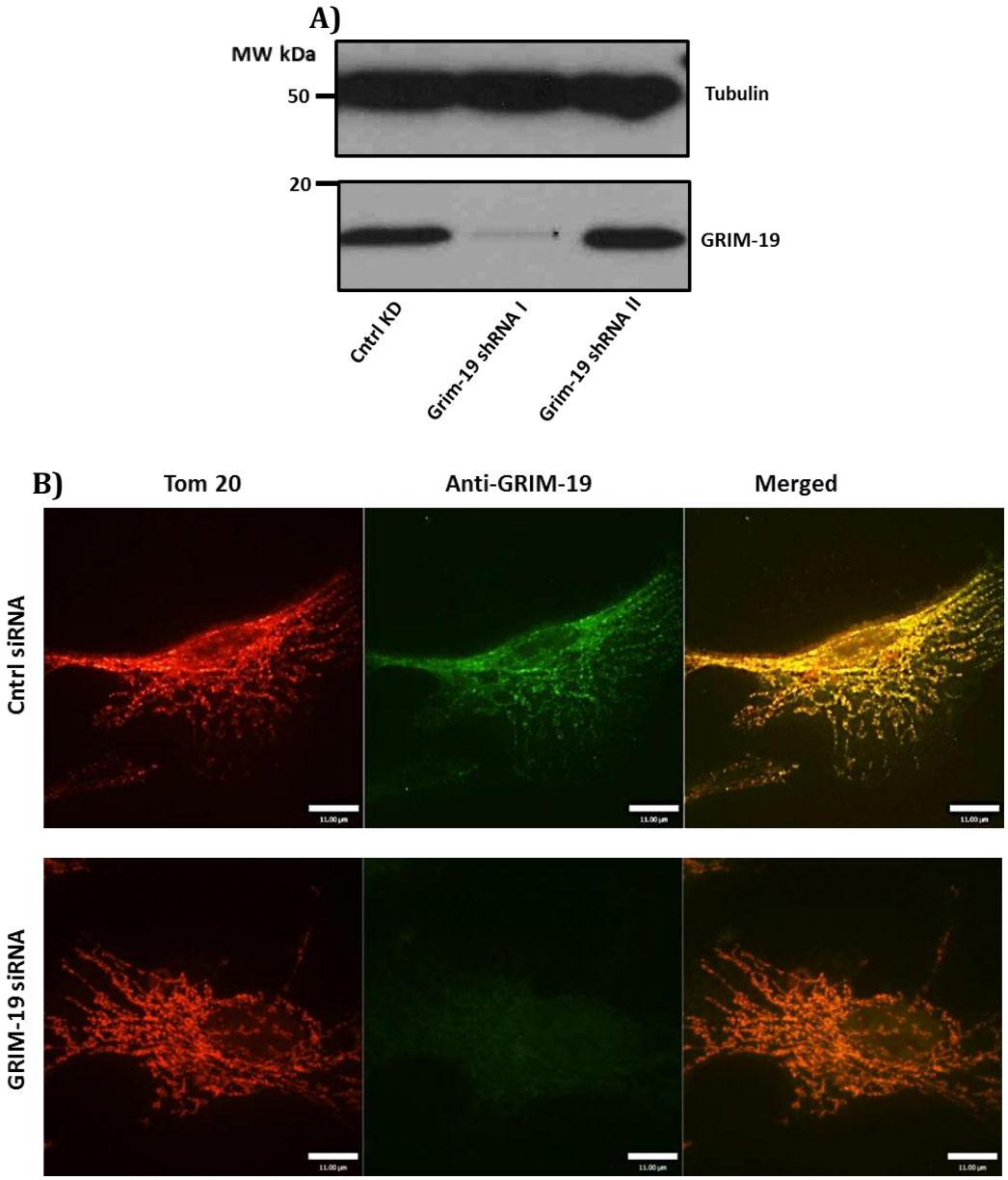

Figure 3-5: Effects of GRIM-19 knockdown on mitochondrial morphology

A) HeLa cells were infected with a pLVRNAi lentiviral system for generation of stable GRIM-19 knock-down cell line. After selection with 2 µM puromycin for cells successfully infected, the cells from control and GRIM-19 siRNA were harvested and analyzed using Western blot to confirm the knock down of GRIM-19 efficiency. As seen from the above figures, shRNA proved to be efficient in knocking down GRIM-19.

B) HeLa cells were transfected with control siRNA or GRIM-19 siRNA before being fixed by 4% paraformaldehyde and permeablizing with 0.5% Triton X-100, followed by staining with Tom20 antibody or a GRIM-19 antibody. Scale bar: 11µm

3.1.3 GRIM-19 does not control mitochondrial dynamics

As mentioned earlier, mitochondria are highly dynamic organelles that constantly undergo fission and fusion (Chan, 2006). Once I confirmed that overexpression of or depletion of GRIM-19 does not affect the mitochondrial morphology, I was curious to find out if GRIM-19 plays a role in mediating mitochondrial dynamics. A Fluorescence Recovery After Photobleaching (FRAP) assay is useful in studying the dynamics of structures (Day et al., 2012). Hence, I employed the same to analyze the effects of overexpression of GRIM-19 and knockdown of it on mitochondrial dynamics. However, a significant difference of fluorescence recovery levels and fluorescence rates between the control and GRIM-19 overexpressing cells were not found (Figure 3.6 A and D). Figures 3.6 B and C show the mean fluorescence recovery curve individually of both control- and GRIM-GFP vectors.

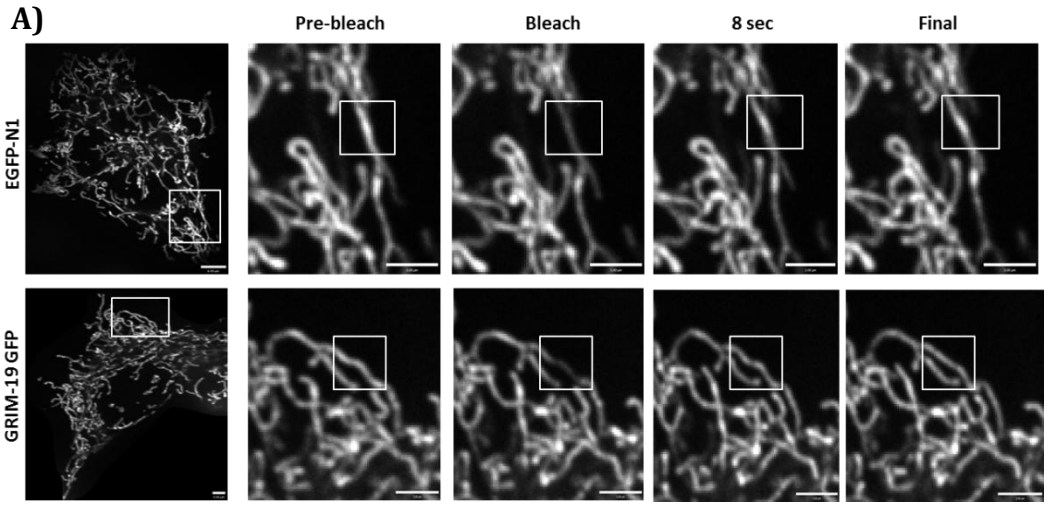
A)
Pre-bleach
Bleach
8 sec
Final
EGFP-N1
GRIM-19 GFP

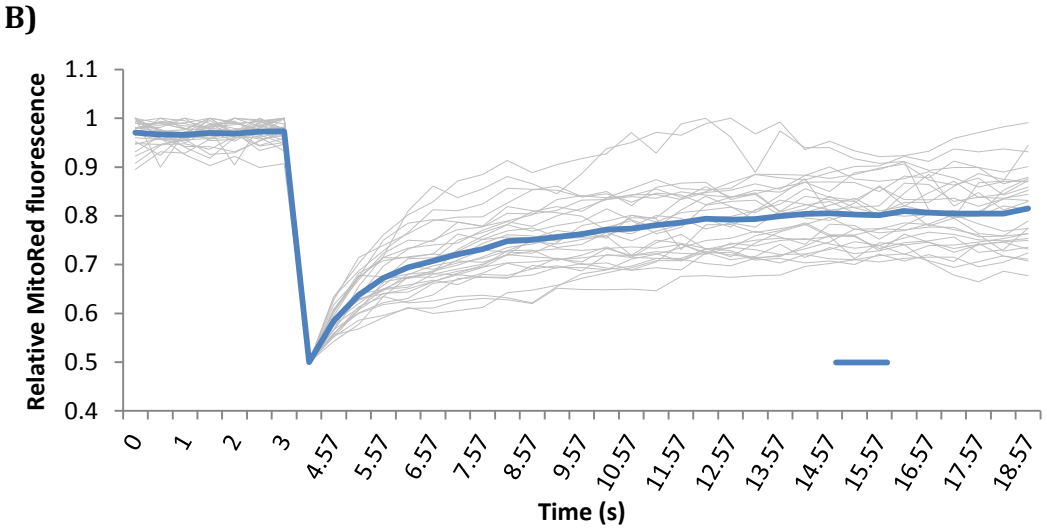
B)
Relative MitoRed fluorescence
1.1
1
0.9
0.8
0.7
0.6
0.5
0.4
0
1
2
3
4.57
5.57
6.57
7.57
8.57
9.57
10.57
11.57
12.57
13.57
14.57
15.57
16.57
17.57
18.57
Time (s)

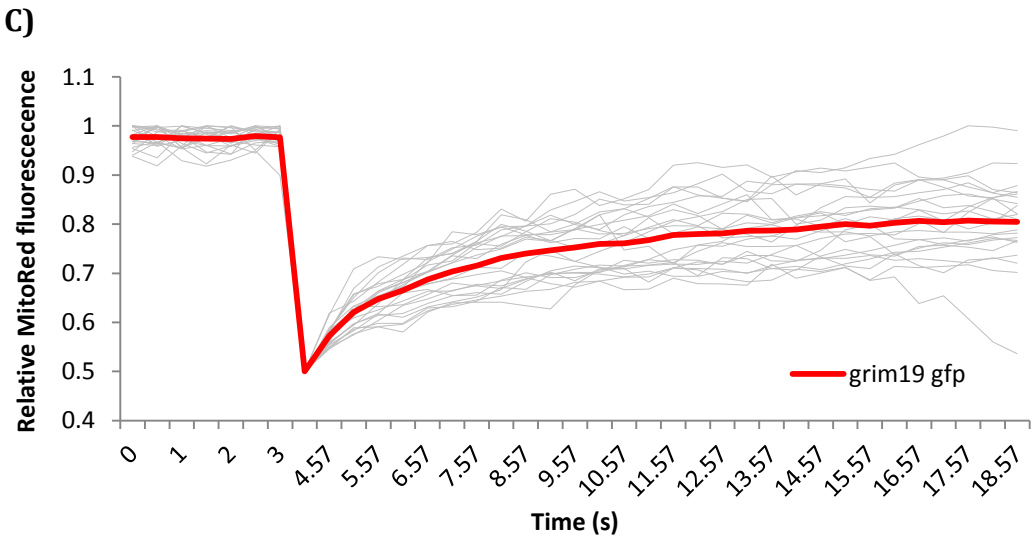
C)
Relative MitoRed fluorescecence
1.1
1
0.9
0.8
0.7
0.6
0.5
0.4
grim19 gfp
0
1
2
3
4.57
5.57
6.57
7.57
8.57
9.57
10.57
11.57
12.57
13.57
14.57
15.57
16.57
17.57
18.57
Time (s)

D)

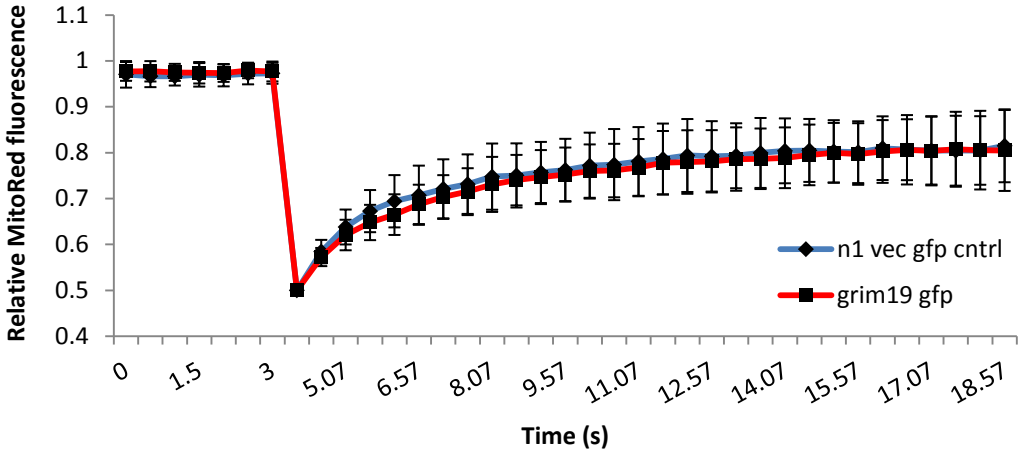

Figure 3-6: Effects of GRIM-19 over expression on mitochondrial dynamics

A) Representative images of mitochondrial signal recovery in fluorescence recovery after photobleaching (FRAP) assay. HeLa cells stably expressing mito-DsRed were transfected with an EGFP-N1 control vector or a GRIM-19 GFP plasmid as indicated.
B) Live-cell imaging was performed at an interval of 0.5 s. A 2 × 2 μm^2 square region of interest (ROI) was selected on the mitochondrial fiber and photobleached
C) Representative curves of individual experiments showing the mean recovery curve. MitoRed cells were transfected with an EGFP-N1 vector.
D) Representative curves of individual experiments showing the mean recovery curve. MitoRed cells were transfected with GRIM-19 GFP.
Normalized recovery curves of mito-DsRed signal intensity after photobleaching.

I also observed that when the FRAP experiment was performed with GRIM-19 depleted cells, the fluorescence recovery levels and rates were comparable to that of control knockdown cells, indicating that GRIM-19 may not play a role by being part of the mitochondrial dynamics machinery. These can be verified from Figures 3.7 A and D which show the representative images for the indicated time points during the FRAP assay. Figures 3.7 B and C are the compilation of fluorescence recovery curves of individual samples with their mean.

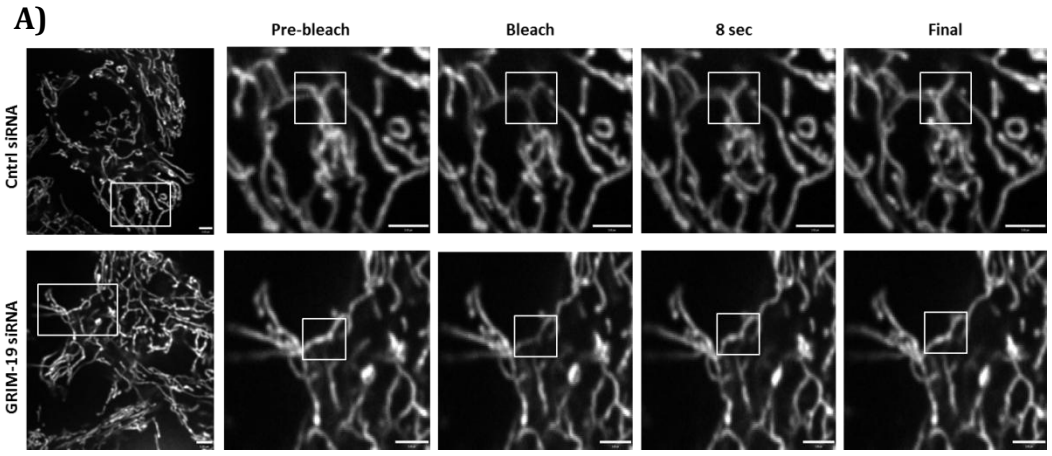
A)
Pre-bleach
Bleach
8 sec
Final
Cntrl siRNA
GRIM-19 siRNA

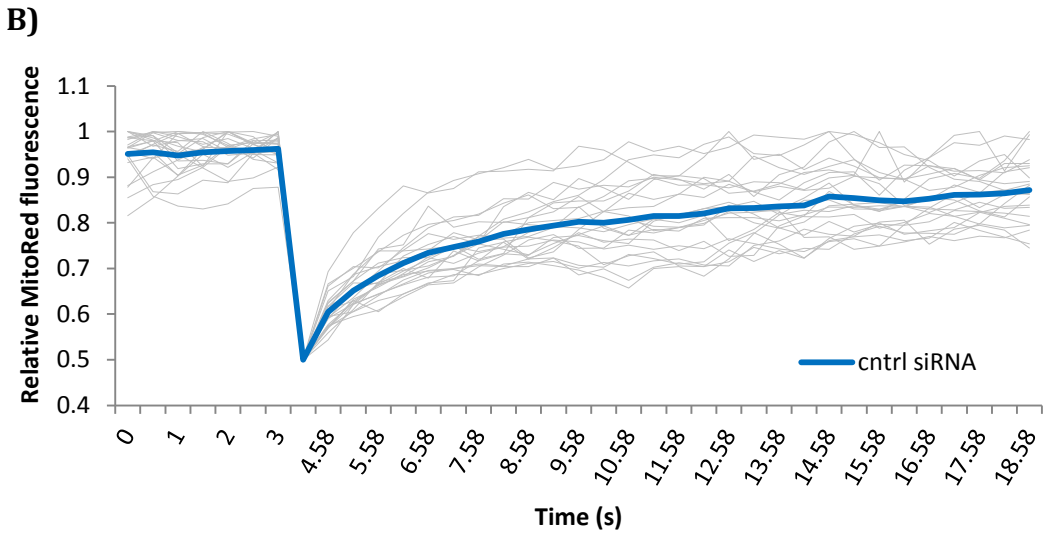
B)
Relative MitoRed fluorescence
1.1
1
0.9
0.8
0.7
0.6
0.5
0.4
cntrl siRNA
0
1
2
3
4.58
5.58
6.58
7.58
8.58
9.58
10.58
11.58
12.58
13.58
14.58
15.58
16.58
17.58
18.58
Time (s)

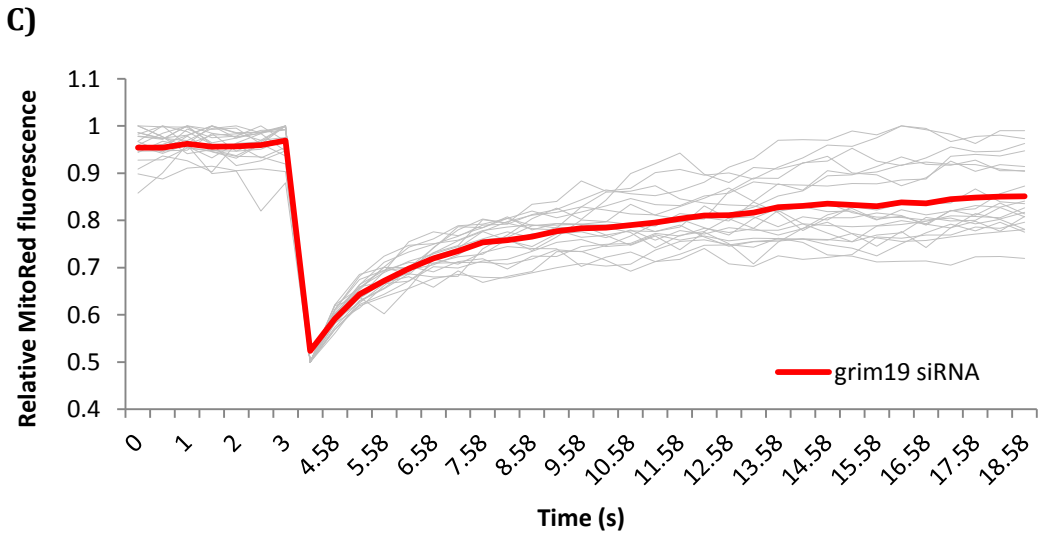
C)
Relative MitoRed fluorescence
1.1
1
0.9
0.8
0.7
0.6
0.5
0.4
grim19 siRNA
0
1
2
3
4.58
5.58
6.58
7.58
8.58
9.58
10.58
11.58
12.58
13.58
14.58
15.58
16.58
17.58
18.58
Time (s)

D)

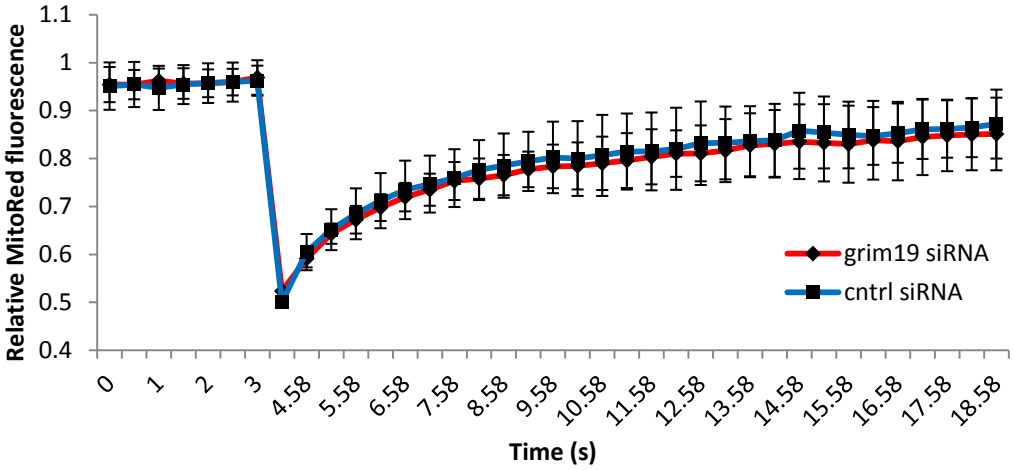

Figure 3-7: Effects of GRIM-19 knockdown on mitochondrial dynamics

A) Representative images of mitochondrial signal recovery in fluorescence recovery after photobleaching (FRAP) assay. HeLa cells stably expressing mito-DsRed were transfected with control siRNA or GRIM-19 siRNA as indicated. Live-cell imaging was performed at an interval of 0.5 s. A 2 × 2 μm2 square region of interest (ROI) was selected on the mitochondrial fiber and photobleached

B) Representative curves of individual experiments showing the mean recovery curve. MitoRed cells were transfected with cntrl siRNA.

C) Representative curves of individual experiments showing the mean recovery curve. MitoRed cells were transfected with GRIM-19 siRNA.

D) Normalized recovery curves of mito-DsRed signal intensity after photobleaching.

3.2 EFFECTS OF GRIM-19 ON MITOCHONDRIAL FUNCTIONS

3.2.1 Depletion of GRIM-19 increases ROS production

Our aim of the project in large was to characterize the GRIM-19 protein and dissect its mitochondria-related roles. Following experiments that were designed to study the mitochondrial morphology and dynamics, I carried out analysis of mitochondrial functions such as production of ROS, maintenance of mitochondrial membrane potential and the generation of ATP under GRIM-19 knockdown conditions. Firstly, I measured the ROS production in control and GRIM-19 knockdown cells

by using the DHE dye. The fluorescence of the dye indicates the level of ROS in the cells. This fluorescence was measured by Fluorescence Activated Cell Sorting (FACS). Quantification analysis revealed that knockdown of GRIM-19 increases the ROS levels in the cells by about 30%. Figure 3.8 A shows the scatter plot as seen from the results of FACS while Figure 3.8 B shows the quantification.

A)

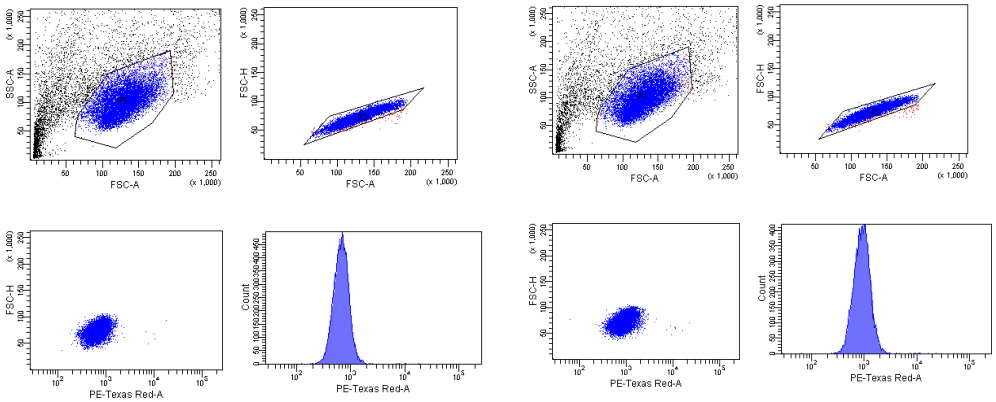

B)

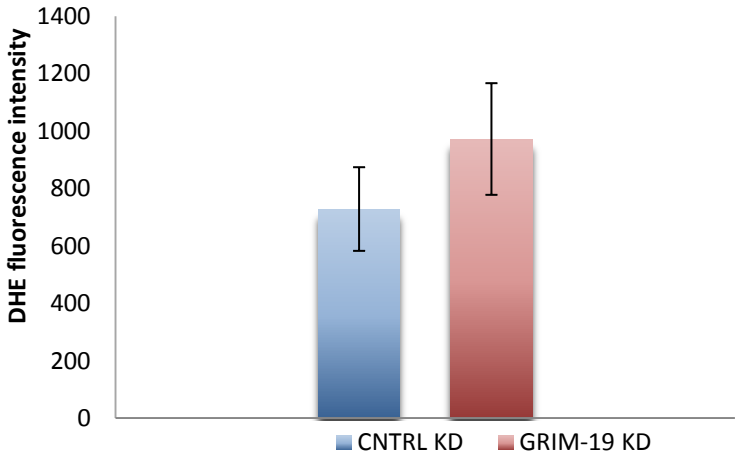

Figure 3-8: Effects of GRIM-19 KD on mitochondrial function- ROS

A) Control KD or GRIM-19 KD stable cells were washed with PBS and trypsinized and collected in medium containing DHE before analyzing by Flow cytometry. Cells were progressively sorted for live and single cells before measuring the intensity of DHE which indicates the amount of ROS in the cells.

B) Bar graph represents the fluorescence intensity of DHE for Control and GRIM-19 KD cells. Results indicate that knock down of GRIM-19 increases ROS production in cells.*$P<0.05$(student t test). Error bars represent + SEM.

3.2.2 Knockdown of GRIM-19 does not alter mitochondrial membrane potential

The next parameter I wanted to study was the alteration of mitochondrial membrane potential upon depletion of GRIM-19. To this end, I used the TMRM dye, a lipophilic slow potential sensitive membrane distribution compound. It distributes in the inner mitochondrial membrane driven by the mitochondrial membrane potential. This leads to an increase in its fluorescence (Gerencser et al., 2012). In apoptotic cells, the reagent is dispersed throughout the cells at a concentration that yields a minimum fluorescence when excited. As mentioned earlier, FACS was used to measure the fluorescence of TMRM as well. As shown in Figure 3.9 A and B, our results show that the read out between knockdown of GRIM-19 and control cells for the TMRM intensity is similar.

A)

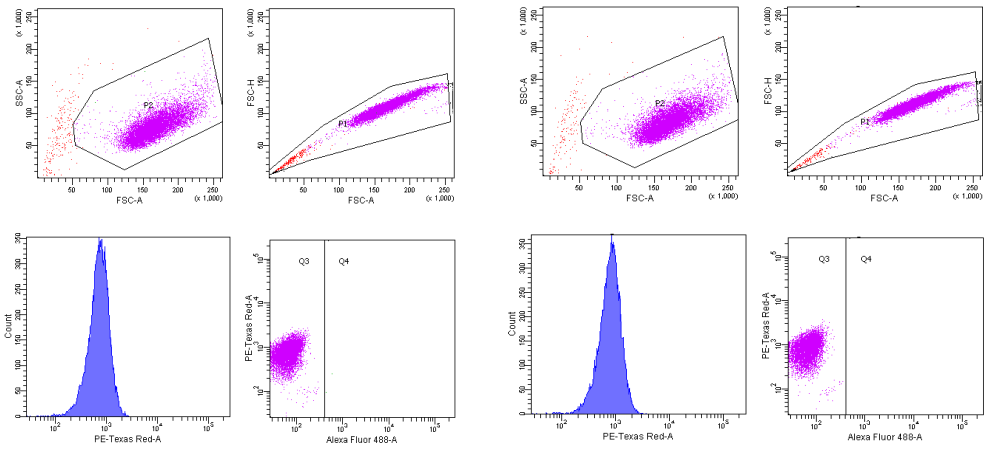

Control KD **GRIM-19 KD**

B)

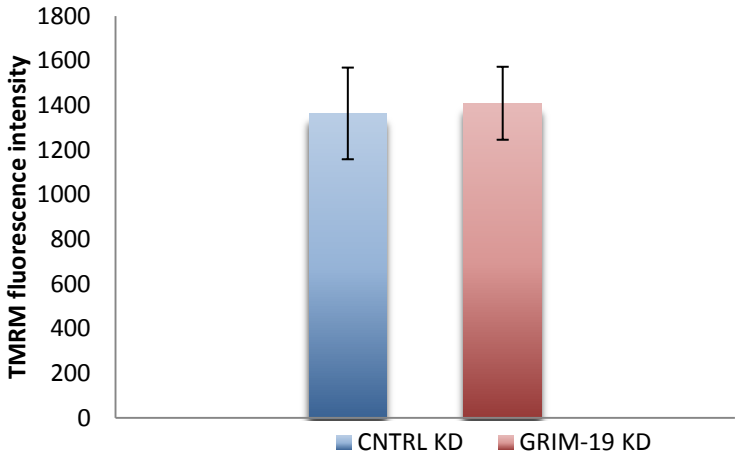

Figure 3-9: Effects of GRIM-19 KD on mitochondrial function- Mitochondrial potential

A) Control KD or GRIM-19 KD stable cells were washed with PBS and trypsinized and collected in medium containing TMRM before analyzing by Flow cytometry. Cells were progressively sorted for live and single cells before measuring the intensity of TMRM which indicates the mitochondrial potential in the cells.

B) Bar graph represents the fluorescence intensity of TMRM for Control and GRIM-19 KD cells. Results indicate that knockdown of GRIM-19 does not affect the maintenance of mitochondrial potential.

3.2.3 ATP generation is not affected by GRIM-19 knockdown

Since GRIM-19 was reported to be a subunit of Complex I of the mitochondrial respiratory chain (Fearnley et al., 2001), I was interested in investigating the effect of depletion of GRIM-19 on ATP production. This assay was carried out using the ATP determination Kit (Invitrogen) that utilizes the luciferase enzyme activity. The conversion of the substrate luciferin to oxyluciferin by the luciferase enzyme requires the presence of ATP. Thus the intensity of luminescence will give an indication of the amount of ATP present in the cells. Results of this assay upon quantification show that there is no significant difference between cells of control and GRIM-19 knockdown.

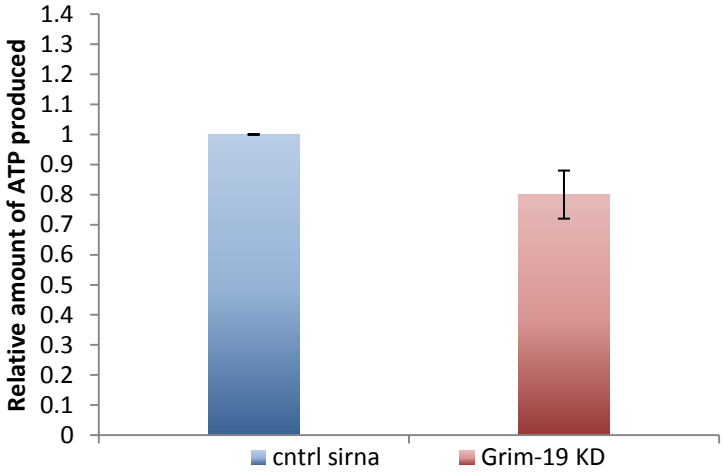

Figure 3-10: Effects of GRIM-19 KD on mitochondrial function- ATP
Control KD or GRIM-19 KD cells were washed with PBS, collected in ATP Buffer and incubated in the same for 5 min followed by centrifugation to obtain the lysate. The lysate is then measured for its ATP content using ATP determination Kit (Invitrogen). This utilizes the luciferase assay. Bar graph represents relative amount of ATP produced. Results indicate that GRIM-19 KD does not significantly affect ATP production.

3.3 ROLE OF GRIM-19 IN CELL CYCLE

There have been several reports as mentioned in detail in the introduction section, about GRIM-19 knockdown favouring cell proliferation and thus leading to cancer (Cheng et al., 2014; Hao et al., 2012; Li et al., 2012; Zhang et al., 2011; Zhou et al., 2013; Zhou et al., 2009). This is understandable since GRIM-19 is proposed to be a cell death regulator. To look into this at a cell division level, I wanted to examine which phase is altered during GRIM-19 knockdown. To this end, I fixed control and GRIM-19 knockdown cells and used the PI dye to stain the DNA, the amount of which indicates the stage of cell cycle. The fluorescence of PI is measured by FACS. As represented in Figure 3.11, there was a marked reduction in the percentage of cells in the sub-G1 phase from 10 % in control knockdown cells to 4.9 % in GRIM-19 KD cells. Similarly the G1 phase also shows a reduction from 59.9% in control KD cells to 49.6% in GRIM-19 KD cells. A corresponding increase in the percentage of cells in G2 was observed as 16.1% in control KD cells to 28.8% GRIM-19 KD cells.

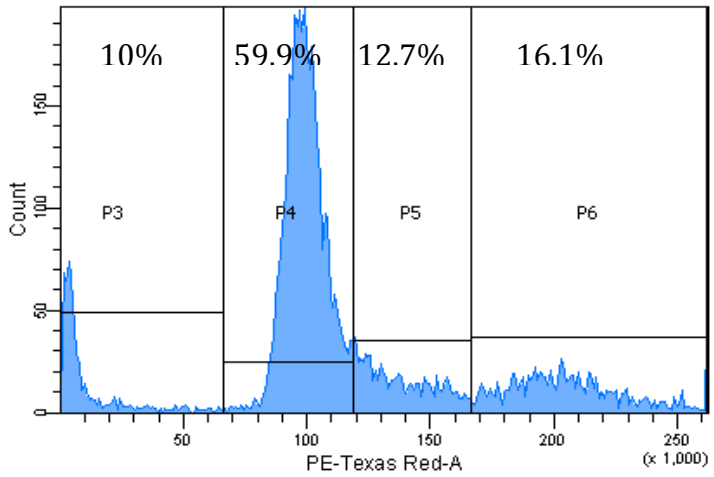

Control KD

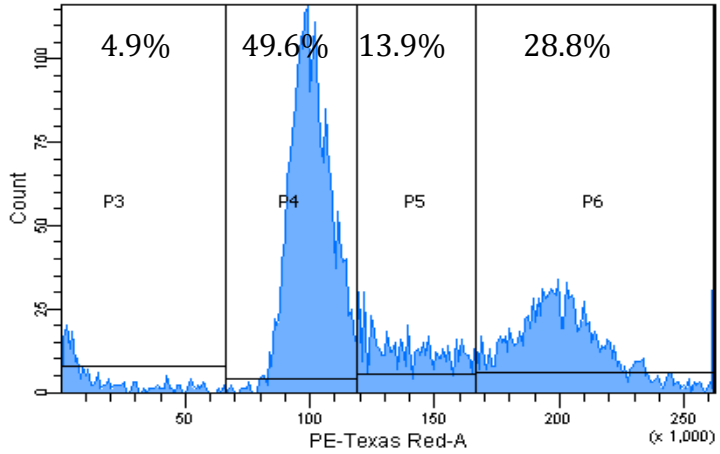

GRIM-19 KD

Figure 3-11: Effects of GRIM-19 KD on cell cycle

Control KD stable line cells or GRIM-19 KD cells were fixed using ice cold 70% percent ethanol after all floating and attached cells were collected. The cells were then treated with RNAse before being stained by PI and subjected to FACS analysis. The percentage value in the scatter plots represents the percentage of cells in sub G0, G1, S and G2 phases.

3.4 EFFECT OF IFNB/RA TREATMENT ON CELLS

3.4.1 The combination of IFNβ/RA causes more cell death than either drug alone

GRIM-19 was identified originally from a screen that provided resistance to IFNβ/RA treatment. However, to validate this in my hands, I resorted to treating HeLa cells with the single agent alone (IFNβ or RA) or the combination of both. It is now widely accepted that the combination causes more cell death than either drug alone. This was found to be true in our trials as well. The various panels labeled with the corresponding treatment in Figure 3.12 show that IFNβ alone causes 25% lesser cell death and RA alone causes about 40% lesser cell death compared to the combination treatment of IFNβ/RA which causes about 50% death of cells. PI was used as the dye for this assay too to detect dead cells by FACS.

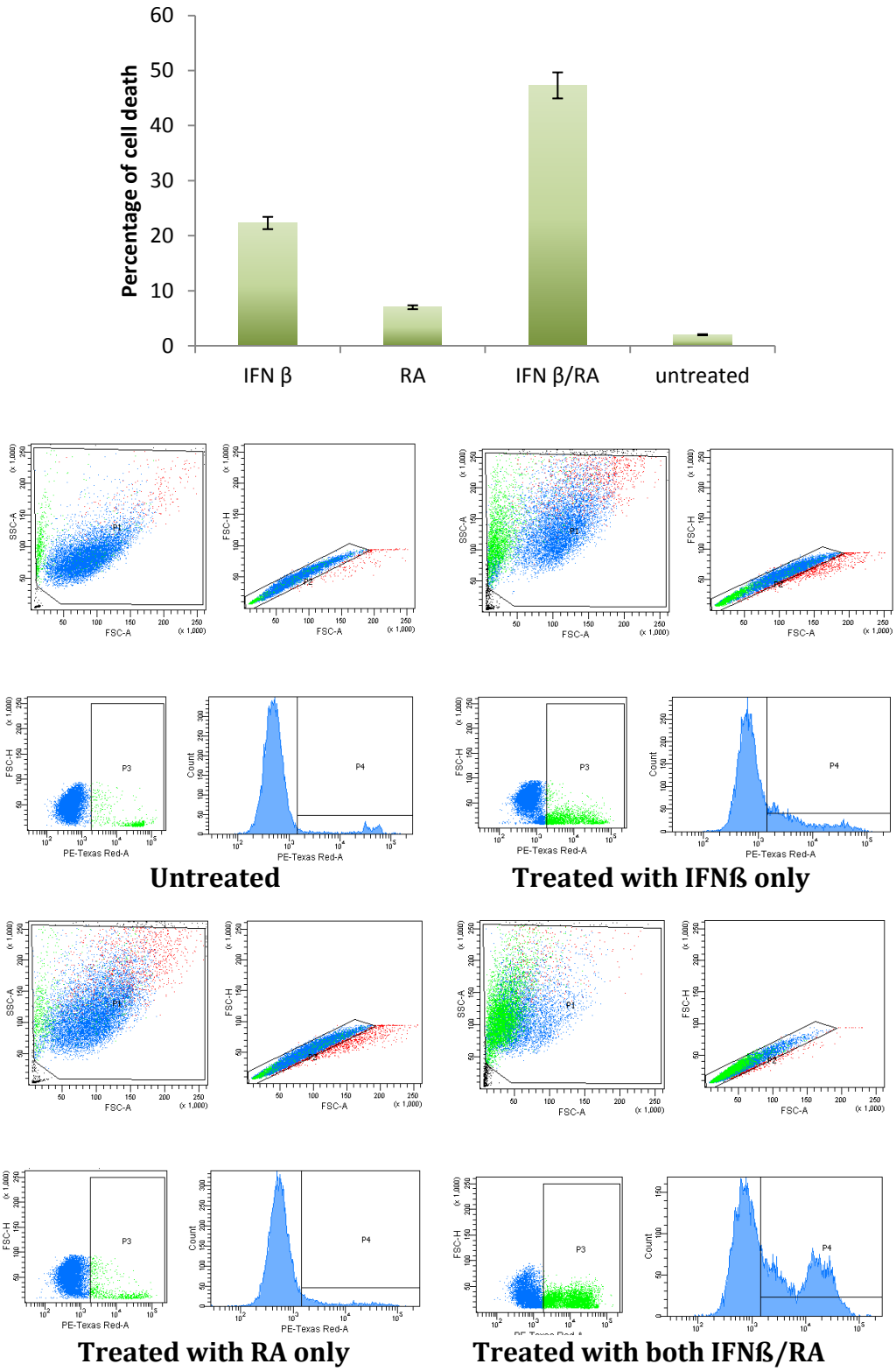

Fugure 3-12: Effects of IFNß/RA treatment on cell death

HeLa cells were subjected to various combinations of treatments. Cells were either untreated or Treated with IFNß only at 30ng/ml or RA only at 1µM or a combination of both IFNß/RA at the indicated concentrations for 48 hours. After 48 hours, floating and attached cells were harvested and stained with PI before subjecting to FACS analysis. Results clearly show that IFNß/RA combination is much more potent in inducing cell death than either drug alone.

3.4.2 Treatment with IFNβ/RA causes fragmentation of mitochondria but does not change the localization of GRIM-19

Once the cell death inducing capabilities of IFNβ/RA were studied, I was curious to know the effects of this treatment on mitochondrial morphology and the localization of GRIM-19. The rationale behind was to identify if GRIM-19 is translocated from mitochondria to cytoplasm to execute the apoptotic signaling pathway induced by the treatment. HeLa cells were treated with IFNβ/RA for 48 hours before being fixed and immunostained to detect protein signals. In Figure 3.13, the top panel shows untreated cell exhibiting normal mitochondrial morphology whereas the bottom panel with treated cells shows fragmented mitochondria. One can also observe from these figures that the localization of GRIM-19 remains in the mitochondria with or without treatment.

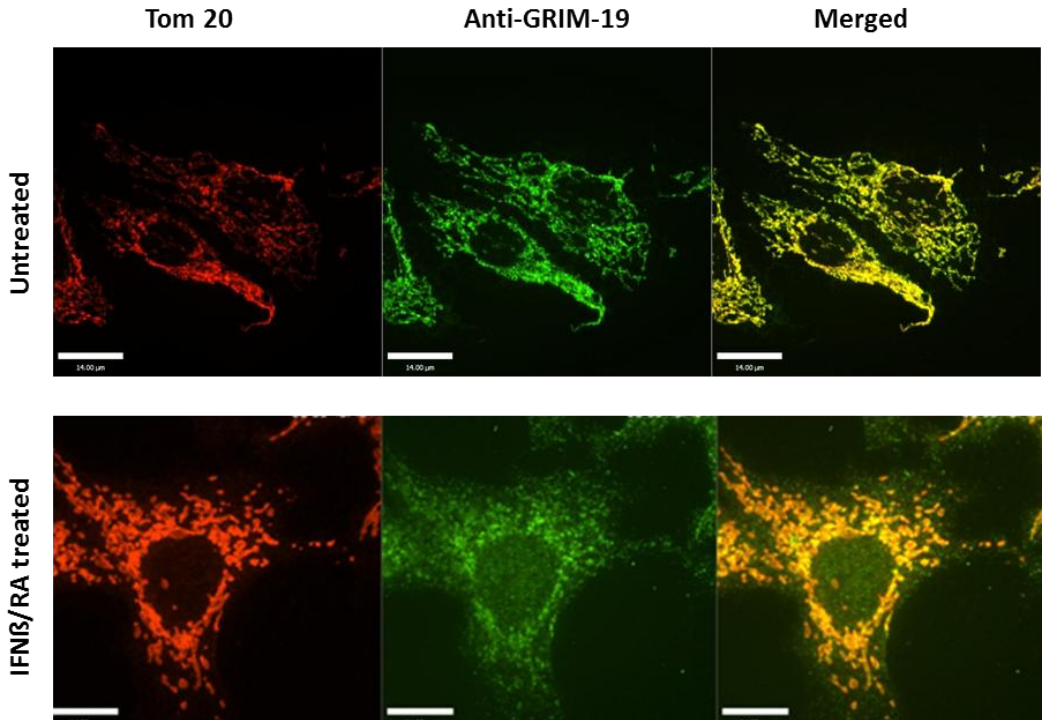

Figure 3-13: Effect of IFNß/RA treatment on the localization of GRIM-19

HeLa cells were either treated or untreated with IFNß/RA for 48 hours at 30ng/ml (IFNß) and RA (1µM. After the treatment, cells were fixed with 4% paraformaldehyde and permeabilized with 0.5 %Triton X 100 for 30 mins followed by staining with an anti Grim-19 antibody or Tom20 antibody. Results indicate that the mitochondria are fragmented upon IFNß/RA. However, this does not change the localization of GRIM-19. Scale bar: 14µm

3.4.3 Knockdown of GRIM-19 provides resistance to IFNβ/RA induced cell death

Although GRIM-19 is shown as an effecter of cell death through the IFNβ/RA pathway (Angell et al., 2000), in order to test the dependency of this apoptotic signaling on GRIM-19, I decided to treat cells depleted of GRIM-19 with IFNβ/RA to see the percentage of rescue of cell death. The methodology of the experiment was similar to previously mentioned ones as I used PI to detect dead cells by FACS. Indeed, as it is clear from Figure 3.14, knockdown of GRIM-19 rescues cell death by about 20%. The

various panels below the quantification graph represent the scatter plots from the Flow Cytometry experiment for the indicated treatment.

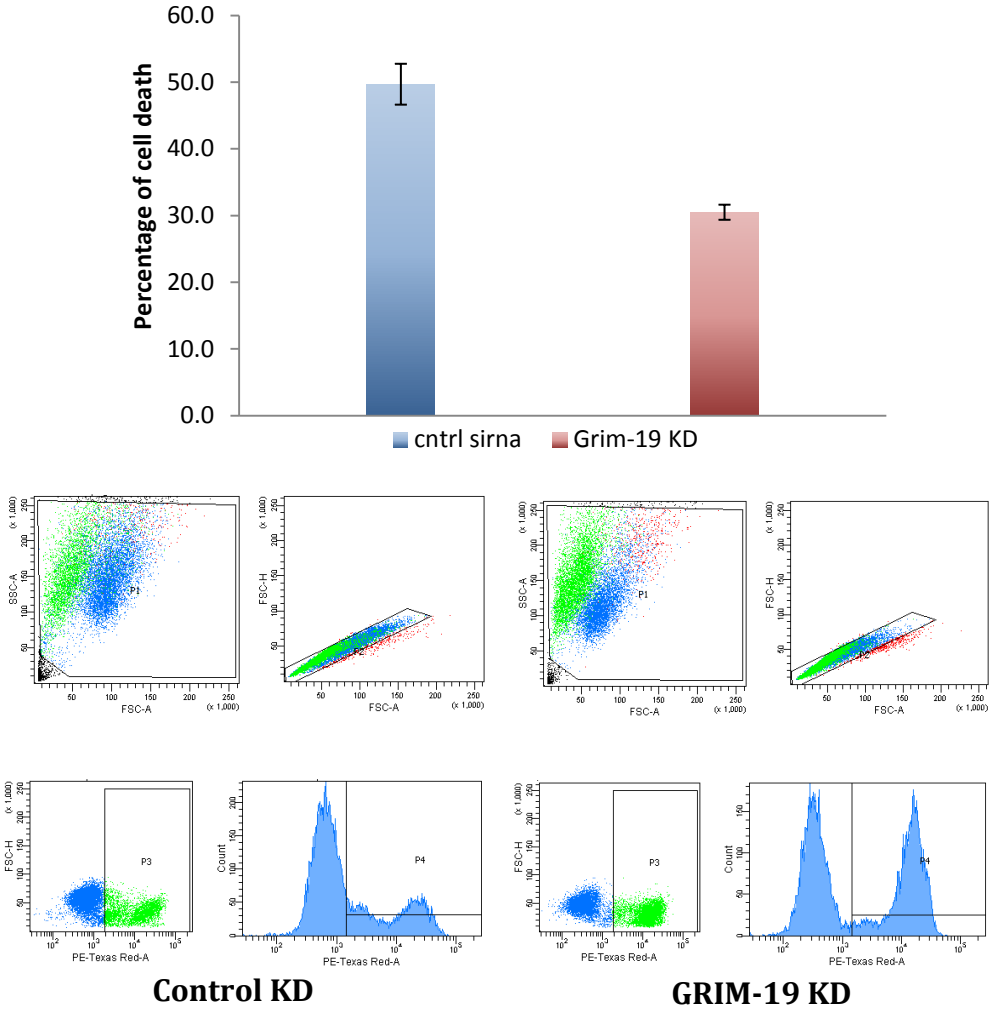

Figure 3-14: GRIM-19 KD rescues cell death induced by IFNß/RA

HeLa cells were transfected with cntrl siRNA or GRIM-19 siRNA. After 48 hours, the cells were treated with IFNß/RA (at 30ng/ml IFNß and 1µM RA) for 48 hours. Following this, all cells (floating and attached) were collected and stained with PI to identify the dead cells and analyzed by Flow cytometry. Bar graph represents the percentage cell death in cntrl and GRIM-19 KD background. Results indicate that GRIM-19 KD provides resistance to IFNß/RA induced cell death. *P<0.01; Error bars represent+SEM

3.4.4 Fragmentation of mitochondria caused by IFNβ/RA is partially rescued by GRIM-19 KD

From the previous results two observations are made clear; firstly, GRIM-19 KD offers resistance to IFNβ/RA treatment and secondly, this

combinatorial treatment causes the fragmentation of mitochondria. My next experiment was to examine the effect of this treatment on the morphology of mitochondria when GRIM-19 is depleted. Figure 3.15 shows mitochondrial morphology in control and GRIM-19 KD cells upon treatment with IFNβ/RA. It is observed that in the GRIM-19 knockdown cells, some mitochondria exhibit normal tubular morphology. A bar graph represents the quantification analysis for the percentage of cells exhibiting different mitochondrial morphology under the indicated treatments.

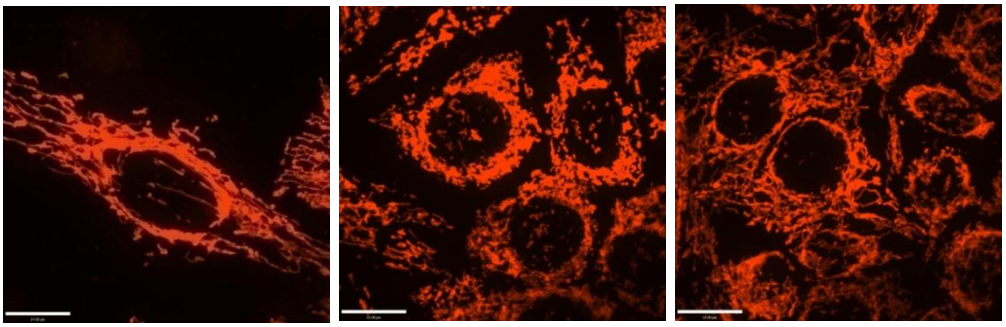

Untreated **cntrl siRNA+IFNβ/RA** **GRIM-19 siRNA+IFNβ/RA**

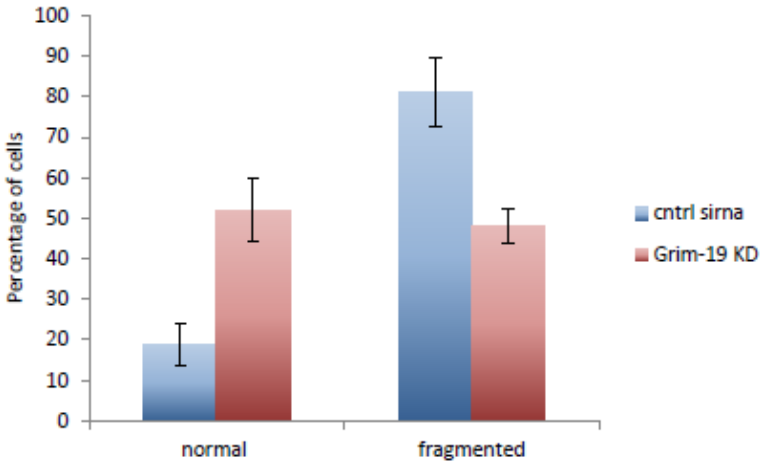

Figure 3-15: Effects of IFNβ/RA on mitochondrial morphology in normal and GRIM-19 depleted cells

HeLa cells were transfected with either control siRNA or GRIM-19 siRNA prior to treatment with IFNβ/RA for 48 hours. Cells were stained with MitoTracker RED before performing live cell imaging. Normal : *P<0.01; Fragmented *P<0.01 Scale bar: 14μm

3.5 CHARACTERIZATION OF PATIENT TUMOR DERIVED GRIM-19 MUTANTS

3.5.1 Mutations in GRIM-19 do not affect the morphology of mitochondria

After a near comprehensive analysis of the wild type GRIM-19, I came across a report that had identified mutations in the tumor tissues of patients with head and neck cancer. I was enthusiastic to know what the possible effects could be of these mutants on the normal functioning of the mitochondria. To begin with, these GRIM-19 mutants, i.e. L71P, L91P, A95T and T113A were cloned into the appropriate C-terminal tags (Flag and GFP). The foremost experiment was to over express these mutant proteins into HeLa cells to see the effect of these mutations on the mitochondrial morphology. In Figure 3.16, the various panels show these mutant proteins with different tags as indicated. As is obvious from the images, the mitochondrial morphology looks normal.

A)

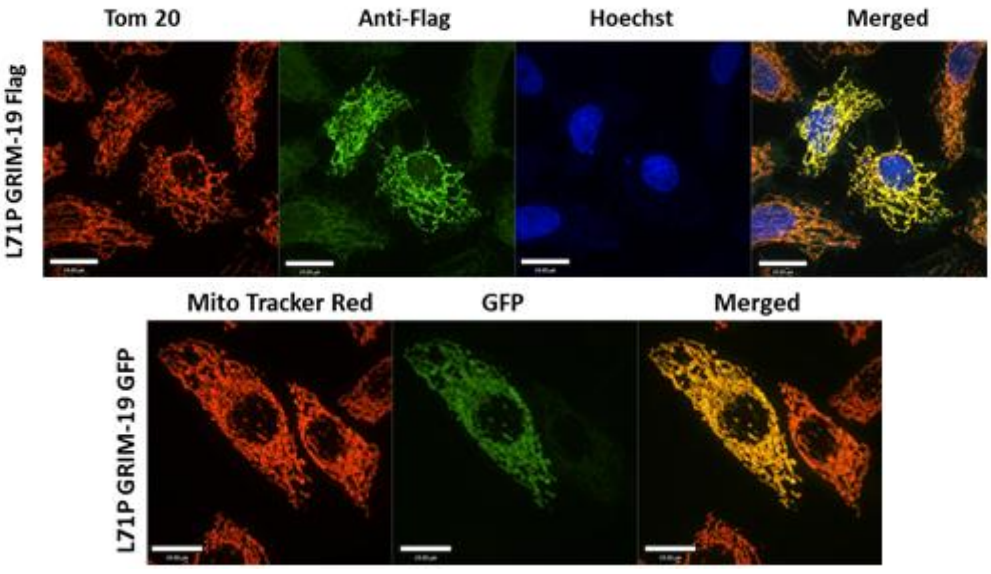

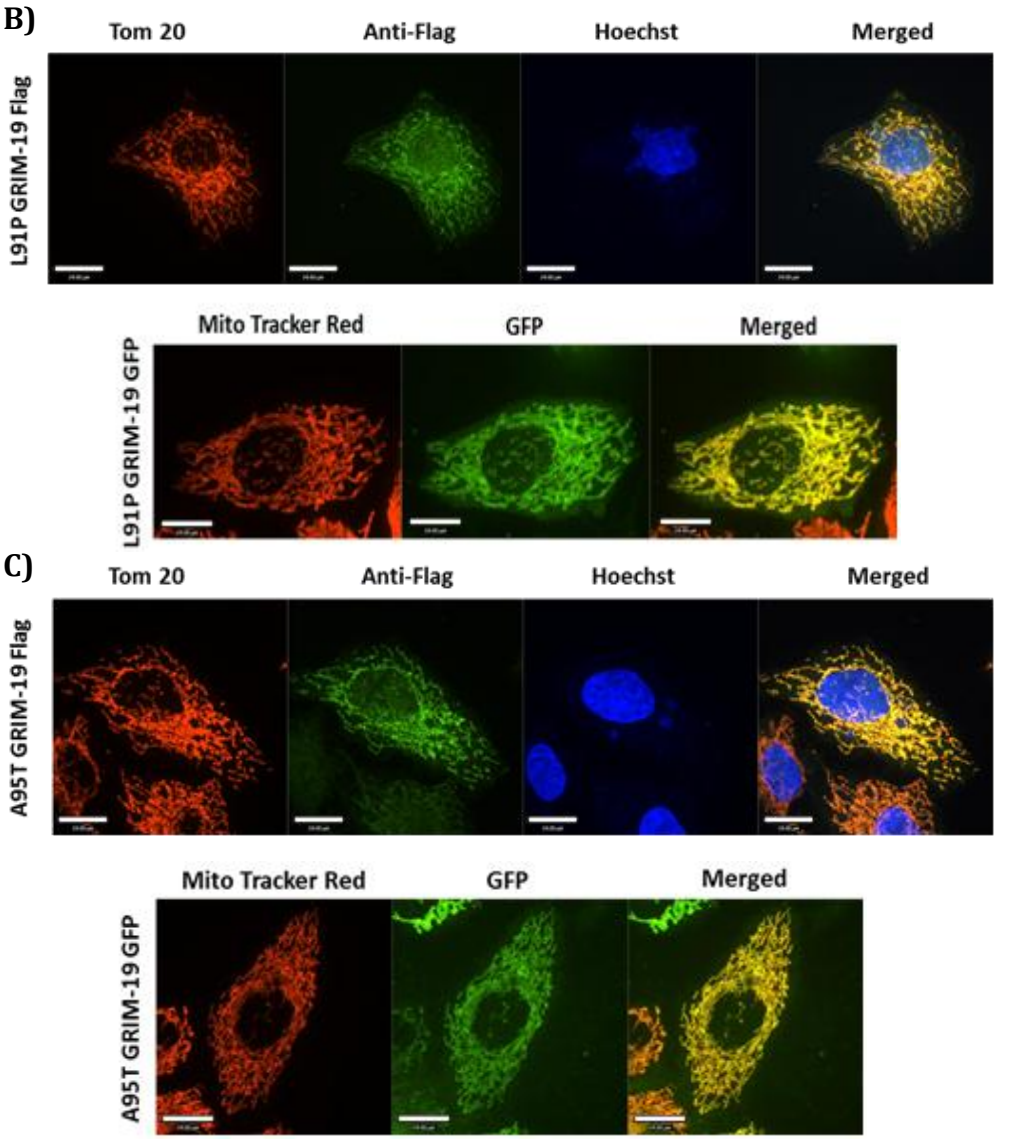
B)
Tom 20
Anti-Flag
Hoechst
Merged
L91P GRIM-19 Flag
Mito Tracker Red
GFP
Merged
L91P GRIM-19 GFP
C)
Tom 20
Anti-Flag
Hoechst
Merged
A95T GRIM-19 Flag
Mito Tracker Red
GFP
Merged
A95T GRIM-19 GFP
D)
Tom 20
Anti-Flag
Hoechst
Merged
T113A GRIM-19 Flag
Mito Tracker Red
GFP
Merged
T113A GRIM-19 GFP

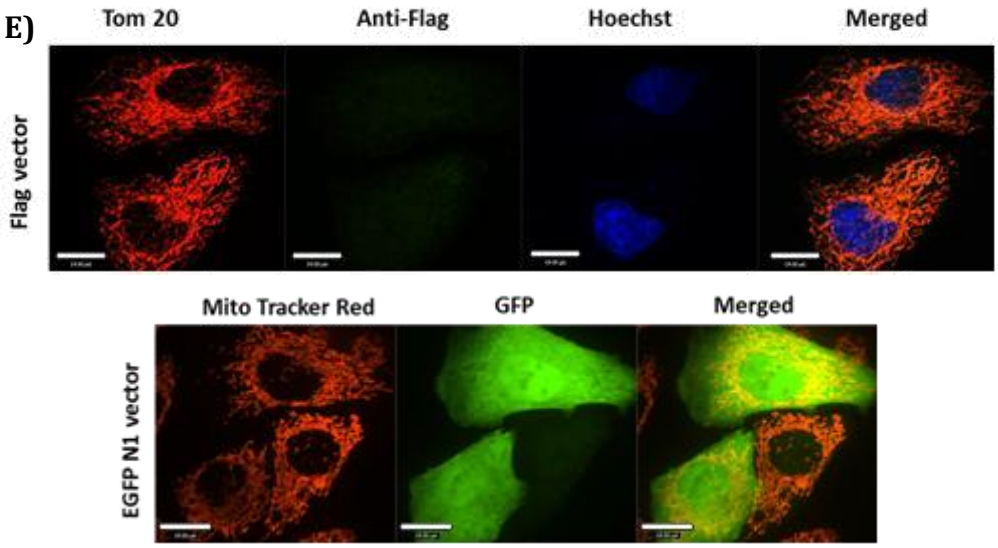

Figure 3-16: Localization of GRIM-19 mutants and their effect on mitochondrial morphology

A) HeLa cells were transfected with either L71P GRIM-19 Flag or L71P GRIM-19 GFP. As in the first panel, cells were fixed with 4% paraformaldehyde and permeabilized with 0.5 % Triton in BSA before staining with Tom20 and Anti-Flag antibody before staining with Hoechst. In the second panel, cells were transfected with L71P GRIM-19 GFP and stained with MitoTracker RED before being subjected to live cell imaging

B) HeLa cells were transfected with either L91P GRIM-19 Flag or L91P GRIM-19 GFP. As in the first panel, cells were fixed with 4% paraformaldehyde and permeabilized with 0.5 % Triton in BSA before staining with Tom20 and Anti-Flag antibody before staining with Hoechst. In the second panel, cells were transfected with L91P GRIM-19 GFP and stained with MitoTracker RED before being subjected to live cell imaging

C) HeLa cells were transfected with either A95T GRIM-19 Flag or A95T GRIM-19 GFP. As in the first panel, cells were fixed with 4% paraformaldehyde and permeabilized with 0.5 % Triton in BSA before staining with Tom20 and Anti-Flag antibody before staining with Hoechst. In the second panel, cells were transfected with A95T GRIM-19 GFP and stained with MitoTracker RED before being subjected to live cell imaging

D) HeLa cells were transfected with either T113A GRIM-19 Flag or T113A GRIM-19 GFP. As in the first panel, cells were fixed with 4% paraformaldehyde and permeabilized with 0.5 % Triton in BSA before staining with Tom20 and Anti-Flag antibody before staining with Hoechst. In the second panel, cells were transfected with T113A GRIM-19 GFP and stained with MitoTracker RED before being subjected to live cell imaging

E) HeLa cells were either transfected with Flag vector or EGFP-N1 as controls. For the Flag vector, cells were processed in the same way as mentioned earlier. EGFP-N1 transfected cells were stained with MitoTracker RED before performing live cell imaging.

Scale bars for all images:14μm

3.5.2 Mutants of GRIM-19 have a similar expression level as that of wild type

My next objective was to clarify if the expression levels of these mutants are different or similar to that of wild type protein. HEK 293Tcells were used for this purpose. The different mutants with their tags were over expressed in HEK 293 T cells and Western blot was run to observe their expression levels. The top panels in Figure 3.17 show that all the mutants are expressed at comparable levels to that of wild type.

Proceeding further with the characterization of mutants, my interest was to analyze their effects on the production of ROS since our previous results showed that knockdown of GRIM-19 increases the ROS production. To this end, my strategy was to overexpress the mutants in the GRIM-19 knockdown stable line. This was conceived to eliminate the possible effects of endogenous GRIM-19. This demands that we verify the overexpression of the mutants in the GRIM-19 knockdown stable line since there is a possibility of degradation of the mutant proteins by the shRNA against wild type GRIM-19. Therefore, I over expressed the GFP tagged mutant proteins *i.e.* L71P, L91P, A95T and T113A in GRIM-19 KD stable line and performed western blot. These results are shown in Figure 3.17 (bottom panel). Expression of the mutant proteins was well observed in the knockdown stable line.

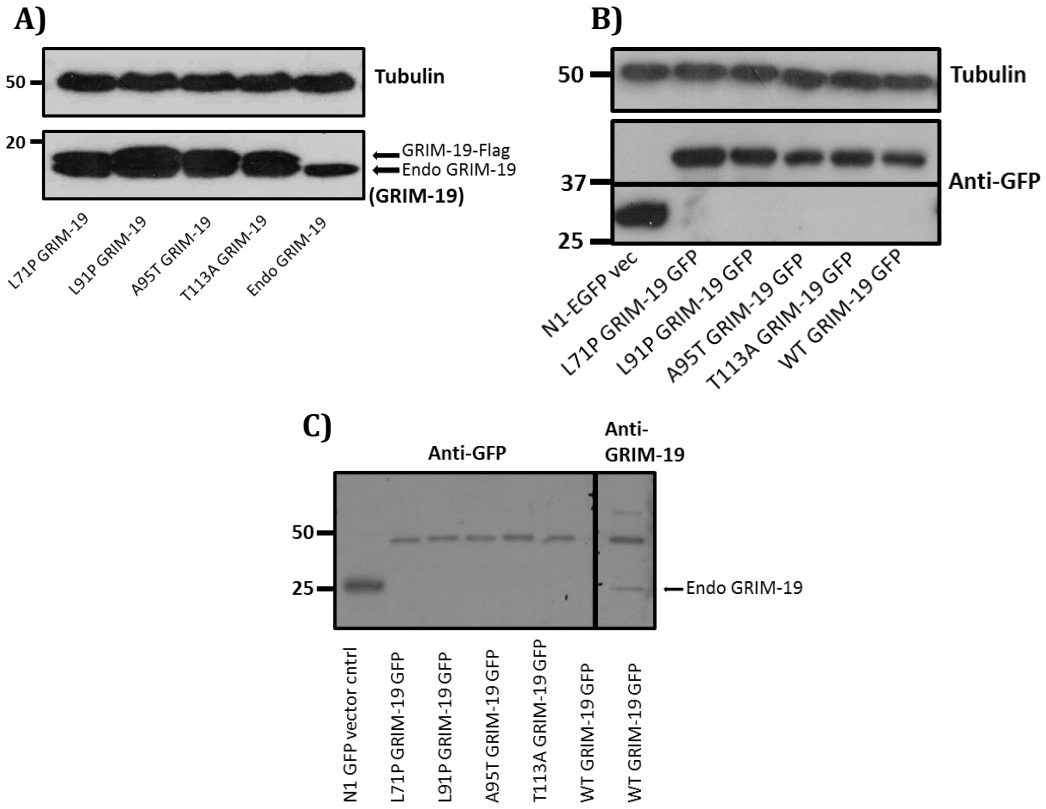

Figure 3-17: Expression levels of GRIM-19 mutants- L71P, L91P, A95T and T113A GRIM-19

A) 293T cells were transfected with L71P, L91P, A95T or T113A GRIM-19 Flag plasmids. Cells were then harvested and subjected to SDS-PAGE. Membranes were probed with Tubulin or GRIM-19 Antibody

B) 293T cells were transfected with L71P, L91P, A95T or T113A or WT GRIM-19 EGFP-N1 plasmids. Cells were harvested thereafter to run SDS-PAGE. Membranes were probed with Anti-GRIM-19 Antibody and Tubulin.

C) Since the following experiments involve over expressing the mutant GRIM-19-GFP proteins in the GRIM-19 KD stable cell line, their expression level in the same is shown as reference. It is clear that the mutants are expressed in the knockdown cells and the level of GRIM-19 KD is also indicated as control in the right half of the same figure. GRIM-19 KD cells were transfected with the mentioned mutants and harvested after 24 hours for Western blot analysis.

3.5.3 Mutant GRIM-19 does not alter the mitochondrial membrane potential

Since the GFP tagged mutants could be successfully over expressed in the knockdown stable line, these could now be used to study the effect of these mutations on the maintenance of mitochondrial membrane potential and the generation of ROS. The measurement was done in a similar method to that mentioned earlier in the results section. TMRM dye was used to indicate the mitochondrial membrane potential, the intensity of which was recorded by FACS. Results as seen from the bar graph in Figure 3.18 have not a significant difference between the various mutants and wild type GRIM-19. These are validated by the scatter plots seen in the same figure that show peaks of TMRM fluorescence for the different mutants, wild type and control vectors.

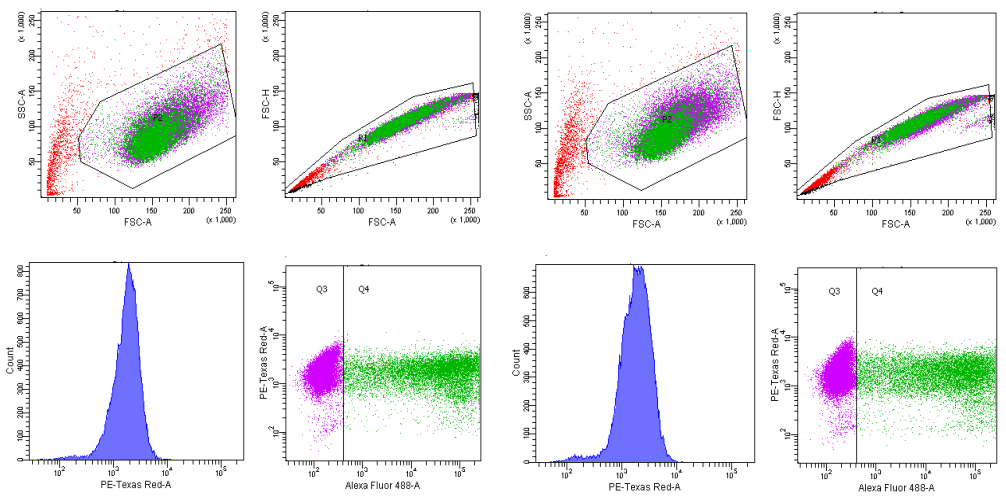

EGFP vector N1 in cntrl KD **EGFP vector in GRIM-19 KD**

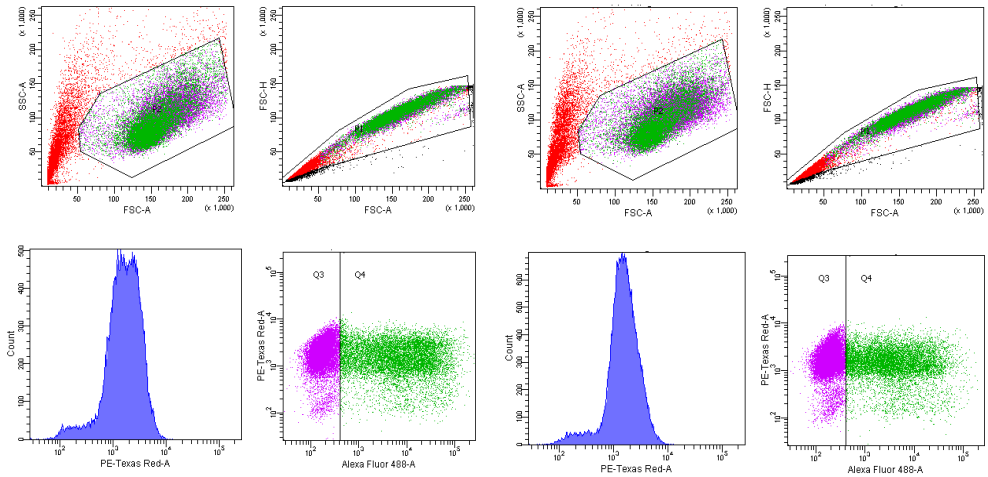

L71P GRIM-19 GFP in cntrl KD

L71P GRIM-19 GFP in GRIM-19 KD

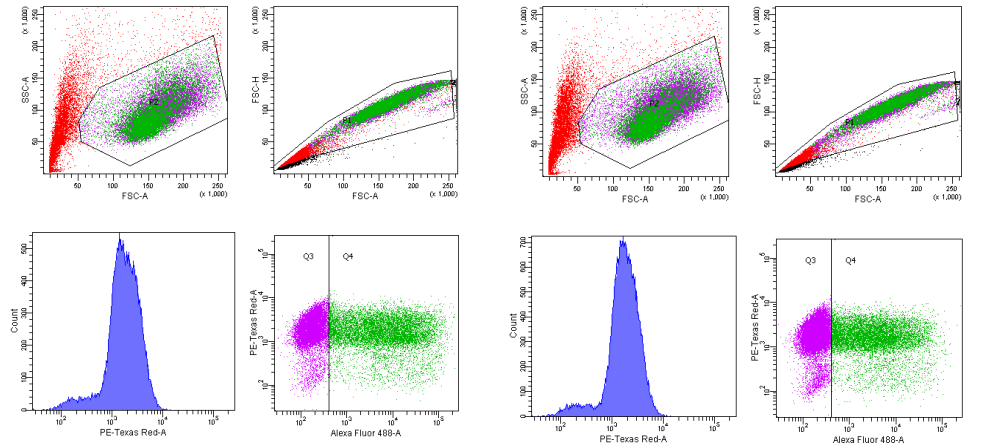

L91P GRIM-19 GFP in cntrl KD

L91P GRIM-19 GFP in GRIM-19 KD

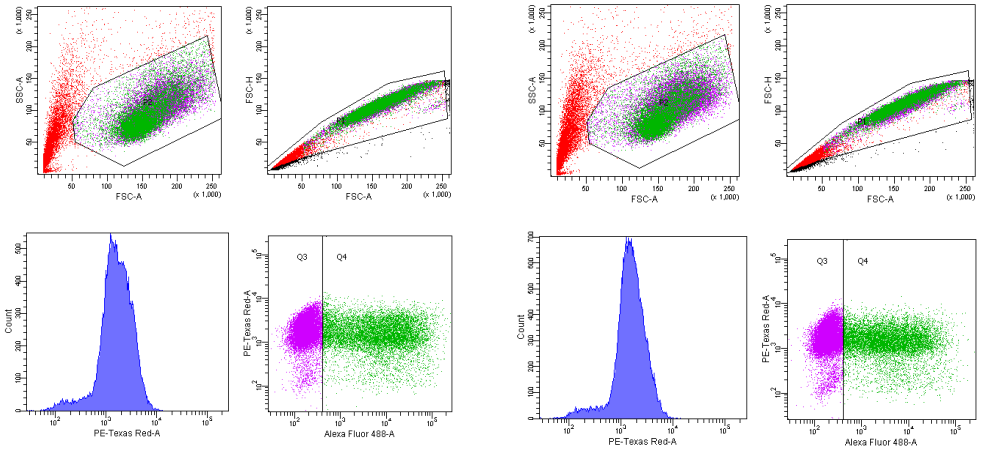

A95T GRIM-19 GFP in cntrl KD

A95T GRIM-19 GFP in GRIM-19 KD

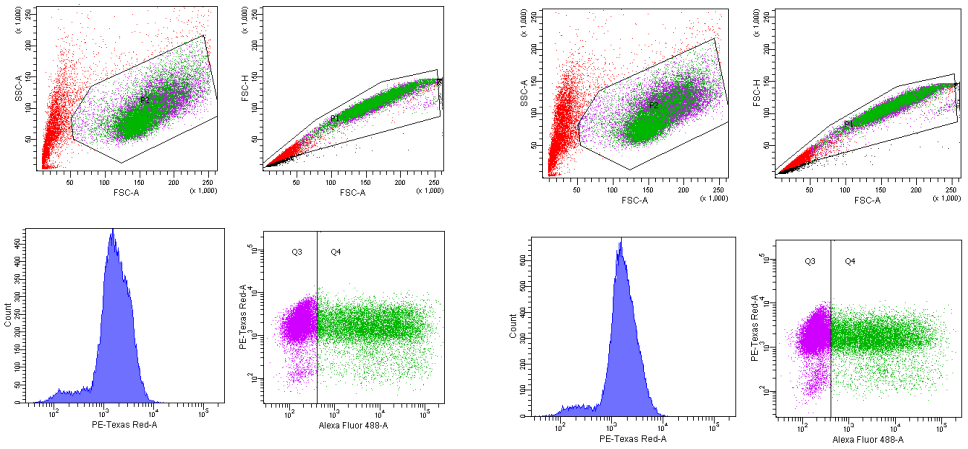

T113A GRIM-19 GFP in cntrl KD **T113A GRIM-19 GFP in GRIM-19 KD**

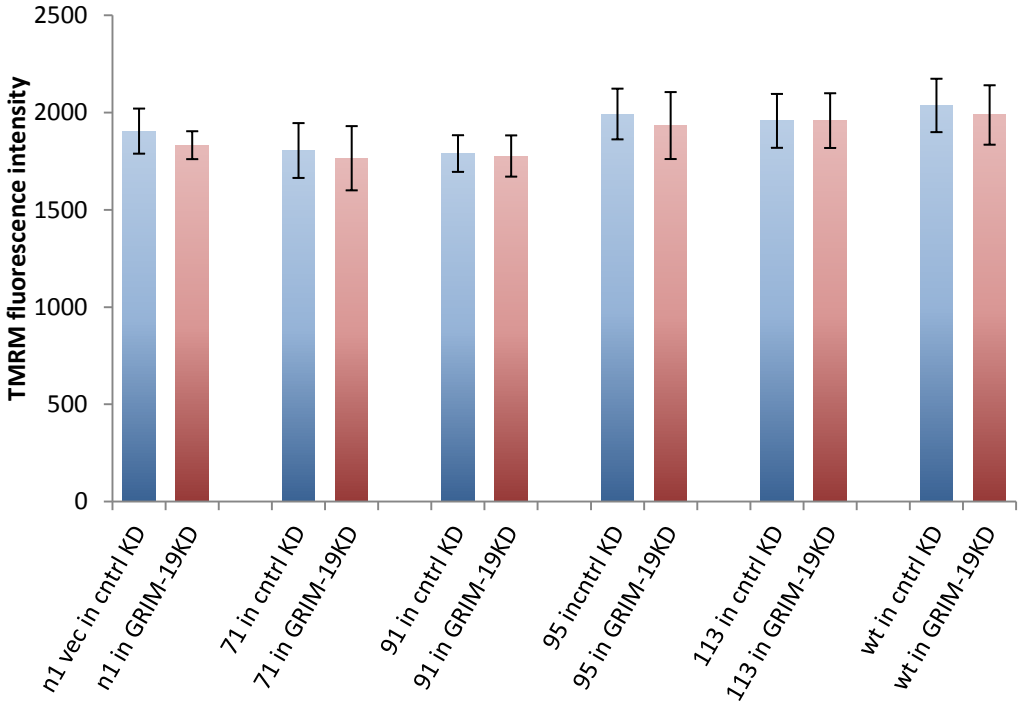

Figure 3-18: Effects of GRIM-19 mutants on mitochondrial functions- Mitochondrial potential

Control KD or GRIM-19 KD stable cells were transfected with the indicated plasmids. One day post transfection, cells were washed with PBS, trypsinized and collected in medium containing TMRM. Fluorescence intensity of TMRM indicates the mitochondrial potential in the cells. This was analyzed by Flow Cytometry. Cells were progressively selected to finally analyze 10,000 live GFP positive single cells. GRIM-19 mutants do not seem to affect the mitochondrial

3.5.4 Mutants of GRIM-19 increase the ROS levels

As shown before, knockdown of GRIM-19 increases the ROS levels of the cell. Having known this, I next wanted to examine the mutants' effect on ROS production. This was measured after over expression of GFP tagged mutant GRIM-19 proteins in GRIM-19 KD stable line. DHE dye was used to measure the amount of ROS in the cells. GFP and TMRM double positive cells were sorted using Flow Cytometry. The results indicate an increase in ROS levels in the mutant expressing cells. The level of ROS was on an average (between the different mutants) 34.68% more in the cells expressing the different mutant forms of GRIM-19 in comparison to the GRIM-19 depleted cells. In the corresponding wild type GRIM-19 expressing cells, there was only a 15.6% increase in ROS levels indicating that when wild type GRIM-19 is supplied it could aid in the rescue of ROS increase. In other words, there is a rescue of about 22.58% in ROS levels when cells are replenished with wild type GRIM-19. These are shown in Figure 3.19. The scatter plots represent the peaks of DHE fluorescence in the various mutant or wild type or control over expressing cells as indicated. Quantification analysis is also presented in the bottom panel.

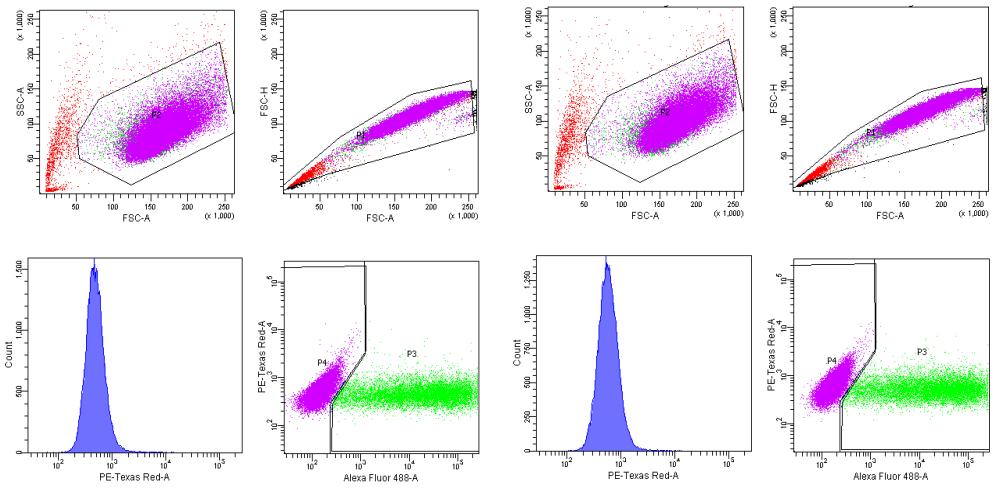

EGFP vector N1 in cntrl KD **EGFP vector in GRIM-19 KD**

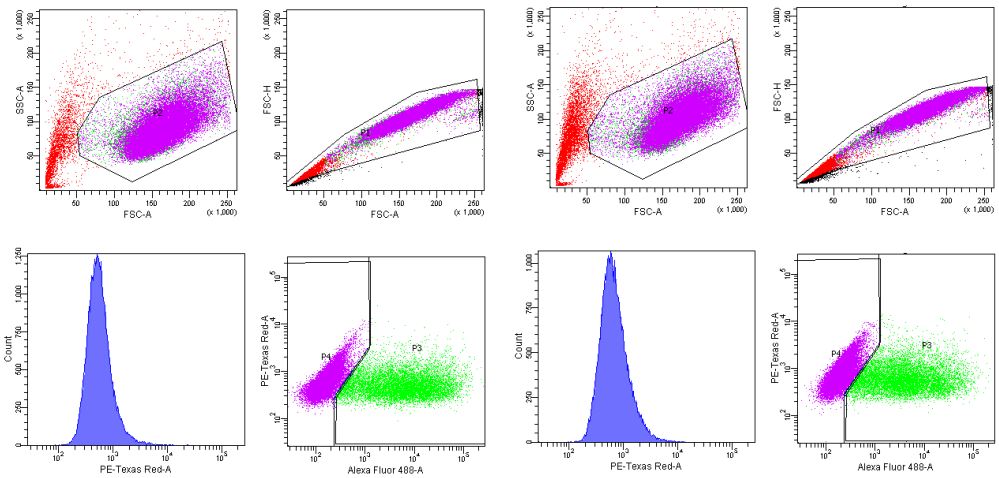

L71P GRIM-19 GFP in cntrl KD **L71P GRIM-19 GFP in GRIM-19 KD**

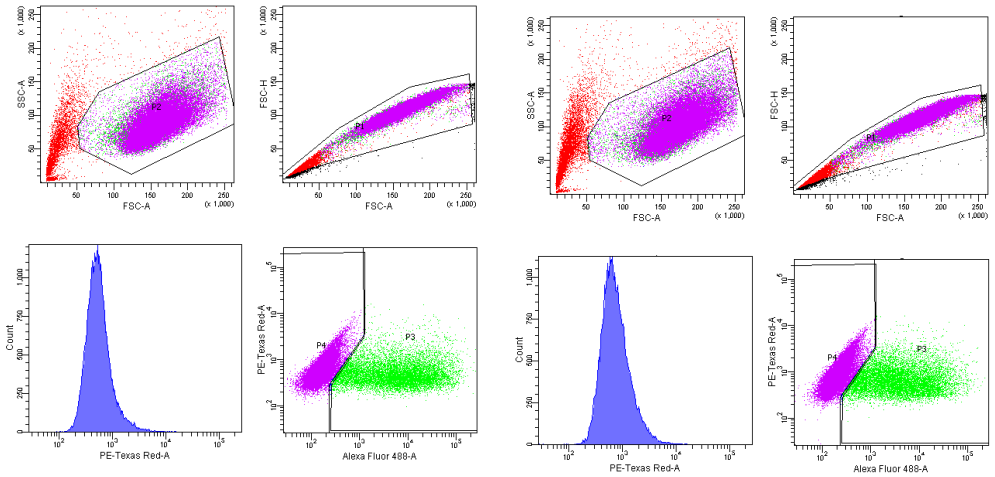

L91P GRIM-19 GFP in cntrl KD **L91P GRIM-19 GFP in GRIM-19 KD**

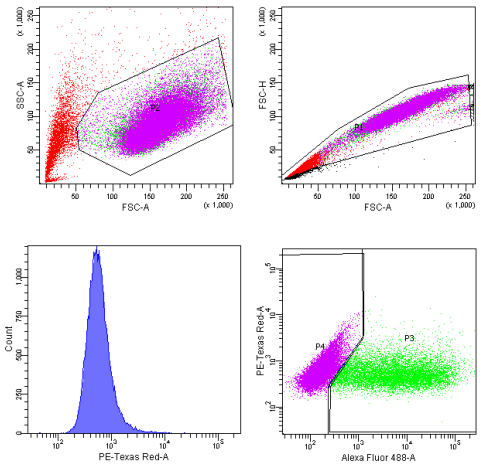

A95T GRIM-19 GFP in cntrl KD

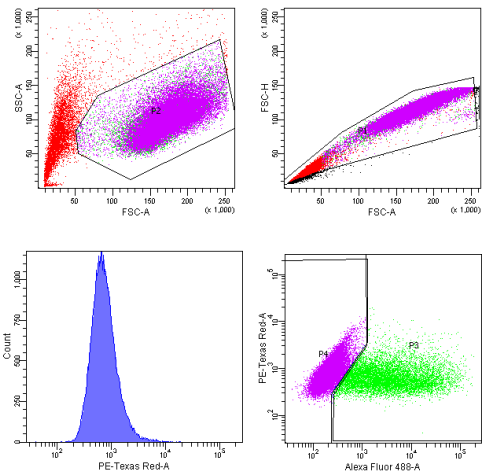

A95T GRIM-19 GFP in GRIM-19

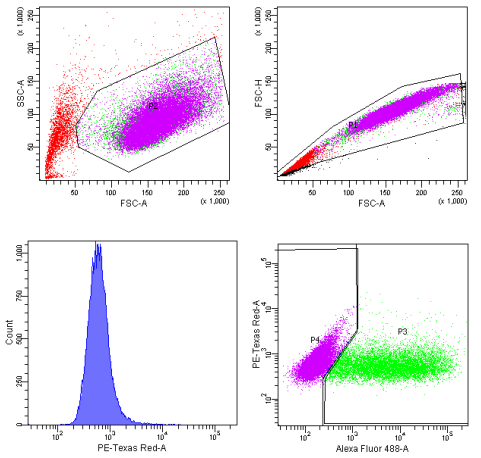

T113A GRIM-19 GFP in cntrl KD

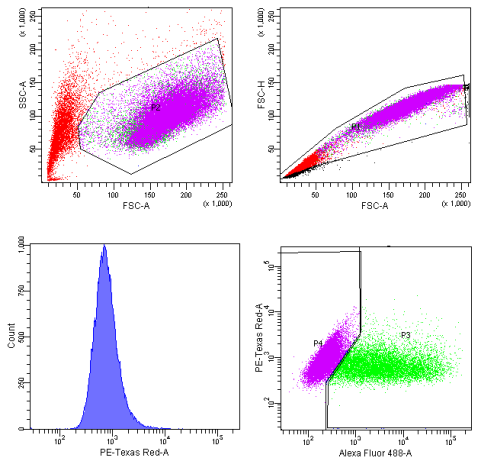

T113A GRIM-19 GFP in GRIM-19

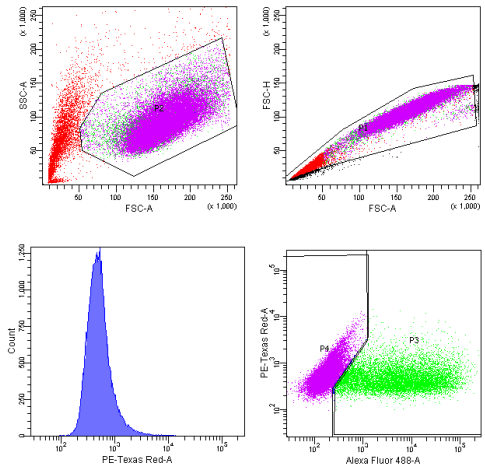

WT GRIM-19 GFP in cntrl KD

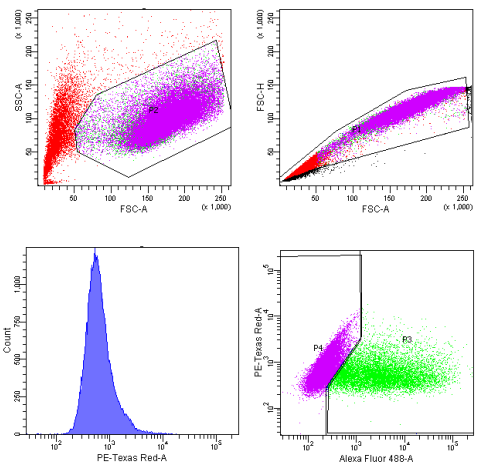

WT GRIM-19 GFP in GRIM-19 KD

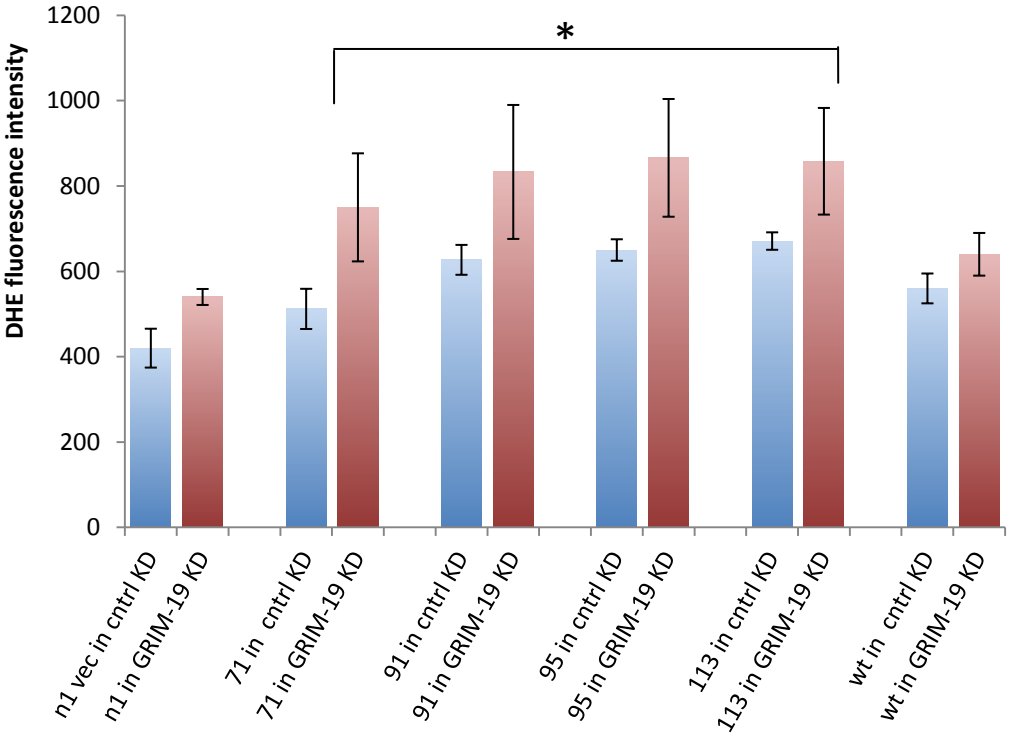

Figure 3-19: Effects of GRIM-19 mutants on mitochondrial functions-ROS

Control KD or GRIM-19 KD stable cells were transfected with the indicated plasmids. One day post transfection, cells were washed with PBS, trypsinized and collected in medium containing DHE. Fluorescence intensity of DHE indicates the ROS in the cells. This was analyzed by Flow Cytometry. Cells were progressively selected to finally analyze 10,000 live GFP positive single cells. GRIM-19 mutants are not able to rescue the increase in ROS caused by the knockdown of GRIM-19 whereas Wild type GRIM-19 transfected into GRIM-19 KD cells reduces the production of ROS. *P<0.05(student t test). Error bars represent + SEM

Chapter 4 DISCUSSION AND CONCLUSIONS

4.1 MITOCHONDRIAL LOCALIZATION OF GRIM-19

A number of groups, from the time of its identification have tried to pin point the localization of GRIM-19 inside the cell. The scientists who discovered GRIM-19 attributed its cellular localization to the nucleus (Angell et al., 2000). However, the immunofluorescence images are far from convincing. This could be the result of lack of developments in the imaging field at the time. Though subsequent studies projected a partial mitochondrial localization of GRIM-19, apart from the wide conviction that most of the protein accumulated in the nucleus at the time, these studies also had their laws which made the results unreliable. For example, in the study by Lufei *et al*., the authors used a tag on the N-terminal of the GRIM-19 protein, doing which, we show, affects the localization of the protein (Refer Figure 3.3 A and B). The reason that the N-terminal tags might affect the localization could be because the mitochondria localization signal (MLS) is usually present in the Nterminus of a mitochondria targeted protein. Hence, the tags have a probability of interfering with the normal translocation to the mitochondria. Later on, studies by the same group had ascertained that majority of GRIM-19 localizes to the mitochondria. Yet again, now with advancement in the imaging techniques, authors failed to provide convincing data (Huang et al., 2004; Lu and Cao, 2008). The MitoTracker

signal was well detected in the nucleus and the mitochondria in cells of both the studies looked highly fragmented not to mention the poor quality of the images. Therefore, before embarking on the characterization of GRIM-19's mitochondrial functions, without a solid proof for the localization of the protein, it was necessary for us to clarify unambiguously, the same. To this end, our results very clearly show that endogenous (Refer Figure 3.1) GRIM-19 and the C-terminal tagged GRIM-19 (Refer Figure 3.4 A and B) localize to only the mitochondria and not the nucleus. We have proved this using Western Blot too. GRIM-19 was observed only in the mitochondrial fraction and not the cytosolic. However, the mitochondrial fraction could be made purer by eliminating the possibility of contamination by ER, nucleus, peroxisomes and other such organelles. Nevertheless, the cytosolic fraction is relatively pure and shows that GRIM-19 does not localize to the cytoplasm. (Refer Figure 3.2 A). A closer look at the blots would reveal that GRIM-19 is not digested at low concentrations of Proteinase K in contrast to Tom20, an outer mitochondrial membrane protein which is digested even at very low Proteinase K concentrations. Only when Triton X-100 is added to the digestion mixture is GRIM-19 digested (Refer Figure 3.2 C). Moreover, it is found only in the pellet fraction of mitochondria (Refer Figure 3.2 B) whereas cytochrome c is found in the supernatant fraction of the mitochondria. These results give a clear understanding of the sub cellular localization of GRIM-19. It can now be concluded that it is part of the inner membrane of mitochondria.

4.2 EFFECTS OF GRIM-19 ON MITOCHONDRIAL MORPHOLOGY AND DYNAMICS

When I overexpressed GRIM-19 with the right C-terminal tags, I did not observe any change in the mitochondrial morphology (Refer Figure 3.4 A and B). A number of studies have thus far reported the downregulation of GRIM-19 in cancer tissues (Zhang et al., 2011; Zhou et al., 2013; Zhou et al., 2009). The majority of the studies to date pertain to the function of GRIM-19 in cancer and the molecular mechanism involved. Very few report its function in the mitochondria. This drove me to observe the anomalies in the mitochondria when GRIM-19 is depleted in the cells. Figures 3.5 A and B show that GRIM-19 was successfully ablated from the cells to a very significant extent. Figure 3.5 B makes clear that reduction in GRIM-19 levels do not disrupt the mitochondrial morphology. However, since our aim was to conduct a comprehensive analysis of the function of GRIM-19 with regard to the mitochondria, I moved on to study mitochondrial dynamics under excess and limiting amounts of GRIM-19. This was done by FRAP analysis. Consistent with the results from the morphology analysis, dynamics study also showed that GRIM-19 does not have a role to play in controlling the fission and fusion of mitochondria. We concluded this after observing from Figures 3.6 A, B, C and D that the recovery of fluorescence of GRIM-19-GFP and GFP vector transfected cells do not differ significantly which implies that mitochondria are able to divide and unite normally under excess GRIM-19

conditions. Similarly, Figures 3.7 A, B, C and D show that control and GRIM-19 KD cells do not suffer any difficulty in maintaining their balance between fission and fusion. This indicates that GRIM-19 is not part of the dynamics controlling machinery.

4.3 THE ROLE OF GRIM-19 IN MITOCHONDRIAL FUNCTION

4.3.1 GRIM-19 KD increases the production of ROS

Though GRIM-19 was identified to be part of mitochondrial Complex I (Fearnley et al., 2001), not much has been discovered of its specific role in the functions of mitochondria such as ROS production, maintenance of mitochondrial membrane potential and generation of ATP. In this direction, my first attempt was to check the levels of ROS in cells with physiological level of GRIM-19 and those which are depleted of the protein. I used the GRIM-19 KD stable cell line and control-shRNA KD stable cell line for the analysis. DHE dye was used to indicate the amount of ROS present in the cells. Upon measuring the fluorescence of DHE in both the samples, it was observed that GRIM-19 KD cells exhibited a greater accumulation of ROS than that in the control KD cells (Refer Figure 3.8 A and B). Literature shows several studies reporting an increase in the ROS levels in cancer cells (Liou and Storz, 2010; Pelicano et al., 2004). Our results corroborate with the present findings that downregulation of GRIM-19 occurs in cancer tissues. In addition, we propose with the backing of our results, that this could be in part by an

increase in ROS levels. Further studies are needed to explore how GRIM-19 KD causes an increase in ROS production.

4.3.2 GRIM-19 depletion does not affect mitochondrial potential

My next test was the alteration of mitochondrial potential upon removal of GRIM-19.. GRIM-19 KD and control KD cells were stained with TMRM, a positively charged fluorescence indicator of mitochondrial potential. When the intensity of fluorescence was measured using FACS, I was surprised to note that there was no change in the mitochondrial potential between the two population of cells (Figure 3.9 A and B). Previous studies have reported that GRIM-19 is essential for the maintenance of potential (Lu and Cao, 2008). The reason for a discrepancy in our results could be because of a few reasons. Firstly, their group had used truncation mutants to assess the role of GRIM-19 in maintenance of potential. The truncation mutants could have caused disturbances to the normal functioning of Complex I. It is not necessary that the total absence of GRIM-19 should also exhibit the same effect since the result from Lu *et al*. could have been caused by the toxicity of the truncated mutants owing to their misfolding or sorts. Knockdown study provides a much more direct evidence of the role of the protein of interest, here GRIM-19, than mutant studies. Secondly, the previous group had carried out their assays using MCF-7 cells and we had used HeLa cells. This could also be the reason for our difference in results pertaining to GRIM-19's function in maintaining mitochondrial potential.

4.3.3 GRIM-19 KD does not hamper ATP production

Another most important functional aspect of mitochondria is its production of ATP. The five complexes in the inner membrane of the mitochondria co-ordinate in shuttling electrons between them that finally results in the generation of ATP molecules. Since GRIM-19 makes up a subunit of Complex I, we wanted to see the effect of GRIM-19 depletion on the production of ATP in cells. To this end, using the ATP determination kit from Invitrogen, luciferase assay based analysis was carried out to reveal the gross amount of ATP in a comparable amount of cells from the two sets of samples (GRIM-19 KD and control KD). Figure 3.10, a quantification analysis of the data from the experiments conducted indicated that GRIM-19 may not be an important factor in the production of ATP. Other subunits of Complex I could contribute more significantly to ATP production and also compensate for the loss of GRIM-19.

4.4 EFFECTS OF GRIM-19 DEPLETION IN CELL CYCLE

GRIM-19 has been proposed to be a cell death regulatory protein through the IFNβ/RA pathway. Apart from this, as mentioned earlier, several reports have been published that claim that downregulation of GRIM-19 is observed in several cancer tissues (Cheng et al., 2014; Li et al., 2012; Zhang et al., 2011; Zhou et al., 2013; Zhou et al., 2009). Most of these studies have been carried out with patient tissue samples. I was curious to know at a cellular level how changes in GRIM-19 reflect in cell cycle. For this, GRIM-19 KD and control cells were fixed using Propidium

Iodide to be followed by FACS analysis. Results as depicted in Figure 3.11 show that depletion of GRIM-19 exhibits an increase in the percentage of the S and G2 phase cells of the population. A previous study reports that GRIM-19 arrests cells at the G1 to S transition phase (Sun et al., 2010). Our results also support this idea since we noted that there is an increase in the percentage of cells progressing towards the S and G2 phase in GRIM-19 depleted cells. This also corroborates findings that report downregulation of GRIM-19 might promote cell growth in turn leading to development of cancers.

4.5 STUDIES ON IFNB/RA TREATMENT

4.5.1 Combination of IFNβ/RA causes more cell death than either drug alone

Before embarking on studies that involve the effects of treatment of IFNβ/RA on mitochondrial morphology, I validated the current understanding about the effect of these drugs on cell health. Consistent with the present literature (Frey et al., 1991; Lindner et al., 1997; Marth et al., 1986; Moore et al., 1994), our results also prove that treatment of cells with either IFNβ or RA alone causes less cell death than when both of them are used in combination (Figure 3.12).

4.5.2 GRIM-19 KD provides resistance to IFNβ/RA treatment

Recollecting from the introduction, GRIM-19 was identified from a screening that scanned for genes that were responsible for executing cell

death through the IFNβ/RA pathway. This was done using an anti-sense technical knockout screen under the treatment of IFNβ/RA. To validate these results, I treated GRIM-19 KD and control KD cells with IFNβ/RA and assessed the percentage of cell death in each population. As expected, a rescue of about 20% was seen in cell death in GRIM-19 depleted cells (Figure 3.14). This conveys that GRIM-19 does play a role in the cell death pathway executed by IFNβ/RA.

4.5.3 FNβ/RA treatment causes fragmentation of mitochondria

After verifying the present data on IFNβ/RA treatment and its effects on cell death, my next aim was to observe the changes if any in the mitochondrial morphology when the cells are treated with the same combination of drugs. Upon treatment, mitochondria of HeLa cells were fragmented (Figure 3.13). This was much to our expectation since one of the first signs of cell health damage would be reflected in the mitochondria. Also, GRIM-19 being an important player in this pathway that is present in the mitochondria itself, could be implementing this phenomenon. There was one more observation that we could make from this experiment. The localization of GRIM-19 is not changed because of the treatment (Figure 3.13 bottom panel), suggesting that unlike cytochrome c, GRIM-19 does not translocate to the cytoplasm prior to execution of cell death. Next, I was to curious to know if GRIM-19 KD could rescue the mitochondrial fragmentation since it could provide resistance to IFNβ/RA induced cell death. We were able to detect some GRIM-19 KD cells with mitochondria that had close to normal morphology

(Figure 3.15). This leads us to propose that as a first indicator of apoptotic stress under IFNβ/RA, GRIM-19 disrupts the mitochondrial morphology.

4.6 CHARACTERIZATION OF PATIENT TUMOR DERIVED GRIM-19 MUTANTS

After having studied the wild type protein with respect to its mitochondrial functions, I was interested in analyzing how certain patient tumour derived mutations affect the normal functioning of the protein. L71P, L91P and A95T were tumours detected in head and neck cancers from patients (Nallar et al., 2013). In this study, the authors conduct assays to prove that these mutations fail to inhibit STAT3 and thereby promote oncogenesis. T113A was identified in another study as a potential site for phosphorylation (Palmisano et al., 2007). I, thus, chose these four mutations to characterize in an effort to elucidate the mechanism of pathogenesis underlying the carcinomas harbouring these mutations. To begin with, these were overexpressed in HeLa cells and the mitochondrial morphology observed. As shown in Figure 3.16, GRIM-19 mutants did not cause alterations in the mitochondrial morphology.

Since our previous results show that knockdown of GRIM-19 causes an increase in ROS production, I examined the effect of mutants on the same. To exclusively study the effects of mutants, a GFP tagged GRIM-19 was overexpressed in the GRIM-19 KD stable cell lines lest the effect of endogenous GRIM-19 could interfere. In doing this, we first had to ensure that the mutants could be expressed in the KD cells. I took to Western Blot

to prove this (Refer Figure 3.17 C). Figure 3.17 A and B show that the expression levels of the mutants are comparable to each other and the wild type protein.

Using this as a technique to assess the effect of mutants, ROS production and mitochondrial potential in cells expressing the mutants were measured. As far as mitochondrial potential was concerned, the mutants did not disrupt the normal maintenance and the intensity of the TMRM dye was comparable across the control KD cells, GRIM-19 KD cells as well as the samples expressing mutants and wild type (Refer Figure 3.18).

All the mutants consistently showed an increase in ROS production which was higher than both the KD cells and wild type overexpressing protein (Figure 3.19). In this scenario, the mutants fail to rescue the ROS production indicating that this may be a factor contributing to their pathogenecity. This is in support with studies reporting an increase cellular ROS levels in various cancer tissues (Liou and Storz, 2010; Pelicano et al., 2004).

4.7 CONCLUSION

In this thesis, I have shown that GRIM-19 localizes mainly to the mitochondria in the cell and that at a sub-mitochondrial level, it is part of the inner mitochondrial membrane. Our results demonstrate that GRIM-19 does not play a significant role in maintenance of mitochondrial morphology or dynamics. However, the depletion of GRIM-19 causes an

increase ROS production which is consistent with previous research. downregulation of GRIM-19 promotes oncogenesis and several cancer tissues exhibit an increase in cellular ROS levels. Furthermore, I show that IFNβ/RA treatment causes the fragmentation of mitochondria which is partially rescued by the knockdown of GRIM-19 indicating that upon the drug treatment, mitochondrial stability is lost via a GRIM-19 dependent mechanism. Further studies are needed to extrapolate the mechanisms behind the increase in ROS levels under GRIM-19 KD and the changes in mitochondrial morphology upon IFNβ/RA treatment.

4.8 FUTURE WORK

Many studies have reported that STAT3 and GRIM-19 interact with each other and this is in particular significant in the pathology of tumor cells (Lufei et al., 2003; Okamoto et al., 2010; Zhang et al., 2003; Zhou et al., 2009). Besides, the relevance of this interaction to my current study stems from few key papers which report the presence of mitochondrial STAT3 (Gough et al., 2009; Wegrzyn et al., 2009; Zhang et al., 2013). However, what is lacking in these studies is the correlation and inter-dependency of GRIM-19 and STAT3 under the investigated conditions. These links play a vital role in designing future experiments in order to formulate a mechanism for pathogenesis of tumor cells in case of an anomaly in GRIM-19 or STAT3 proteins. For this, a mito-targeted STAT3 could be used. The level of STAT3 in the mitochondria in the presence and absence of GRIM-19 will provide an idea of the dependency of the two proteins on each other to be present on the mitochondria. Once this is

established, the effect of mito-targeted STAT3 on ROS in the presence and absence of GRIM-19 could be investigated. This is would help complement the physiological significance of the interaction of the two proteins. One possible theory of an increase in ROS causing cancer could be through activation of STAT3. To verify the same, ROS scavengers could be used in the background of GRIM-19 KD to ascertain the level of activated STAT3. Results from such experiments would form a framework of working model involving GRIM-19 and STAT3 in light of cancer cells.

Another dimension to the cell death activity of GRIM-19 could be investigated by conducting studies on the interaction of GRIM-19 and GW112, a putative binding partner of GRIM-19 that impedes its pro-apoptotic function. Knock down of GW112 should lead to a more profound effect of the cell death activity of GRIM-19. Also, the site of interaction of GRIM-19 and GW112 could be determined by truncation mutant studies of both proteins. Once this is established, further tests on the effect of the interaction on mitochondrial functions such as ROS and mitochondrial potential would provide an evidence of the balance maintained under normal conditions which otherwise go haywire. These would go on to widen the knowledge on the housekeeping activities of GRIM-19.

Another branch of study that could be undertaken related to the current project is one involving the IFNβ/RA pathway. Since not many proteins that are part of this cascade are known, it would be useful to stimulate the cells with IFNβ/RA and identify other unique proteins that help in

execution of cell death through this pathway. For the same, after stimulation of cells with IFNβ/RA, an SDS-PAGE could be carried out to identify bands that are exclusive in lanes loaded with stimulated cells as against unstimulated control cells. These bands could be cut and analyzed through mass spectrometry to check for other potential players in this pathway. This could lead to further investigations on the downstream effect of the signalling cascade and its implications in cell death.

REFERENCES

Alchanati, I., Nallar, S.C., Sun, P., Gao, L., Hu, J., Stein, A., Yakirevich, E., Konforty, D., Alroy, I., Zhao, X.*, et al.* (2006). A proteomic analysis reveals the loss of expression of the cell death regulatory gene GRIM-19 in human renal cell carcinomas. Oncogene *25*, 7138-7147.

Alnemri, E.S. (1999). Hidden powers of the mitochondria. Nature cell biology *1*, E40-42.

Altucci, L., and Gronemeyer, H. (2001). The promise of retinoids to fight against cancer. Nature reviews Cancer *1*, 181-193.

Anderson, S., Bankier, A.T., Barrell, B.G., de Bruijn, M.H., Coulson, A.R., Drouin, J., Eperon, I.C., Nierlich, D.P., Roe, B.A., Sanger, F.*, et al.* (1981). Sequence and organization of the human mitochondrial genome. Nature *290*, 457-465.

Angell, J.E., Lindner, D.J., Shapiro, P.S., Hofmann, E.R., and Kalvakolanu, D.V. (2000). Identification of GRIM-19, a novel cell death-regulatory gene induced by the interferon-beta and retinoic acid combination, using a genetic approach. The Journal of biological chemistry *275*, 33416-33426.

Balachandran, S., Kim, C.N., Yeh, W.C., Mak, T.W., Bhalla, K., and Barber, G.N. (1998). Activation of the dsRNA-dependent protein kinase, PKR, induces apoptosis through FADD-mediated death signaling. The EMBO journal *17*, 6888-6902.

Barnich, N., Hisamatsu, T., Aguirre, J.E., Xavier, R., Reinecker, H.C., and Podolsky, D.K. (2005). GRIM-19 interacts with nucleotide oligomerization domain 2 and serves as downstream effector of anti-bacterial function in intestinal epithelial cells. The Journal of biological chemistry *280*, 19021-19026.

Berard, J., Laboune, F., Mukuna, M., Masse, S., Kothary, R., and Bradley, W.E. (1996). Lung tumors in mice expressing an antisense RARbeta2 transgene. FASEB journal : official publication of the Federation of American Societies for Experimental Biology *10*, 1091-1097.

Bjelke, E. (1975). Dietary vitamin A and human lung cancer. International journal of cancer Journal international du cancer *15*, 561-565.

Bromberg, J.F., Wrzeszczynska, M.H., Devgan, G., Zhao, Y., Pestell, R.G., Albanese, C., and Darnell, J.E., Jr. (1999). Stat3 as an oncogene. Cell *98*, 295-303.

Bu, X., Zhao, C., Wang, W., and Zhang, N. (2013). GRIM-19 inhibits the STAT3 signaling pathway and sensitizes gastric cancer cells to radiation. Gene *512*, 198-205.

Buettner, R., Mora, L.B., and Jove, R. (2002). Activated STAT signaling in human tumors provides novel molecular targets for therapeutic intervention. Clinical cancer

research : an official journal of the American Association for Cancer Research *8*, 945-954.

Chambon, P. (1996). A decade of molecular biology of retinoic acid receptors. FASEB journal : official publication of the Federation of American Societies for Experimental Biology *10*, 940-954.

Chan, D.C. (2006). Mitochondrial fusion and fission in mammals. Annual review of cell and developmental biology *22*, 79-99.

Chan, D.C. (2012). Fusion and fission: interlinked processes critical for mitochondrial health. Annual review of genetics *46*, 265-287.

Chelbi-Alix, M.K., Quignon, F., Pelicano, L., Koken, M.H., and de The, H. (1998). Resistance to virus infection conferred by the interferon-induced promyelocytic leukemia protein. Journal of virology *72*, 1043-1051.

Chen, Y., Lu, H., Liu, Q., Huang, G., Lim, C.P., Zhang, L., Hao, A., and Cao, X. (2012). Function of GRIM-19, a mitochondrial respiratory chain complex I protein, in innate immunity. The Journal of biological chemistry *287*, 27227-27235.

Chen, Y., Yuen, W.H., Fu, J., Huang, G., Melendez, A.J., Ibrahim, F.B., Lu, H., and Cao, X. (2007). The mitochondrial respiratory chain controls intracellular calcium signaling and NFAT activity essential for heart formation in Xenopus laevis. Molecular and cellular biology *27*, 6420-6432.

Cheng, Y., Zhang, H.Y., Zhou, Y., Tao, F., and Yu, Y.H. (2014). Decreased expression of GRIM-19 and its association with high-risk HPV infection in cervical squamous intraepithelial neoplasias and cancer. Clinical and investigative medicine Medecine clinique et experimentale *37*, E77-84.

Chidambaram, N.V., Angell, J.E., Ling, W., Hofmann, E.R., and Kalvakolanu, D.V. (2000). Chromosomal localization of human GRIM-19, a novel IFN-beta and retinoic acid-activated regulator of cell death. Journal of interferon & cytokine research : the official journal of the International Society for Interferon and Cytokine Research *20*, 661-665.

Chin, Y.E., Kitagawa, M., Su, W.C., You, Z.H., Iwamoto, Y., and Fu, X.Y. (1996). Cell growth arrest and induction of cyclin-dependent kinase inhibitor p21 WAF1/CIP1 mediated by STAT1. Science *272*, 719-722.

Chipuk, J.E., Bouchier-Hayes, L., and Green, D.R. (2006). Mitochondrial outer membrane permeabilization during apoptosis: the innocent bystander scenario. Cell death and differentiation *13*, 1396-1402.

Chomienne, C., Ballerini, P., Balitrand, N., Daniel, M.T., Fenaux, P., Castaigne, S., and Degos, L. (1990). All-trans retinoic acid in acute promyelocytic leukemias. II. In vitro studies: structure-function relationship. Blood *76*, 1710-1717.

Dal Col, J., Mastorci, K., Fae, D.A., Muraro, E., Martorelli, D., Inghirami, G., and Dolcetti, R. (2012). Retinoic acid/alpha-interferon combination inhibits growth and

promotes apoptosis in mantle cell lymphoma through Akt-dependent modulation of critical targets. Cancer research *72*, 1825-1835.

Day, C.A., Kraft, L.J., Kang, M., and Kenworthy, A.K. (2012). Analysis of protein and lipid dynamics using confocal fluorescence recovery after photobleaching (FRAP). Current protocols in cytometry / editorial board, J Paul Robinson, managing editor [et al] *Chapter 2*, Unit2 19.

de The, H., Lavau, C., Marchio, A., Chomienne, C., Degos, L., and Dejean, A. (1991). The PML-RAR alpha fusion mRNA generated by the t(15;17) translocation in acute promyelocytic leukemia encodes a functionally altered RAR. Cell *66*, 675-684.

Diaz, N., Minton, S., Cox, C., Bowman, T., Gritsko, T., Garcia, R., Eweis, I., Wloch, M., Livingston, S., Seijo, E.*, et al.* (2006). Activation of stat3 in primary tumors from high-risk breast cancer patients is associated with elevated levels of activated SRC and survivin expression. Clinical cancer research : an official journal of the American Association for Cancer Research *12*, 20-28.

Dyson, N. (1998). The regulation of E2F by pRB-family proteins. Genes & development *12*, 2245-2262.

Ekchariyawat, P., Thitithanyanont, A., Sirisinha, S., and Utaisincharoen, P. (2013). Involvement of GRIM-19 in apoptosis induced in H5N1 virus-infected human macrophages. Innate immunity *19*, 655-662.

el-Deiry, W.S. (1998). p21/p53, cellular growth control and genomic integrity. Current topics in microbiology and immunology *227*, 121-137.

Evan, G.I., and Vousden, K.H. (2001). Proliferation, cell cycle and apoptosis in cancer. Nature *411*, 342-348.

Fan, X.Y., Jiang, Z.F., Cai, L., and Liu, R.Y. (2012). Expression and clinical significance of GRIM-19 in lung cancer. Medical oncology *29*, 3183-3189.

Fanjul, A., Dawson, M.I., Hobbs, P.D., Jong, L., Cameron, J.F., Harlev, E., Graupner, G., Lu, X.P., and Pfahl, M. (1994). A new class of retinoids with selective inhibition of AP-1 inhibits proliferation. Nature *372*, 107-111.

Fearnley, I.M., Carroll, J., Shannon, R.J., Runswick, M.J., Walker, J.E., and Hirst, J. (2001). GRIM-19, a cell death regulatory gene product, is a subunit of bovine mitochondrial NADH:ubiquinone oxidoreductase (complex I). The Journal of biological chemistry *276*, 38345-38348.

Frey, J.R., Peck, R., and Bollag, W. (1991). Antiproliferative activity of retinoids, interferon alpha and their combination in five human transformed cell lines. Cancer letters *57*, 223-227.

Friedman, J.R., and Nunnari, J. (2014). Mitochondrial form and function. Nature *505*, 335-343.

Frohlich, C., Grabiger, S., Schwefel, D., Faelber, K., Rosenbaum, E., Mears, J., Rocks, O., and Daumke, O. (2013). Structural insights into oligomerization and mitochondrial remodelling of dynamin 1-like protein. The EMBO journal *32*, 1280-1292.

Fujita, T., Kimura, Y., Miyamoto, M., Barsoumian, E.L., and Taniguchi, T. (1989). Induction of endogenous IFN-alpha and IFN-beta genes by a regulatory transcription factor, IRF-1. Nature *337*, 270-272.

Gaboli, M., Gandini, D., Delva, L., Wang, Z.G., and Pandolfi, P.P. (1998). Acute promyelocytic leukemia as a model for cross-talk between interferon and retinoic acid pathways: from molecular biology to clinical applications. Leukemia & lymphoma *30*, 11-22.

Galluzzi, L., Kepp, O., and Kroemer, G. (2012). Mitochondria: master regulators of danger signalling. Nature reviews Molecular cell biology *13*, 780-788.

Gao, A.C., Lou, W., Ichikawa, T., Denmeade, S.R., Barrett, J.C., and Isaacs, J.T. (1999). Suppression of the tumorigenicity of prostatic cancer cells by gene(s) located on human chromosome 19p13.1-13.2. The Prostate *38*, 46-54.

Gerencser, A.A., Chinopoulos, C., Birket, M.J., Jastroch, M., Vitelli, C., Nicholls, D.G., and Brand, M.D. (2012). Quantitative measurement of mitochondrial membrane potential in cultured cells: calcium-induced de- and hyperpolarization of neuronal mitochondria. The Journal of physiology *590*, 2845-2871.

Gianni, M., Terao, M., Fortino, I., LiCalzi, M., Viggiano, V., Barbui, T., Rambaldi, A., and Garattini, E. (1997). Stat1 is induced and activated by all-trans retinoic acid in acute promyelocytic leukemia cells. Blood *89*, 1001-1012.

Gongora, C., David, G., Pintard, L., Tissot, C., Hua, T.D., Dejean, A., and Mechti, N. (1997). Molecular cloning of a new interferon-induced PML nuclear body-associated protein. The Journal of biological chemistry *272*, 19457-19463.

Gough, D.J., Corlett, A., Schlessinger, K., Wegrzyn, J., Larner, A.C., and Levy, D.E. (2009). Mitochondrial STAT3 supports Ras-dependent oncogenic transformation. Science *324*, 1713-1716.

Gray, M.W. (1989). Origin and evolution of mitochondrial DNA. Annual review of cell biology *5*, 25-50.

Gray, M.W., Burger, G., and Lang, B.F. (1999). Mitochondrial evolution. Science *283*, 1476-1481.

Gutterman, J.U. (1994). Cytokine therapeutics: lessons from interferon alpha. Proceedings of the National Academy of Sciences of the United States of America *91*, 1198-1205.

Hansen, L.A., Sigman, C.C., Andreola, F., Ross, S.A., Kelloff, G.J., and De Luca, L.M. (2000). Retinoids in chemoprevention and differentiation therapy. Carcinogenesis *21*, 1271-1279.

Hao, H., Liu, J., Liu, G., Guan, D., Yang, Y., Zhang, X., Cao, X., and Liu, Q. (2012). Depletion of GRIM-19 accelerates hepatocellular carcinoma invasion via inducing EMT and loss of contact inhibition. Journal of cellular physiology *227*, 1212-1219.

Hao, S.X., and Ren, R. (2000). Expression of interferon consensus sequence binding protein (ICSBP) is downregulated in Bcr-Abl-induced murine chronic myelogenous leukemia-like disease, and forced coexpression of ICSBP inhibits Bcr-Abl-induced myeloproliferative disorder. Molecular and cellular biology *20*, 1149-1161.

Hay, R., Bohni, P., and Gasser, S. (1984). How mitochondria import proteins. Biochimica et biophysica acta *779*, 65-87.

He, X., and Cao, X. (2010). Identification of alternatively spliced GRIM-19 mRNA in kidney cancer tissues. Journal of human genetics *55*, 507-511.

Hegde, R., Srinivasula, S.M., Zhang, Z., Wassell, R., Mukattash, R., Cilenti, L., DuBois, G., Lazebnik, Y., Zervos, A.S., Fernandes-Alnemri, T.*, et al.* (2002). Identification of Omi/HtrA2 as a mitochondrial apoptotic serine protease that disrupts inhibitor of apoptosis protein-caspase interaction. The Journal of biological chemistry *277*, 432-438.

Herrmann, J.M., and Neupert, W. (2000). Protein transport into mitochondria. Current opinion in microbiology *3*, 210-214.

Hertzog, P.J., and Williams, B.R. (2013). Fine tuning type I interferon responses. Cytokine & growth factor reviews *24*, 217-225.

Holtschke, T., Lohler, J., Kanno, Y., Fehr, T., Giese, N., Rosenbauer, F., Lou, J., Knobeloch, K.P., Gabriele, L., Waring, J.F.*, et al.* (1996). Immunodeficiency and chronic myelogenous leukemia-like syndrome in mice with a targeted mutation of the ICSBP gene. Cell *87*, 307-317.

Huang, G., Lu, H., Hao, A., Ng, D.C., Ponniah, S., Guo, K., Lufei, C., Zeng, Q., and Cao, X. (2004). GRIM-19, a cell death regulatory protein, is essential for assembly and function of mitochondrial complex I. Molecular and cellular biology *24*, 8447-8456.

Huang, Y., Yang, M., Yang, H., and Zeng, Z. (2010). Upregulation of the GRIM-19 gene suppresses invasion and metastasis of human gastric cancer SGC-7901 cell line. Experimental cell research *316*, 2061-2070.

Kalakonda, S., Nallar, S.C., Gong, P., Lindner, D.J., Goldblum, S.E., Reddy, S.P., and Kalvakolanu, D.V. (2007a). Tumor suppressive protein gene associated with retinoid-interferon-induced mortality (GRIM)-19 inhibits src-induced oncogenic transformation at multiple levels. The American journal of pathology *171*, 1352-1368.

Kalakonda, S., Nallar, S.C., Jaber, S., Keay, S.K., Rorke, E., Munivenkatappa, R., Lindner, D.J., Fiskum, G.M., and Kalvakolanu, D.V. (2013). Monoallelic loss of tumor suppressor GRIM-19 promotes tumorigenesis in mice. Proceedings of the National Academy of Sciences of the United States of America *110*, E4213-4222.

Kalakonda, S., Nallar, S.C., Lindner, D.J., Hu, J., Reddy, S.P., and Kalvakolanu, D.V. (2007b). Tumor-suppressive activity of the cell death activator GRIM-19 on a constitutively active signal transducer and activator of transcription 3. Cancer research *67*, 6212-6220.

Kalvakolanu, D.V. (2000). Interferons and cell growth control. Histology and histopathology *15*, 523-537.

Kalvakolanu, D.V. (2004). The GRIMs: a new interface between cell death regulation and interferon/retinoid induced growth suppression. Cytokine & growth factor reviews *15*, 169-194.

Kaplan, D.H., Shankaran, V., Dighe, A.S., Stockert, E., Aguet, M., Old, L.J., and Schreiber, R.D. (1998). Demonstration of an interferon gamma-dependent tumor surveillance system in immunocompetent mice. Proceedings of the National Academy of Sciences of the United States of America *95*, 7556-7561.

Kastner, P., Mark, M., and Chambon, P. (1995). Nonsteroid nuclear receptors: what are genetic studies telling us about their role in real life? Cell *83*, 859-869.

Kjellin, H., Johansson, H., Hoog, A., Lehtio, J., Jakobsson, P.J., and Kjellman, M. (2014). Differentially expressed proteins in malignant and benign adrenocortical tumors. PloS one *9*, e87951.

Kolla, V., Weihua, X., and Kalvakolanu, D.V. (1997). Modulation of interferon action by retinoids. Induction of murine STAT1 gene expression by retinoic acid. The Journal of biological chemistry *272*, 9742-9748.

Koshida, S., Kobayashi, D., Moriai, R., Tsuji, N., and Watanabe, N. (2007). Specific overexpression of OLFM4(GW112/HGC-1) mRNA in colon, breast and lung cancer tissues detected using quantitative analysis. Cancer science *98*, 315-320.

Kroemer, G., Galluzzi, L., and Brenner, C. (2007). Mitochondrial membrane permeabilization in cell death. Physiological reviews *87*, 99-163.

Krysko, D.V., Agostinis, P., Krysko, O., Garg, A.D., Bachert, C., Lambrecht, B.N., and Vandenabeele, P. (2011). Emerging role of damage-associated molecular patterns derived from mitochondria in inflammation. Trends in immunology *32*, 157-164.

Kuida, K., Lippke, J.A., Ku, G., Harding, M.W., Livingston, D.J., Su, M.S., and Flavell, R.A. (1995). Altered cytokine export and apoptosis in mice deficient in interleukin-1 beta converting enzyme. Science *267*, 2000-2003.

Kuwata, T., Wang, I.M., Tamura, T., Ponnamperuma, R.M., Levine, R., Holmes, K.L., Morse, H.C., De Luca, L.M., and Ozato, K. (2000). Vitamin A deficiency in mice causes a systemic expansion of myeloid cells. Blood *95*, 3349-3356.

Lee, H.Y., Dohi, D.F., Kim, Y.H., Walsh, G.L., Consoli, U., Andreeff, M., Dawson, M.I., Hong, W.K., and Kurie, J.M. (1998). All-trans retinoic acid converts E2F into a transcriptional suppressor and inhibits the growth of normal human bronchial

epithelial cells through a retinoic acid receptor- dependent signaling pathway. The Journal of clinical investigation *101*, 1012-1019.

Levy-Strumpf, N., and Kimchi, A. (1998). Death associated proteins (DAPs): from gene identification to the analysis of their apoptotic and tumor suppressive functions. Oncogene *17*, 3331-3340.

Levy, D.E., and Darnell, J.E., Jr. (2002). Stats: transcriptional control and biological impact. Nature reviews Molecular cell biology *3*, 651-662.

Li, F., Ren, W., Zhao, Y., Fu, Z., Ji, Y., Zhu, Y., and Qin, C. (2012). Downregulation of GRIM-19 is associated with hyperactivation of p-STAT3 in hepatocellular carcinoma. Medical oncology *29*, 3046-3054.

Li, H., Kolluri, S.K., Gu, J., Dawson, M.I., Cao, X., Hobbs, P.D., Lin, B., Chen, G., Lu, J., Lin, F*., et al.* (2000). Cytochrome c release and apoptosis induced by mitochondrial targeting of nuclear orphan receptor TR3. Science *289*, 1159-1164.

Li, M., Li, Z., Liang, C., Han, C., Huang, W., and Sun, F. (2014). Upregulation of GRIM-19 suppresses the growth of oral squamous cell carcinoma in vitro and in vivo. Oncology reports *32*, 2183-2190.

Lindner, D.J., Borden, E.C., and Kalvakolanu, D.V. (1997). Synergistic antitumor effects of a combination of interferons and retinoic acid on human tumor cells in vitro and in vivo. Clinical cancer research : an official journal of the American Association for Cancer Research *3*, 931-937.

Liou, G.Y., and Storz, P. (2010). Reactive oxygen species in cancer. Free radical research *44*, 479-496.

Liu, Q., Wang, L., Wang, Z., Yang, Y., Tian, J., Liu, G., Guan, D., Cao, X., Zhang, Y., and Hao, A. (2013). GRIM-19 opposes reprogramming of glioblastoma cell metabolism via HIF1alpha destabilization. Carcinogenesis *34*, 1728-1736.

Liu, Y., Lee, M.O., Wang, H.G., Li, Y., Hashimoto, Y., Klaus, M., Reed, J.C., and Zhang, X. (1996). Retinoic acid receptor beta mediates the growth-inhibitory effect of retinoic acid by promoting apoptosis in human breast cancer cells. Molecular and cellular biology *16*, 1138-1149.

Love, J.M., and Gudas, L.J. (1994). Vitamin A, differentiation and cancer. Current opinion in cell biology *6*, 825-831.

Lu, H., and Cao, X. (2008). GRIM-19 is essential for maintenance of mitochondrial membrane potential. Molecular biology of the cell *19*, 1893-1902.

Lufei, C., Ma, J., Huang, G., Zhang, T., Novotny-Diermayr, V., Ong, C.T., and Cao, X. (2003). GRIM-19, a death-regulatory gene product, suppresses Stat3 activity via functional interaction. The EMBO journal *22*, 1325-1335.

Ly, J.D., Grubb, D.R., and Lawen, A. (2003). The mitochondrial membrane potential (deltapsi(m)) in apoptosis; an update. Apoptosis : an international journal on programmed cell death *8*, 115-128.

Ma, X., Kalakonda, S., Srinivasula, S.M., Reddy, S.P., Platanias, L.C., and Kalvakolanu, D.V. (2007). GRIM-19 associates with the serine protease HtrA2 for promoting cell death. Oncogene *26*, 4842-4849.

Mangelsdorf, D.J., and Evans, R.M. (1995). The RXR heterodimers and orphan receptors. Cell *83*, 841-850.

Mannella, C.A. (2006). Structure and dynamics of the mitochondrial inner membrane cristae. Biochimica et biophysica acta *1763*, 542-548.

Marth, C., Daxenbichler, G., and Dapunt, O. (1986). Synergistic antiproliferative effect of human recombinant interferons and retinoic acid in cultured breast cancer cells. Journal of the National Cancer Institute *77*, 1197-1202.

Martin, G.S. (2001). The hunting of the Src. Nature reviews Molecular cell biology *2*, 467-475.

Martins, L.M., Iaccarino, I., Tenev, T., Gschmeissner, S., Totty, N.F., Lemoine, N.R., Savopoulos, J., Gray, C.W., Creasy, C.L., Dingwall, C*., et al.* (2002). The serine protease Omi/HtrA2 regulates apoptosis by binding XIAP through a reaper-like motif. The Journal of biological chemistry *277*, 439-444.

Matikainen, S., Ronni, T., Lehtonen, A., Sareneva, T., Melen, K., Nordling, S., Levy, D.E., and Julkunen, I. (1997). Retinoic acid induces signal transducer and activator of transcription (STAT) 1, STAT2, and p48 expression in myeloid leukemia cells and enhances their responsiveness to interferons. Cell growth & differentiation : the molecular biology journal of the American Association for Cancer Research *8*, 687-698.

Maximo, V., Botelho, T., Capela, J., Soares, P., Lima, J., Taveira, A., Amaro, T., Barbosa, A.P., Preto, A., Harach, H.R*., et al.* (2005). Somatic and germline mutation in GRIM-19, a dual function gene involved in mitochondrial metabolism and cell death, is linked to mitochondrion-rich (Hurthle cell) tumours of the thyroid. British journal of cancer *92*, 1892-1898.

Melamed, D., Tiefenbrun, N., Yarden, A., and Kimchi, A. (1993). Interferons and interleukin-6 suppress the DNA-binding activity of E2F in growth-sensitive hematopoietic cells. Molecular and cellular biology *13*, 5255-5265.

Mishra, P., and Chan, D.C. (2014). Mitochondrial dynamics and inheritance during cell division, development and disease. Nature reviews Molecular cell biology *15*, 634-646.

Moore, D.M., Kalvakolanu, D.V., Lippman, S.M., Kavanagh, J.J., Hong, W.K., Borden, E.C., Paredes-Espinoza, M., and Krakoff, I.H. (1994). Retinoic acid and interferon in human cancer: mechanistic and clinical studies. Seminars in hematology *31*, 31-37.

Nagpal, S., Saunders, M., Kastner, P., Durand, B., Nakshatri, H., and Chambon, P. (1992). Promoter context- and response element-dependent specificity of the transcriptional activation and modulating functions of retinoic acid receptors. Cell *70*, 1007-1019.

Nallar, S.C., Kalakonda, S., Lindner, D.J., Lorenz, R.R., Lamarre, E., Weihua, X., and Kalvakolanu, D.V. (2013). Tumor-derived mutations in the gene associated with retinoid interferon-induced mortality (GRIM-19) disrupt its anti-signal transducer and activator of transcription 3 (STAT3) activity and promote oncogenesis. The Journal of biological chemistry *288*, 7930-7941.

Nallar, S.C., Kalakonda, S., Sun, P., Ohmori, Y., Hiroi, M., Mori, K., Lindner, D.J., and Kalvakolanu, D.V. (2010). Identification of a structural motif in the tumor-suppressive protein GRIM-19 required for its antitumor activity. The American journal of pathology *177*, 896-907.

Nason-Burchenal, K., Gandini, D., Botto, M., Allopenna, J., Seale, J.R., Cross, N.C., Goldman, J.M., Dmitrovsky, E., and Pandolfi, P.P. (1996). Interferon augments PML and PML/RAR alpha expression in normal myeloid and acute promyelocytic cells and cooperates with all-trans retinoic acid to induce maturation of a retinoid-resistant promyelocytic cell line. Blood *88*, 3926-3936.

Niederreither, K., Subbarayan, V., Dolle, P., and Chambon, P. (1999). Embryonic retinoic acid synthesis is essential for early mouse post-implantation development. Nature genetics *21*, 444-448.

Okamoto, T., Inozume, T., Mitsui, H., Kanzaki, M., Harada, K., Shibagaki, N., and Shimada, S. (2010). Overexpression of GRIM-19 in cancer cells suppresses STAT3-mediated signal transduction and cancer growth. Molecular cancer therapeutics *9*, 2333-2343.

Ozato, K., Tailor, P., and Kubota, T. (2007). The interferon regulatory factor family in host defense: mechanism of action. The Journal of biological chemistry *282*, 20065-20069.

Palmisano, G., Sardanelli, A.M., Signorile, A., Papa, S., and Larsen, M.R. (2007). The phosphorylation pattern of bovine heart complex I subunits. Proteomics *7*, 1575-1583.

Pelicano, H., Carney, D., and Huang, P. (2004). ROS stress in cancer cells and therapeutic implications. Drug resistance updates : reviews and commentaries in antimicrobial and anticancer chemotherapy *7*, 97-110.

Pelicano, L., Li, F., Schindler, C., and Chelbi-Alix, M.K. (1997). Retinoic acid enhances the expression of interferon-induced proteins: evidence for multiple mechanisms of action. Oncogene *15*, 2349-2359.

Perry, S.W., Norman, J.P., Barbieri, J., Brown, E.B., and Gelbard, H.A. (2011). Mitochondrial membrane potential probes and the proton gradient: a practical usage guide. BioTechniques *50*, 98-115.

Piedrafita, F.J., and Pfahl, M. (1997). Retinoid-induced apoptosis and Sp1 cleavage occur independently of transcription and require caspase activation. Molecular and cellular biology *17*, 6348-6358.

Ranger, J.J., Levy, D.E., Shahalizadeh, S., Hallett, M., and Muller, W.J. (2009). Identification of a Stat3-dependent transcription regulatory network involved in metastatic progression. Cancer research *69*, 6823-6830.

Raveh, T., Hovanessian, A.G., Meurs, E.F., Sonenberg, N., and Kimchi, A. (1996). Double-stranded RNA-dependent protein kinase mediates c-Myc suppression induced by type I interferons. The Journal of biological chemistry *271*, 25479-25484.

Resnitzky, D., Tiefenbrun, N., Berissi, H., and Kimchi, A. (1992). Interferons and interleukin 6 suppress phosphorylation of the retinoblastoma protein in growth-sensitive hematopoietic cells. Proceedings of the National Academy of Sciences of the United States of America *89*, 402-406.

Ruas, M., and Peters, G. (1998). The p16INK4a/CDKN2A tumor suppressor and its relatives. Biochimica et biophysica acta *1378*, F115-177.

Ruotsalainen, T., Halme, M., Isokangas, O.P., Pyrhonen, S., Mantyla, M., Pekonen, M., Sarna, S., Joensuu, H., and Mattson, K. (2000). Interferon-alpha and 13-cis-retinoic acid as maintenance therapy after high-dose combination chemotherapy with growth factor support for small cell lung cancer--a feasibility study. Anti-cancer drugs *11*, 101-108.

Schmidt, M., Nagel, S., Proba, J., Thiede, C., Ritter, M., Waring, J.F., Rosenbauer, F., Huhn, D., Wittig, B., Horak, I.*, et al.* (1998). Lack of interferon consensus sequence binding protein (ICSBP) transcripts in human myeloid leukemias. Blood *91*, 22-29.

Sen, G.C. (2000). Novel functions of interferon-induced proteins. Seminars in cancer biology *10*, 93-101.

Seo, T., Lee, D., Shim, Y.S., Angell, J.E., Chidambaram, N.V., Kalvakolanu, D.V., and Choe, J. (2002). Viral interferon regulatory factor 1 of Kaposi's sarcoma-associated herpesvirus interacts with a cell death regulator, GRIM19, and inhibits interferon/retinoic acid-induced cell death. Journal of virology *76*, 8797-8807.

Shuai, K., Schindler, C., Prezioso, V.R., and Darnell, J.E., Jr. (1992). Activation of transcription by IFN-gamma: tyrosine phosphorylation of a 91-kD DNA binding protein. Science *258*, 1808-1812.

Shulga, N., and Pastorino, J.G. (2012). GRIM-19-mediated translocation of STAT3 to mitochondria is necessary for TNF-induced necroptosis. Journal of cell science *125*, 2995-3003.

Stadler, W.M., Kuzel, T., Dumas, M., and Vogelzang, N.J. (1998). Multicenter phase II trial of interleukin-2, interferon-alpha, and 13-cis-retinoic acid in patients with metastatic renal-cell carcinoma. Journal of clinical oncology : official journal of the American Society of Clinical Oncology *16*, 1820-1825.

Stark, G.R., Kerr, I.M., Williams, B.R., Silverman, R.H., and Schreiber, R.D. (1998). How cells respond to interferons. Annual review of biochemistry *67*, 227-264.

Sun, P., Nallar, S.C., Kalakonda, S., Lindner, D.J., Martin, S.S., and Kalvakolanu, D.V. (2009). GRIM-19 inhibits v-Src-induced cell motility by interfering with cytoskeletal restructuring. Oncogene *28*, 1339-1347.

Sun, P., Nallar, S.C., Raha, A., Kalakonda, S., Velalar, C.N., Reddy, S.P., and Kalvakolanu, D.V. (2010). GRIM-19 and p16(INK4a) synergistically regulate cell cycle progression and E2F1-responsive gene expression. The Journal of biological chemistry *285*, 27545-27552.

Sun, Q.A., Wu, Y., Zappacosta, F., Jeang, K.T., Lee, B.J., Hatfield, D.L., and Gladyshev, V.N. (1999). Redox regulation of cell signaling by selenocysteine in mammalian thioredoxin reductases. The Journal of biological chemistry *274*, 24522-24530.

Suzuki, Y., Imai, Y., Nakayama, H., Takahashi, K., Takio, K., and Takahashi, R. (2001). A serine protease, HtrA2, is released from the mitochondria and interacts with XIAP, inducing cell death. Molecular cell *8*, 613-621.

Tait, S.W., and Green, D.R. (2010). Mitochondria and cell death: outer membrane permeabilization and beyond. Nature reviews Molecular cell biology *11*, 621-632.

Tammineni, P., Anugula, C., Mohammed, F., Anjaneyulu, M., Larner, A.C., and Sepuri, N.B. (2013). The import of the transcription factor STAT3 into mitochondria depends on GRIM-19, a component of the electron transport chain. The Journal of biological chemistry *288*, 4723-4732.

Thacher, S.M., Vasudevan, J., and Chandraratna, R.A. (2000). Therapeutic applications for ligands of retinoid receptors. Current pharmaceutical design *6*, 25-58.

Thar, R., and Kuhl, M. (2004). Propagation of electromagnetic radiation in mitochondria? Journal of theoretical biology *230*, 261-270.

Tiefenbrun, N., Melamed, D., Levy, N., Resnitzky, D., Hoffman, I., Reed, S.I., and Kimchi, A. (1996). Alpha interferon suppresses the cyclin D3 and cdc25A genes, leading to a reversible G0-like arrest. Molecular and cellular biology *16*, 3934-3944.

Toshchakov, V., Jones, B.W., Perera, P.Y., Thomas, K., Cody, M.J., Zhang, S., Williams, B.R., Major, J., Hamilton, T.A., Fenton, M.J*., et al.* (2002). TLR4, but not TLR2, mediates IFN-beta-induced STAT1alpha/beta-dependent gene expression in macrophages. Nature immunology *3*, 392-398.

Tupper, J.T., and Tedeschi, H. (1969). Microelectrode studies on the membrane properties of isolated mitochondria. Proceedings of the National Academy of Sciences of the United States of America *63*, 370-377.

Tzagoloff, A. (1974). Assembly of inner membrane complexes. Annals of the New York Academy of Sciences *227*, 521-526.

van Loo, G., van Gurp, M., Depuydt, B., Srinivasula, S.M., Rodriguez, I., Alnemri, E.S., Gevaert, K., Vandekerckhove, J., Declercq, W., and Vandenabeele, P. (2002). The serine protease Omi/HtrA2 is released from mitochondria during apoptosis. Omi interacts with caspase-inhibitor XIAP and induces enhanced caspase activity. Cell death and differentiation *9*, 20-26.

Wang, G.M., Ren, Z.X., Wang, P.S., Su, C., Zhang, W.X., Liu, Z.G., Zhang, L., Zhao, X.J., and Chen, G. (2014). Plasmid-based Stat3-specific siRNA and GRIM-19 inhibit the growth of thyroid cancer cells in vitro and in vivo. Oncology reports *32*, 573-580.

Wang, T., Yan, X.B., Zhao, J.J., Ye, J., Jiang, Z.F., Wu, D.R., Xiao, W.H., and Liu, R.Y. (2011). Gene associated with retinoid-interferon-induced mortality-19 suppresses growth of lung adenocarcinoma tumor in vitro and in vivo. Lung cancer *72*, 287-293.

Wang, Z.G., Delva, L., Gaboli, M., Rivi, R., Giorgio, M., Cordon-Cardo, C., Grosveld, F., and Pandolfi, P.P. (1998). Role of PML in cell growth and the retinoic acid pathway. Science *279*, 1547-1551.

Wegrzyn, J., Potla, R., Chwae, Y.J., Sepuri, N.B., Zhang, Q., Koeck, T., Derecka, M., Szczepanek, K., Szelag, M., Gornicka, A.*, et al.* (2009). Function of mitochondrial Stat3 in cellular respiration. Science *323*, 793-797.

Willman, C.L., Sever, C.E., Pallavicini, M.G., Harada, H., Tanaka, N., Slovak, M.L., Yamamoto, H., Harada, K., Meeker, T.C., List, A.F.*, et al.* (1993). Deletion of IRF-1, mapping to chromosome 5q31.1, in human leukemia and preleukemic myelodysplasia. Science *259*, 968-971.

Yang, J., Chatterjee-Kishore, M., Staugaitis, S.M., Nguyen, H., Schlessinger, K., Levy, D.E., and Stark, G.R. (2005). Novel roles of unphosphorylated STAT3 in oncogenesis and transcriptional regulation. Cancer research *65*, 939-947.

Youle, R.J., and van der Bliek, A.M. (2012). Mitochondrial fission, fusion, and stress. Science *337*, 1062-1065.

Yu, M., Tong, J.H., Mao, M., Kan, L.X., Liu, M.M., Sun, Y.W., Fu, G., Jing, Y.K., Yu, L., Lepaslier, D.*, et al.* (1997). Cloning of a gene (RIG-G) associated with retinoic acid-induced differentiation of acute promyelocytic leukemia cells and representing a new member of a family of interferon-stimulated genes. Proceedings of the National Academy of Sciences of the United States of America *94*, 7406-7411.

Zamzami, N., Marchetti, P., Castedo, M., Zanin, C., Vayssiere, J.L., Petit, P.X., and Kroemer, G. (1995). Reduction in mitochondrial potential constitutes an early irreversible step of programmed lymphocyte death in vivo. The Journal of experimental medicine *181*, 1661-1672.

Zhang, J., Yang, J., Roy, S.K., Tininini, S., Hu, J., Bromberg, J.F., Poli, V., Stark, G.R., and Kalvakolanu, D.V. (2003). The cell death regulator GRIM-19 is an inhibitor of signal transducer and activator of transcription 3. Proceedings of the National Academy of Sciences of the United States of America *100*, 9342-9347.

Zhang, L., Gao, L., Li, Y., Lin, G., Shao, Y., Ji, K., Yu, H., Hu, J., Kalvakolanu, D.V., Kopecko, D.J*., et al.* (2008). Effects of plasmid-based Stat3-specific short hairpin RNA and GRIM-19 on PC-3M tumor cell growth. Clinical cancer research : an official journal of the American Association for Cancer Research *14*, 559-568.

Zhang, Q., Raje, V., Yakovlev, V.A., Yacoub, A., Szczepanek, K., Meier, J., Derecka, M., Chen, Q., Hu, Y., Sisler, J*., et al.* (2013). Mitochondrial localized Stat3 promotes breast cancer growth via phosphorylation of serine 727. The Journal of biological chemistry *288*, 31280-31288.

Zhang, X., Huang, Q., Yang, Z., Li, Y., and Li, C.Y. (2004). GW112, a novel antiapoptotic protein that promotes tumor growth. Cancer research *64*, 2474-2481.

Zhang, Y., Hao, H., Zhao, S., Liu, Q., Yuan, Q., Ni, S., Wang, F., Liu, S., Wang, L., and Hao, A. (2011). Downregulation of GRIM-19 promotes growth and migration of human glioma cells. Cancer science *102*, 1991-1999.

Zhou, A., Paranjape, J., Brown, T.L., Nie, H., Naik, S., Dong, B., Chang, A., Trapp, B., Fairchild, R., Colmenares, C*., et al.* (1997). Interferon action and apoptosis are defective in mice devoid of 2',5'-oligoadenylate-dependent RNase L. The EMBO journal *16*, 6355-6363.

Zhou, T., Chao, L., Rong, G., Wang, C., Ma, R., and Wang, X. (2013). Down-regulation of GRIM-19 is associated with STAT3 overexpression in breast carcinomas. Human pathology *44*, 1773-1779.

Zhou, Y., Li, M., Wei, Y., Feng, D., Peng, C., Weng, H., Ma, Y., Bao, L., Nallar, S., Kalakonda, S*., et al.* (2009). Down-regulation of GRIM-19 expression is associated with hyperactivation of STAT3-induced gene expression and tumor growth in human cervical cancers. Journal of interferon & cytokine research : the official journal of the International Society for Interferon and Cytokine Research *29*, 695-703.

Zhou, Y., Wei, Y., Zhu, J., Wang, Q., Bao, L., Ma, Y., Chen, Y., Feng, D., Zhang, A., Sun, J*., et al.* (2011). GRIM-19 disrupts E6/E6AP complex to rescue p53 and induce apoptosis in cervical cancers. PloS one *6*, e22065.